CHALMERS
UNIVERSITY OF TECHNOLOGY

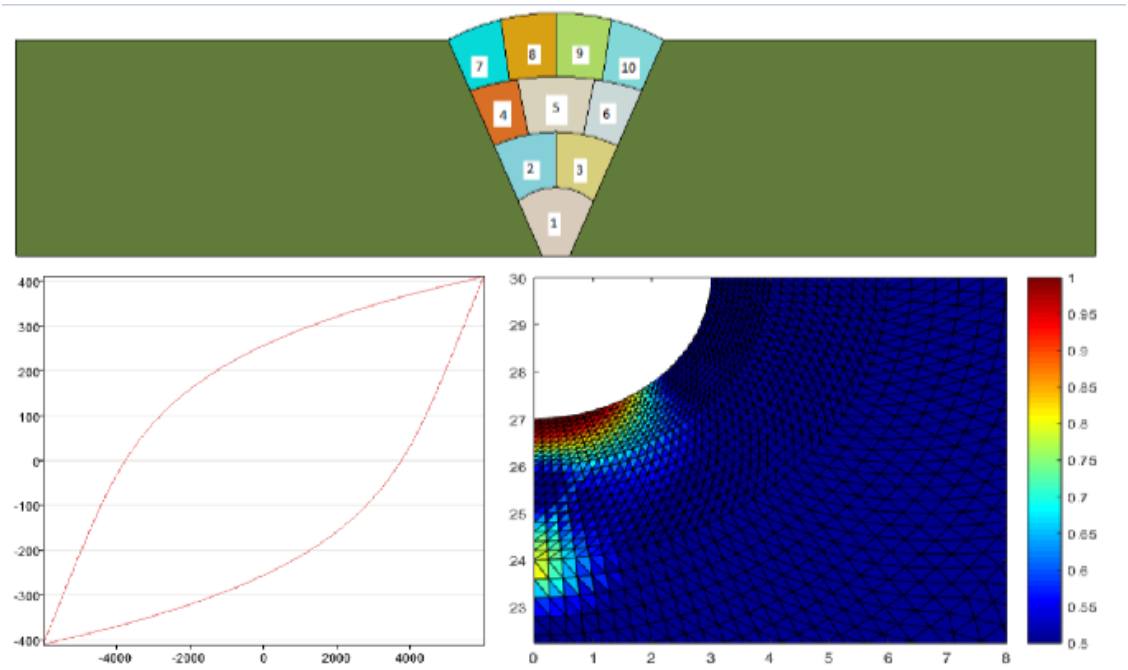

A study of fatigue damage models for assessment of steel structures

Master's thesis in structural engineering and building technology
Master's thesis ACEX30-18-79

HASSAN AYAD ABDULATEEF ALKARAWI

Department of civil and architectural engineering
CHALMERS UNIVERSITY OF TECHNOLOGY
Gothenburg, Sweden 2018

Master's thesis ACEX30-18-79

A STUDY ON FATIGUE DAMAGE MODELING

A study of fatigue damage models for assessment of steel structures

Master's thesis in structural engineering and building technology

ALKARAWI HASSAN

CHALMERS
UNIVERSITY OF TECHNOLOGY

Department of civil and architectural engineering
Division of structural engineering
Steel and timber structure research group
Chalmers University of Technology
Gothenburg, Sweden 2018

A study on fatigue damage modeling

Supervisor: Mohammad Elemrani, Asma Manai, Chalmers university of technology

Master's Thesis ACEX30-18-79
Department of civil and architectural engineering
Division structural engineering
Steel and timber structures research group
Chalmers University of Technology
SE-412 96 Gothenburg
Telephone +46 72 045 345

Typeset in LaTeX
Printed by Chalmers press
Gothenburg, Sweden 2018

Acknowledgements

I would like to express my love to the prettiest flowers in my life: my mother, my father, my lovely sister Fatima and to the soul of my late friend Alaa; you might not be familiar with fatigue problems but you were always in my mind and heart in every single layer of my work. Also a great acknowledgment for my teachers Mohammad Elemrani, Asma Manai and Andreas Ekeberg who didn't save any effort to support me in my work.

Hassan Alkarawi, Gothenburg, June 2018

ABSTRACT

In steel structures, the ultimate and serviceability limits states are not enough to be checked; this is because fatigue is also a decisive criteria. Fatigue damage consumes the life of the structure due to repetitive loading. In general, fatigue life can be divided into stages: crack initiation and crack propagation stages. The first stage is generally much longer in un-welded steel structures and in welded details where critical locations are treated to reduce local stress raisers and remove determinantal weld defects. Different models already existed to estimate the fatigue life of steel structures and components, some of these models the damage as a function of the number of applied cycles (e.g Miner's rule, modified miner rules) while others simulate the damage through a degradation mechanical proprieties .

The aim of the study is to present and implement different fatigue damage models for both high and low cycles fatigue. The fatigue life of selected cases will be estimated, and comparison between these models will be done to show the benefits and drawbacks of each model. Besides, a light is thrown on the role of residual stress and to use some of studied fatigue models to study the relaxation of residual stresses due to fatigue loading.

A detailed literature study in continuum damage mechanics has been conducted to get a comprehensive insight into these damage models. To simulate these models different numerical techniques was used. Elastic and elastoplastic mechanical finite element simulations are conducted through finite element software (Abaqus), and the fatigue life extension software (FE-Safe) was also be used to carry on the simulation conducted by Abaqus. Direct programming also was used to implement many models through Calfem toolbox. For welding simulation the interactive welding interface (AWI) is used in parallel with the thermomechanical models by Abaqus.

Different accumulation techniques have been studied, some of them are superior to the others in a meaning of including the load sequence and interaction effect. The critical plane methods show different results and the closest to reality are Fatemi-socie and Bannantine-Socie models. Some models are sensitive to the material parameters, these models are Chaboche, Xiao and Miao models. Xiao is found to be less conservative than the other two models. Another fatigue damage models are used for studying the residual stress relaxation.

The aim of many of these models is to simulate the effect of microplasticity which is the driving force that cause high cycle fatigue. Studying residual stress and its relaxation is simulated though overloading, temperature filed, stress field and true thermal simulation which found to be the most accurate among them.

Elemental stiffness degradation is reasonable method, physically appealing, doesn't require material parameters and able to simulate the relaxation of residual stress due to fatigue loading. However further testing and numerical studies are required to investigate more models and to compare the studied models to test results.

Keywords: Fatigue damage, Damage initiation, Damage modeling, Critical plane, Pragmatic fatigue, Residual stress relaxation, Abaqus welding interface, FE-Safe, Continuum damage mechanics, Stiffness degradation, High cycle fatigue, Low cycle fatigue, S-N curve.

Contents

1 INTRODUCTION **1**
1.1 Background . . . 1
1.2 Aim and objectives . . . 1
1.3 Methodology . . . 1
1.4 Limitations . . . 2

2 HIGH CYCLE FATIGUE DAMAGE MODELS (HCF) **3**
2.1 Nonlinear fatigue damage model based only on S-N curve parameters* . . . 3
2.2 Chaboche model* . . . 4
2.3 Xiao model . . . 6
2.4 Chow model . . . 7
2.5 Zhang model . . . 9
2.6 Miao model* . . . 10
2.7 Damage Accumulation Model Based on Damage Curve Approach* . . . 11
2.8 Peerlings model* . . . 12
2.9 Socie's proposal for HCF regime [**So**]* . . . 15
2.10 A new modified model based on Xiao model* . . . 15
2.11 Elemental stiffness reduction method* . . . 16
2.12 Yield strength reduction* . . . 17

3 LOW CYCLE FATIGUE DAMAGE MODELS (LCF) **19**
3.1 Pirondi- Bonora model [**PB**] . . . 19
3.2 LPD model . . . 20
3.3 CDM for heat affected zone under LCF* . . . 22
3.4 Ductility exhaustion model . . . 23
3.5 Fatemi–Socie model [**FS**]* . . . 23
3.6 Bannantine and Socie model [**Ba**]* . . . 24
3.7 Wang and Brown's model [**WB**]* . . . 24
3.8 Ductile damage model in Abaqus* . . . 25
3.9 Damage coupled with plasticity* . . . 26

4 METHODS **28**

5 RESULTS **29**
5.1 FE-Safe damage models . . . 29
5.1.1 Elastic block models . . . 30
5.1.2 Elastic plastic block . . . 31
5.1.3 Other features in FE-Safe . . . 31
5.2 Damage accumulation techniques . . . 34
5.3 Notch stress effect . . . 38
5.4 Residual stresses application . . . 40
5.5 Abaqus welding interface (AWI) . . . 43
5.6 Residual stress relaxation . . . 46
5.7 Ductile damage model in Abaqus . . . 49
5.8 Miao model implementation . . . 49
5.9 Xiao model implementation . . . 50
5.10 Chaboche model implementation . . . 51
5.11 Critical plane method . . . 52
5.12 Model describing the damage due to reduction in yield strength . . . 54
5.13 Model describing the damage due to reduction of elemental stiffness . . . 56
5.14 Damage coupled with plasticity . . . 60

5.15 Finite element tricks 60
5.15.1 Adaptive mesh refinement 60
5.15.2 Sub modeling 61

6 DISCUSSION **63**

7 CONCLUSION **66**

8 APPENDIX A: MATLAB CODES **I**
8.1 The main code used for Miao, Xiao and Chaboche models I
8.1.1 Main code I
8.2 Finite element implementation code I
8.3 Miao , Xiao , Chaboche models implementation III
8.3.1 Miao's model III
8.3.2 Xiao's model V
8.3.3 Chaboche's model VI
8.4 Critical plane methods VII
8.5 Reading from Abaqus VIII
8.6 Elemental stiffness degradation code VIII
8.7 Rainflow counting algorithm X

9 APPENDIX B: Material proprieties change with temperature **X**

10 REFERENCES **XII**

*: The marked models will be studied and implemented in the results chapter while the rest of the models will only be displayed in the literature study part without any numerical or analytical implementation.

1 INTRODUCTION

1.1 Background

The fatigue in metals was mentioned for the first time by Wilhelm Albert (1837) but it was until 1880 it starts to be taken seriously in the design when Wöhler found his curve to describe the number of cycles to cause failure as a function of the stress range. Later in 1954 Coffin and Masnon explain crack growth in terns if plastic strain at the crack tip and seven years later Paris proposed his model to calculate the crack growth rate.

Palmgren and Miner put their hypothesis in 1945 and 1924 respectively about the damage accumulation and it achieved great success, that's why it's still widely used for engineering purposes. However, their hypothesis fails to consider the non-liner accumulation behaviour which makes it conservative in some occasions and non conservative in others. After Palmgren-Miner many hypotheses were put to get more realistic models for high and low cycles fatigue. The necessity of these models came from the complexity of the geometry, material and the loading history in real structure.

Different cycle accounting methods have been proposed but the most useful and the best among them was proposed by the Japaneses engineer Tatsuo Endo in 1968. In 1973 the multiaxial fatigue was understood more effectively Brown and Miller when they proposed that both tension and shear stresses contributes to fatigue in their critical planes.

In this study a number of selected fatigue models will be classified according to their objective; so the stress based methods which are applicable and usable for high cycle fatigue problem will be presented in the next chapter while the strain based methods where the plastic strain represents the damage indecatior will be handled in third chapter.

Many of these models are based on the *effective stress concept* in parallel with *strain equivalence principle*. The later was explained by Chaboche and Lemaitre who stated that any deformation behaviour, whether uniaxial or multiaxial, of a damaged material is represented by the constitutive laws of the virgin material in which the stress is replaced by the effective stress; which assumes that all the different types of behaviours (elasticity, plasticity, viscoplasticity) are affected in the same way by the surface density of the damage defects. The former concept (Effective stress) is stated in the same source and it means the ability to replace the stress acting on a damaged area with the effective stress acting on a virgin area.

1.2 Aim and objectives

The aim of the study can be summarized by:

- Studying different fatigue damage models that are able to describe the progression of damage in steel structure in the presence of notch.
- Checking the validity of these models in term of different criterion (mean stress and sequence effect inclusion, conformity with test results and plasticity handling).
- Adopting a model can fulfill these criterion and showing the features of the selected model.
- Consideration of residual stress using different modeling techniques and study of relaxation of residual stresses due to fatigue damage.

1.3 Methodology

In order to achieve the objectives defined above the following methodologies are used:

- A literature study on different fatigue damage models; that requires a solid ground in fatigue theory, damage mechanics and material sciences so these topics will be part of the study.

- A numerical analyses for the selected models using (Abaqus/CAE 6.8) and its extension for fatigue assessment (FE-Safe 2017). Also Abaqus welding interface (AWI) will be used to ease the residual stress evaluation.
- Programming effort to simulate some models which can't be simulated using Abaqus. The coding will be done using Matlab and its FEM toolbox Calfem.

1.4 Limitations

The study will only include fatigue damage models for an isotropic material. Also the study will be limited to the crack initiation phase; so the propagation mechanisms and modeling will not be part of the study. Besides, some models require writing a script using Fortran/Matlab for the constitutive material behaviour if they are not included in Abaqus, this could be very essential for many models but it's not part of this study.

2 HIGH CYCLE FATIGUE DAMAGE MODELS (HCF)

HCF is defined according to the number of cycles to cause failure. However, it can also be a title for the fatigue which does not induced macro plastic strains. The studied models are applicable for high cycle fatigue; but some of them are capable of describing the plasticity term as well (e.g Zhang model).

2.1 Nonlinear fatigue damage model based only on S-N curve parameters*

A new and easy to apply fatigue damage model that does not require any material parameter and depends only on the S-N curve without modification. The proposed model includes the effect of the load sequence and the interaction between the load cycles(Aeran et al., 2017).

Proposed damage index

According to the proposed model [(Aeran et al., 2017) p (328)] the fatigue damage can be represented by the absolute value of proposed D_i given in the following equation:

$$D_i = 1 - [1 - \frac{n_i}{N_i}]^{\delta_i} \tag{1}$$

$$D = |D_i| \tag{2}$$

The selection of the model value δ_i is essential in defining the method, when δ_i =1 then it is Miner rule (Miner, 1954). In the proposed model(Aeran et al., 2017) the δ_i value is given as:

$$\delta_i = \frac{-1.25}{\ln N_i} \tag{3}$$

And that makes it dependent only on the S-N curve without need for any material parameters.

Damage transfer concept

Variable amplitude loading requires a special treatment for the load sequence and interaction factor between the sequential loading; these treatments are included in the model in the form of factor which makes the damage estimation more precise and accurate.

load interaction factor μ

The load sequence represents the sequence of stress ranges in a random stress-time history [(Aeran et al., 2017) P-330].The proposed load sequence factor must take into account that high loading cycles followed by low loading cycles (high-low) results in shorter fatigue life and vice versa. The proposed factor is given as:

$$\mu_{i+1} = \frac{\sigma_i}{\sigma_{i+1}} \tag{4}$$

This is physically appealing since under the (high-low) loading initial micro cracks start to appear in early stage as a result of initial large strains (large stresses). Subsequently these micro cracks start propagating even under small strains (small stresses) and result in more material damage earlier than those predicted by Miner's rule. Another explanation could be that the initial large strains will cause a roughening of the surface and will lead to the creation of more potential crack initiation spots under the subsequent small strains (Aeran et al., 2017) and the new and corrected formula of the damage for the load sequence can be written as(Aeran et al., 2017):

$$D_i = 1 - \left[1 - \frac{n_{(i+1),eff}}{N_{i+1}}\right]^{\frac{\delta_{i+1}}{\mu_{i+1}}} \tag{5}$$

So $n_{(i+1),eff}$ can be given by the following relation:

$$n_{(i+1),eff} = \left[1 - (1 - D_i)^{\frac{\delta_{i+1}}{\mu_{i+1}}}\right] .N_{i+1} \tag{6}$$

where:
n_{i+1}: The number of cycles for stress state σ_{i+1}.
μ: The load interaction factor.

The full algorithm for this model which shows how the damage transfer concept proposed in (Aeran et al., 2017) and it's shown in figure 2. The damage transfer is a continuous process until the fatigue damage value reaches unity. The graphical representation of this process is given in figure 1.

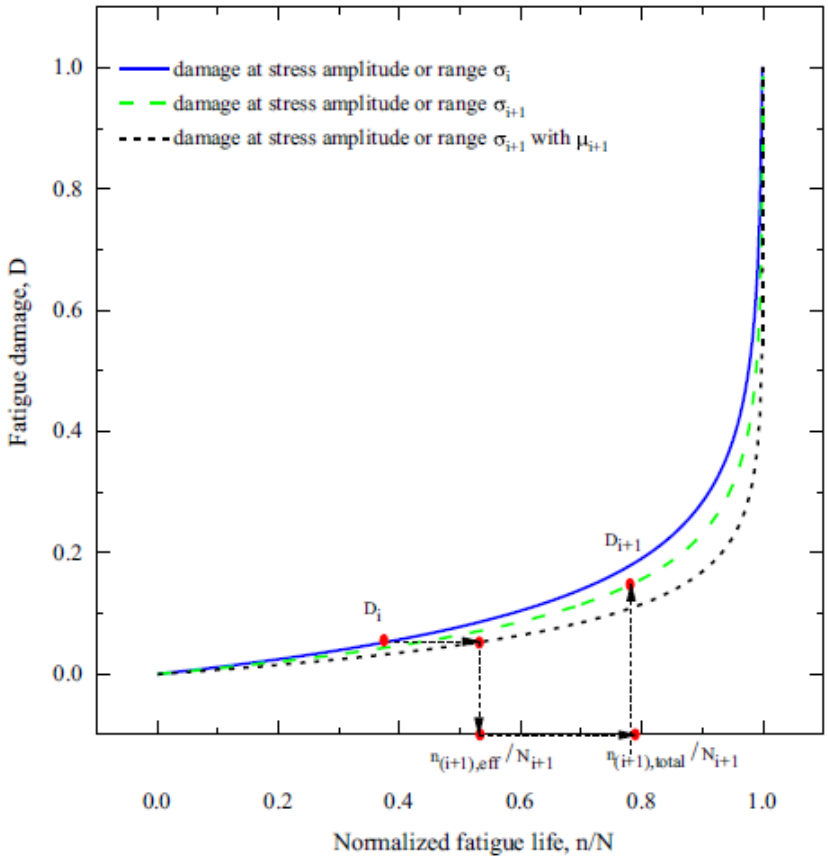

Figure 1: damage transfer concept(Aeran et al., 2017).

Validation

This model was verified on both butt and fillet weld joints. The test preparations and the samples description are given in [(Aeran et al., 2017) p (338-339)]. Good matching was found between the experimental results and the models as shown in figure (3) which compares the proposed model to different known models including Miner rules. These models are discussed and compared in details in [(Aeran et al., 2017) p(329-330)].

2.2 Chaboche model*

A phenomenological model describes the damage evolution in each cycle as a function of maximum stress (σ_{max}), mean stress (σ_m) and the damage variable (D) [(Silitonga et al., 2013) p(329-330)]. This accumulative model is nonlinear since the damage evolution $\dot{D}$ is a function of damage (D) which is given in the following expression:

$$dD = \left[1-(1-D)^{\beta+1}\right]^{\alpha}.\left[\frac{\sigma_{max}-\sigma_m}{M(\sigma_m)(1-D)}\right]^{\beta}.dN \tag{7}$$

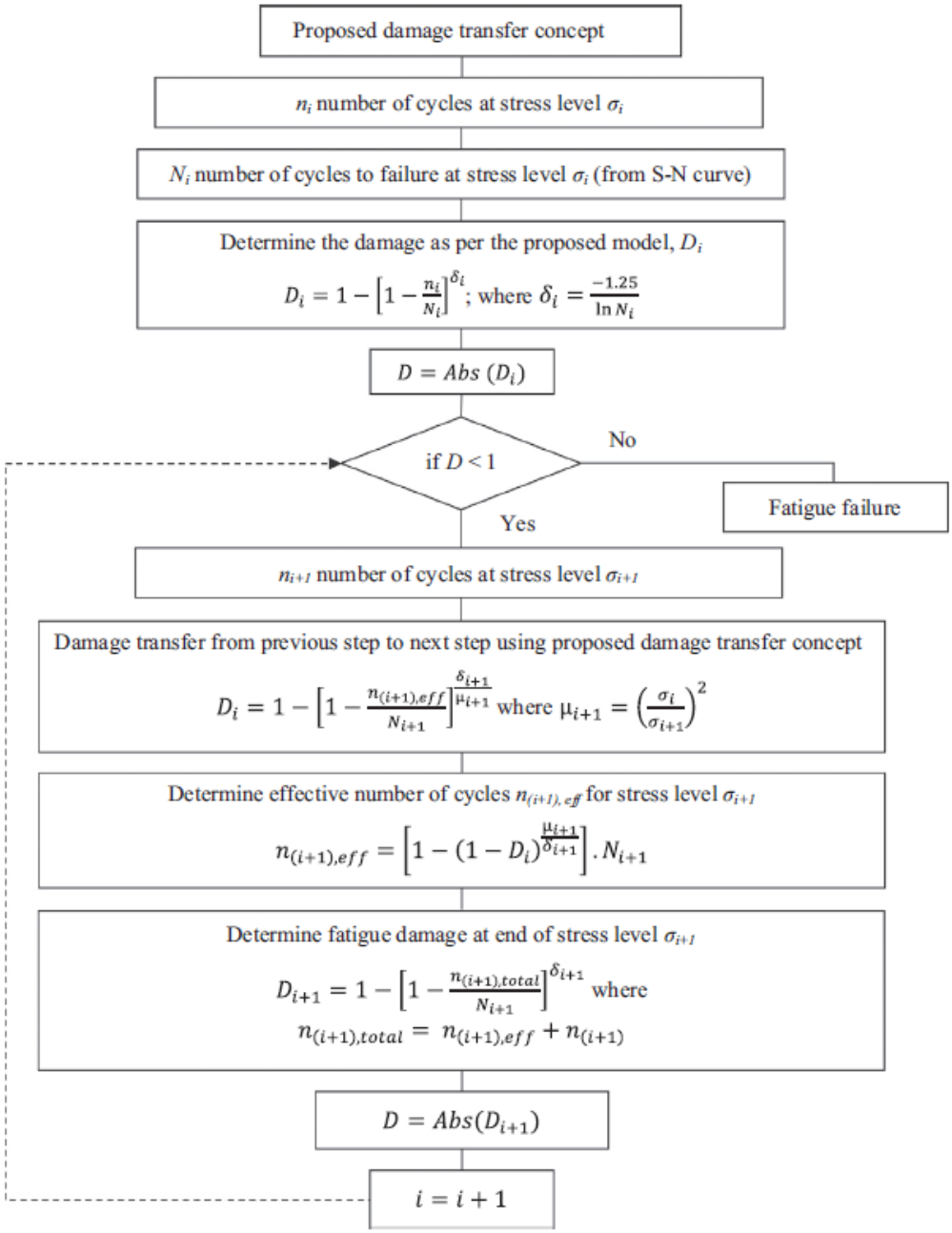

Figure 2: Flow chart of the proposed damage transfer concept.(Aeran et al., 2017)

Where $M(\sigma_m)$ describes the linear relationship between the mean stress and the fatigue limit σ_{fl}. Different models give different expression for that variable [(Silitonga et al., 2013) and (Van Do et al., 2015)] but both sources agree on the expression of the exponent (α):

$$\alpha = 1 - a \left\langle \frac{\sigma_{max} - \sigma_f(\sigma_m)}{\sigma_u - \sigma_{max}} \right\rangle \tag{8}$$

Where $\langle x \rangle$: is a positive argument parenthesis which applies the argument if $x \geq 0$ and zero otherwise.
β, α, a and M_0 are material parameters can be determined from the experimental S-N curve for the predicted of fatigue crack nucleation life (Van Do et al., 2015). The calibration and evaluation of these coefficient are given in the same paper. The fatigue damage can be evaluated by integrating

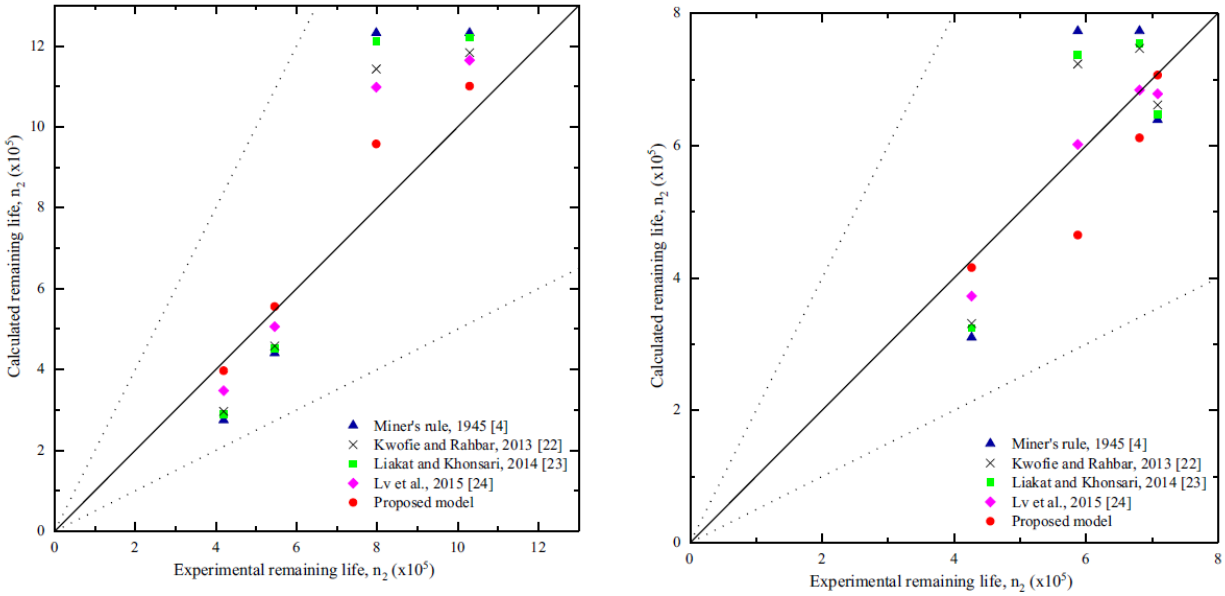

Figure 3: The accuracy of the proposed model for butt and fillet welded joints respectively (Aeran et al., 2017).

equation 7 and the final expression is given by:

$$D = 1 - \left[\frac{N}{N_f}\left(\frac{1}{1-\alpha}\right)\right]^{\left[\frac{1}{1+\beta}\right]} \tag{9}$$

The effective mean stress ($\overline{\sigma_m}$) can replace mean stress (σ_m) so residual stress can be included

$$\overline{\sigma_m} = \sigma_r + \sigma_m \tag{10}$$

The deficiencies of this model are given in [(Chaboche and Lesne, 1988) p(16)] and they can be summarized by the definition of the damage given in this model which includes both initiation phase and micro-propagation as well. On the other hand this method includes the effect of the mean stress and the material parameters can be easily determined from the S-N curve.

Below fatigue limit (α) value can be chosen to be 1 so the damage caused by the undamaging loading is equal to zero according to equation 9. This principle is demonstrated and shown in details in (Dattoma et al., 2006).

Validation

The model was validated on V groove welded joint and the S-N curve obtained from the model was matching the experimental results for different stress ratio as shown in figure 4. There the readers are referred to see detailed discussion about the validity of this model and the detailed procedure of the experiment.

2.3 Xiao model

A continuum mechanics damage (**CDM**) model which is based on thermodynamics framework. The main idea of these kind of models is the effective stress concept in parallel with strain equivalence concepts. Both of these concepts are given in many literature (Lemaitre and Chaboche, 1994). This model does not give an explicit formulation of the damage but instead it gives the damage evolution with time (dD/dN) and the number of cycles can be derived from that by integrating over time; which makes it must be combined with one of the accumulation techniques (e.g Miner).

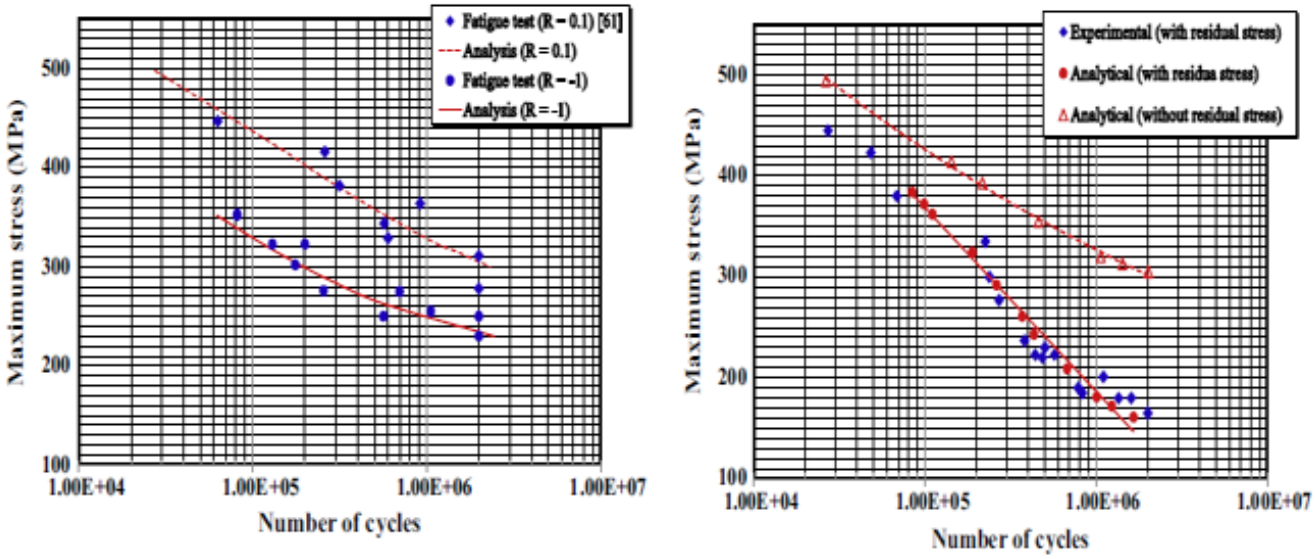

Figure 4: Validation of one of the Chaboche adapted models(Van Do et al., 2015).
L: Different stress ratio.
R: With and without residual stresses effects.

The integration is taken from 0 to 1 to give the total life. Instead, the life can be evaluated at any damage stage if the integration limits set to be from zero to the specified value of the damage, in this study the full integration will be presented.
The damage evolution and the life expectancy respectively are given in the following expressions

$$\frac{dD}{dN} = \left[\frac{\sigma_{max} - \sigma_m}{M(\sigma_m)(1-D)}\right]^{2q} (1-D)^P \tag{11}$$

$$N = \frac{1}{2q - p + 1}\left[\frac{\sigma_{max} - \sigma_m}{M(\sigma_m)}\right]^{-2q} \tag{12}$$

where :
p, q: material parameters.
C_{-1} : material coefficient identified experimentally for symmetric loading.
$M(\sigma_m)$: is the same as defined in Chaboche models (Van Do et al., 2015).

One of the extensions of this models allows to introduce an initial ductile and creep damages before the fatigue damage has commenced. That could be very useful if the ductile damage can be evaluated and there are different models describing that evolution Tai and Yang (1986) and Chandrakanth and Pandey (1995). This multi-mechanism damage coupling model which is capable of describing any damage mechanism (ductile, brittle or creep) in presence of initial different damage is described in Xiao (2004). Also it's capable of describing multi-mechanisms working and evolving together but that requires many calibrations and material parameters.

Validation

It is shown in [(Xiao et al., 1998)p (506)] that this model is a generalization for both Chaboche and (Lemaitre and Plumtree) models; and because of the similarities with Chaboche model the material parameters are also found using Woehler curve [(Xiao et al., 1998)p (508)]. The model was validated and compared to experiments for different mean stresses and good agreement has been obtained by (Xiao et al., 1998), the validation for Aluminum alloy is shown in figure 5.

2.4 Chow model

All of the previous damage models discussed before define the damage by one damage variable which represents the degradation of the material stiffness with cycles.On contrary, Chow introduces

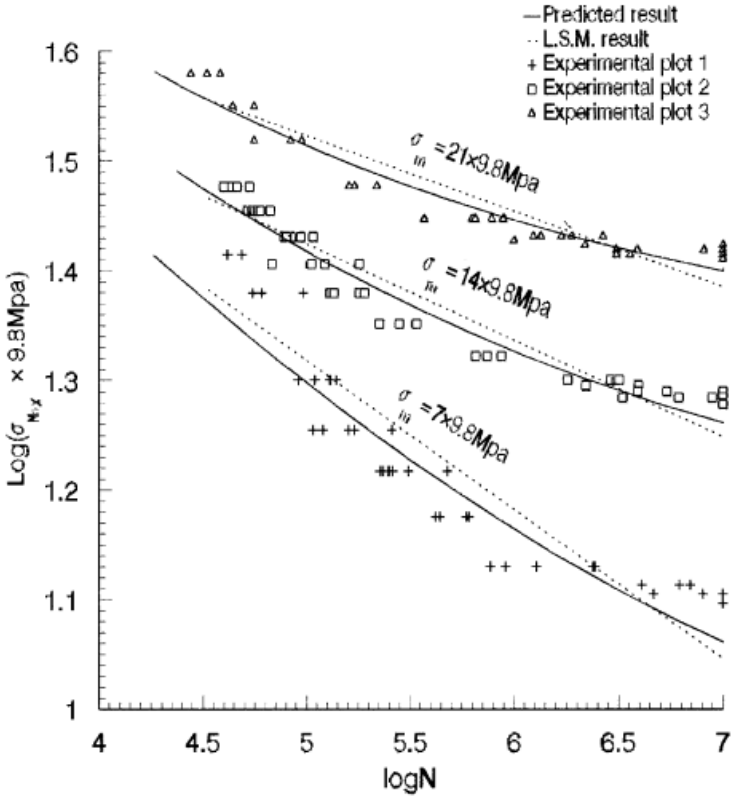

Figure 5: Validation of Xiao model for different mean stresses (Xiao et al., 1998).

a damage tensor consisting of two variables μ_f and D_f. The former represents the degradation of Poisson's ration while the later represents the stiffness loss. The damage tensor evolution is given in the following relations:

$$dw_f = \frac{Y_{Df}dY_{Df} + Y_{\mu f}dY_{\mu f}}{2\sqrt{Y_{df}}K(w_f)} \quad dD_f = -dw_f\frac{Y_{Df}}{2\sqrt{Y_{fd}}} \quad d\mu_f = -dw_f\frac{\gamma Y_{\mu f}}{2\sqrt{Y_{fd}}} \tag{13}$$

$$Y_{fd} = \frac{Y_{Df}^2 + \gamma Y_{\mu f}^2}{2} \quad Y_{Df} = -\frac{\sigma^T : C^{-1} : \sigma}{1 - D_f} \quad Y_{\mu f} = -\frac{\sigma^T : A : \sigma}{1 - D_f} \tag{14}$$

$$K(w_f) = K_0(1 - \frac{w_f}{w_c}) \tag{15}$$

Where:
K_0, γ: Material parameters
C, A: damage effect tensors for Poisson's ratio and elasticity respectively [6 × 6];their matrices are given in [(Chow and Wei, 1991)p(303-304)].
w_f: Overall fatigue damage.
w_c: Intrinsic material property represents critical value of overall damage which can be evaluated using conventional tensile test.

Validation

One deficiency of this model is the necessity for precise measurement of small strains to evaluate the effective elastic modulus $\widetilde{E}$ and Poisson's ratio $\widetilde{\mu}$. This model is very expensive in term of required material parameters and the tests needed for evaluating these parameters. On the other hand The model is very precis and shows excellent agreement with the test results conducted on A1 2024-T3. The test preparation and material parameters evaluation are given in [(Chow and Wei, 1991)p(313-315)]. the validation of this model is shown in figure 6.

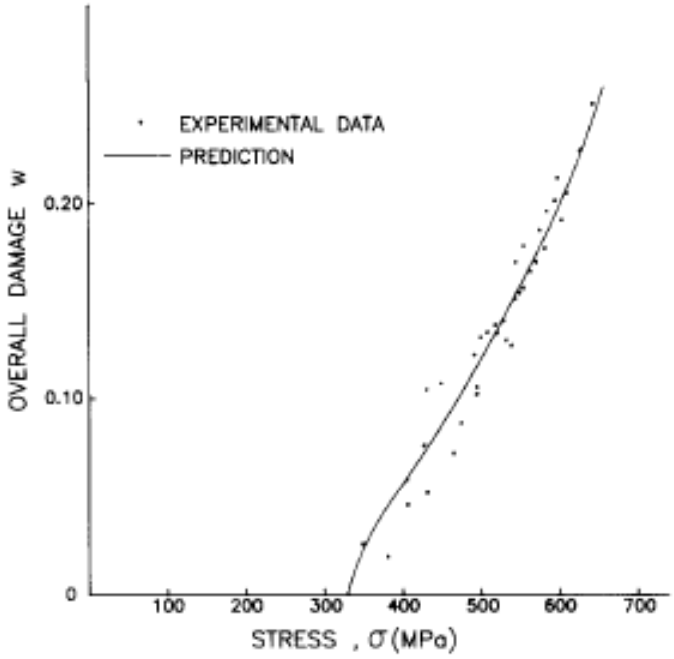

Figure 6: The accuracy of the proposed model for butt and fillet welded joints respectively (Chow and Wei, 1991).

2.5 Zhang model

Similarly to Xiao model (Xiao et al., 1998) this model does not offer an explicit expression for the damage but rather it gives expressions for the damage evolution and fatigue life, so the same procedure mentioned before also applies for Zhang model. Effective stress and strain equivalence concepts are also used here.

Zhang model is a non linear continuum damage model based on the irreversible thermodynamics framework developed by Chaboche and Lemaitre. One of the facilities of this model is the capacity of predicting the fatigue life for both frequency dependent and independent materials (Zhang et al., 2012).
The damage evolution is expressed by:

$$\dot{D} = \frac{Q(f)\sigma_{eq}^{q(f)}\dot{\sigma_{eq}}{R_v}^p}{(1-D)^{q(f)+1}} \tag{16}$$

$$Q(f) = \frac{BM(f)}{(2E)^P K^{M(f)}} \tag{17}$$

$$q(f) = 2p + M(f) - 1 \tag{18}$$

Where:
B, P: Material parameters.
R_v: The triaxiality expression which relates the hydrostatic stress to the equivalent stress and it's equal to 1 in case of uniaxial loading. The full expression for R_v is given in [(Zhang et al., 2012)p(2778)].
M: The strain hardening exponent which depends on the strain rate so it is related the loading frequency.
σ_{eq} $\dot{\sigma_{eq}}$: Von Mises equivalent stress and equivalent stress rate respectively.

Contrary to other models, this model account for the micro plasticity and include the plastic hardening which makes it distinguished from other models since and according to many authors (Silitonga et al., 2013) and (Zhang et al., 2012) micro plasticity is the driving process for high cycle fatigue and implicating this factor would be necessary. It is also capable of accounting for

multiaxial loading represented by the triaxiality function R_v. Also it accounts for both alternating and pulsating loading's (i.e. different R ratio).

Validation

The fatigue life for fully reversed loading (R = -1) is given by:

$$N_f = \frac{[q(f)+1]\left[{\sigma_{eq}}^{q(f)+1}\right]^{-1}}{4[q(f)+2]Q(f){R_v}^p} \tag{19}$$

This can be compressed to:

$$N_f = H(f)\left[\sigma_{eq}^{C(f)}\right]^{-1} \tag{20}$$

Where *H(f)* and *C(f)* are identified from S-N curve [(Zhang et al., 2012) p (2780)]. The model was verified for both frequency dependent (e.g Aluminum alloy) material and independent material (e.g Titanium) as shown in figure 7.

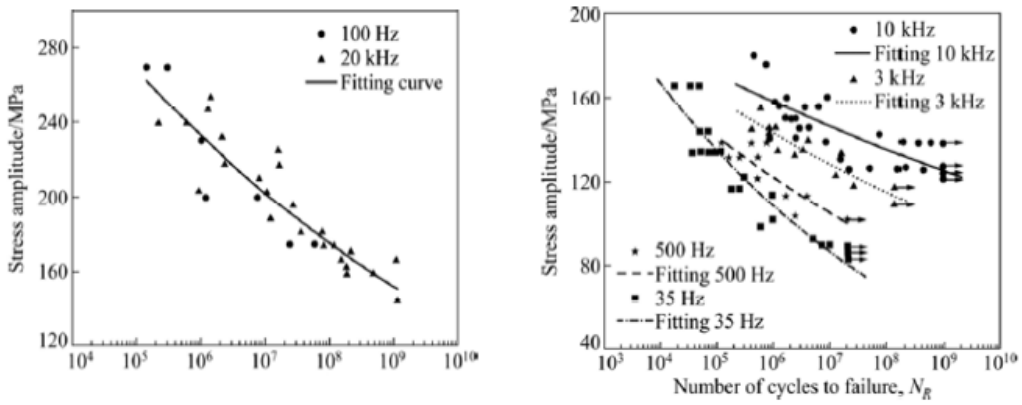

Figure 7: Fatigue life of Aluminum alloy and Titanium respectively (Zhang et al., 2012).

2.6 Miao model*

This model was developed to predict the fatigue life of Pitch-Change-Link as shown in 8L. It's based on thermodynamics framework accompanied with effective stress and strain equivalence concepts. In this method both smooth and notched specimens damage are described. Here only the notched specimen damage is described. The damage evolution for the specimen is given by:

$$\frac{dD}{dN} = \alpha_k \frac{\epsilon_{(k,D,max)} - \epsilon_{(k,0,th)}}{(1-D)^{m_k}} \tag{21}$$

$$\epsilon_{(k,D,max)} = \epsilon_{(k,0,max)}/\sqrt{1-D} \quad \epsilon_{(k,D,th)} = \epsilon_{(k,0,th)}/\sqrt{1-D} \tag{22}$$

$$\epsilon_{(k,0,max)} = \frac{\sigma_{th,k}}{E} \tag{23}$$

Where:
k: The stress concentration factor.
$\sigma_{th,k}$: Is the threshold of stress without damage.
$\epsilon_{(k,D,th)}$: Threshold of strain with damage
$\epsilon_{(k,0,th)}$: Threshold of strain without damage.
$\epsilon_{(k,D,max)}$: Maximum strain with damage.
$\epsilon_{(k,0,max)}$:Maximum strain without damage.
α_k, m_k: Material and geometric proprieties. They can be optimized from high cycle fatigue experimental for fully reversed loading and the following equation must be used for optimization

$$\log N_f = \log S - m_k \log Y \tag{24}$$

The detailed expressions which contain the explicit form of S and Y are given in [(Zhang et al., 2010)p (1685)]

Solution strategy (Zhang et al., 2010)

. The stresses firstly are evaluated without considering the damage and the critical element can be found which is assigned by the maximum principle tensile stress element. The damage increment ΔD is chosen (by the user), For this given increment (N_i) the life cycle increment can be evaluated using equation 21. For the other elements the damage increment ΔD is evaluated by the same equation 21. The new stress state is evaluated by including the damage in the stiffness matrix which is given in the following equation:

$$(K - \sum_{e} D_e A^T k_e A)\Delta = p \tag{25}$$

So the new stress state is given by:

$$\sigma = (E[1 - D])\, B\Delta \tag{26}$$

The same procedure continues until the damage reaches the specified value (specified by the user). Since the loading history is given so the solution will be passive; which means the damage accumulation must be continue until the load cycles covers the whole loading history. The material parameters are obtained by data fitting on experimental fatigue tests; these parameters are given in (Zhang et al., 2010).

$$N = N_t + \Delta N \tag{27}$$

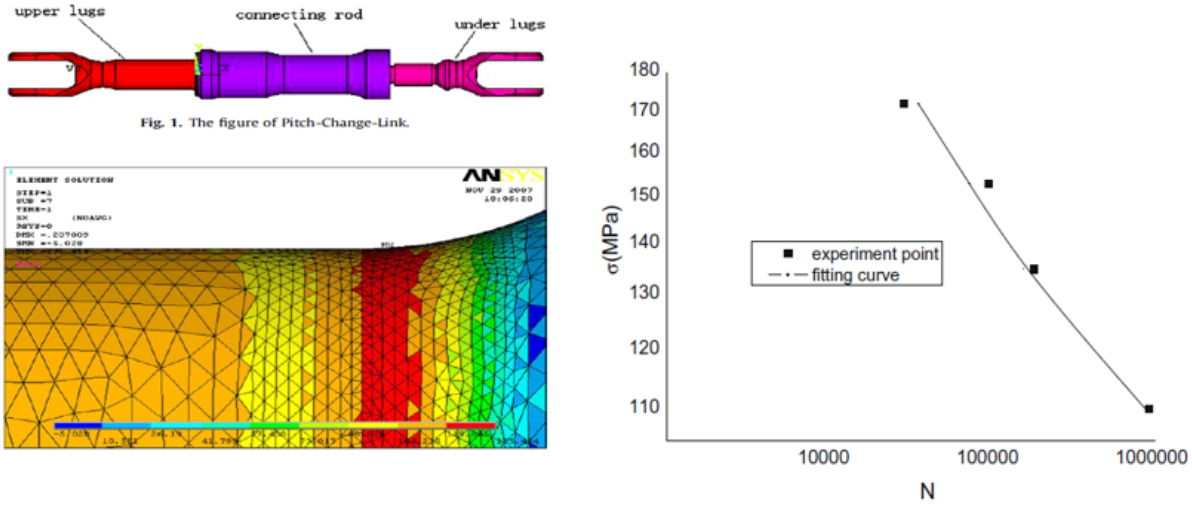

Figure 8: R: The computational and experimental S–N curve of of $K_T = 2$ when σ_m= 69MPa
L: The Pitch-change-link modeled using Ansys (Zhang et al., 2010).

2.7 Damage Accumulation Model Based on Damage Curve Approach*

Manson and Halford proposed the damage curve approach and they were able to express the damage accumulation through the crack length evolution with time by the following expression [(Gao et al., 2014)p (2)]:

$$D = \frac{1}{0.18}\left[(a_0 + (0.18 - a_0))\left(\frac{n_a}{N_f}\right)^{0.67N_f^{0.4}}\right] \tag{28}$$

One of the features of this model is the capacity to include loading sequence effect, this idea is shown in the following equation; which shows the accumulation to the failure point:

$$\left[\left[\left(\frac{n_1}{N_{f1}}\right)^{\alpha_{1,2}} + \frac{n_2}{N_{f2}}\right]^{\alpha_{2,3}} + ... \frac{n_{i-1}}{N_f(i-1)}\right]^{\alpha_{i-1,i}} + \frac{n_i}{N_{fi}} = 1 \tag{29}$$

$$\alpha_{i-1,i} = \left[\frac{N_{f(i-1)}}{N_f(i)}\right]^{0.4} \tag{30}$$

Under constant amplitude loading and (α) values are chosen to be unity then it's simplified to Miner's rule (Miner, 1954).However, Including the loading sequence effect will increase the accuracy of the predicted life.

Load interaction effects

The proposed model consider the interaction effect by adjusting the value of (α) to include the relation between the sequential stresses as follow:

$$\alpha_{i-1,i} = \left[\frac{N_{f(i-1)}}{N_f(i)}\right]^{0.4\min(\frac{\sigma_i}{\sigma_{i-1}},\frac{\sigma_{i-1}}{\sigma_i})} \tag{31}$$

It was explained in the first discussed damage model why low stress cycles preceded by high stress cycles are more detrimental physically.That is also confirmed in this model; since the exponent given in equation 31 would be less than 0.4 regardless of the load sequence. But the base $[n_{i-1}/N_f(i-1)]$ would be smaller since σ_{i-1} is larger; which means that the fraction is smaller and raised to a smaller exponent which means higher damage and vice versa.

Validation

The results show that nearly 80% of proposed model predictions are better than that by the Manson-Halford model, and the inaccuracy under high-low and low-high loading conditions has been both reduced [(Gao et al., 2014)P(4)]. The accuracy of Miner's linear accumulation rule is compared to Masnon model [**M-H**] and the proposed model [**P**] and the results are shown in figure 9. The experiment was conducted on steel.

Another experiment was conducted on welded Aluminum alloy butt and fillet joints and the proposed model was compared to the existing model which will not be discussed here, but interested reader is referred to (Tian et al., 2012). The results are displayed in figure 10. Notice that the error percentage did not exceed 10 %.

2.8 Peerlings model*

A high cycle fatigue damage model assumes the damage does not commence until a threshold value has been exceeded; so in this method a damage loading surface is defined as shown in figure 11L. Peerlings model defines the damage development due to reduction of elastic modulus of the material; this deterioration process accumulates until fracture point is reached which corresponds to D = 1.

The damage (D), damage evolution ($\dot{D}$) and the strain amplitude (ϵ_a) respectively are given in following equations :

$$D = -\frac{1}{\alpha}\ln 1 - (1 - e^{-\alpha})\frac{N}{N_f} \tag{32}$$

$$\frac{dD}{dN} = Ce^{\alpha D}e^{\ \beta} \tag{33}$$

$$\epsilon_a = \left(\frac{\beta+1}{2C}(1-e^{-\alpha})\epsilon_a{}^{-(\beta+1)}\right) \tag{34}$$

Where:
β and C : Material parameters are found from the elastic part of Coffin-Manson equation [(Dowling, 2012)p (750)] which has the same form of strain amplitude equation given in equation 34. The loading history should be divided into time increment and the damage can be evalaluated by integration.
α : A material parameter affects the growth of the damage with time as shown in figure 12.

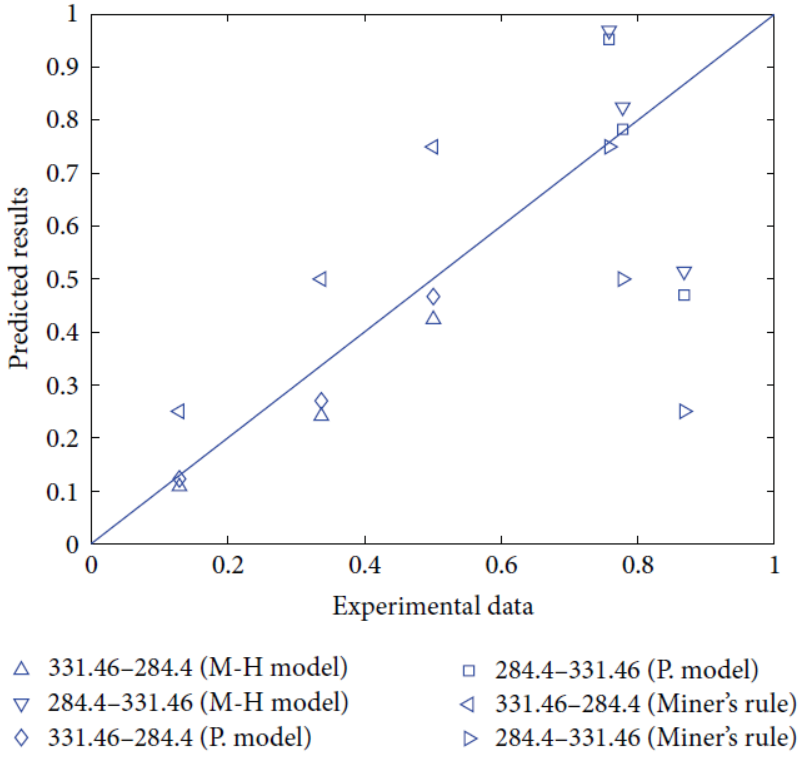

Figure 9: Comparison of prediction results of the proposed model, Miner's rule, and experimental data for 45 steel (Gao et al., 2014).

Load mode	σ_1/Mpa	σ_2/Mpa	$n_1/10^3$	$n_2/10^3$	N_{f1}	N_{f2}	D (by the existing model)	D (by the proposed model)
Mode 1	104	74	109.9	797.6	549,300	1,540,100	0.9260	0.8988
Mode 2	89	74	176.1	1029.2	880,500	1,540,100	1.0810	0.9372
Mode 3	74	89	770.1	545.6	1,540,100	880,500	0.9290	1.0660
Mode 4	74	104	770.1	418.9	1,540,100	549,300	1.0140	1.1053

Load mode	σ_1/Mpa	σ_2/Mpa	$n_1/10^3$	$n_2/10^3$	N_{f1}	N_{f2}	D (by the existing model)	D (by the proposed model)
Mode 5	93	73	309.9	587.5	619,800	1,546,100	1.0140	0.9056
Mode 6	83	73	476.1	681.1	952,300	1,546,100	1.0270	0.9426
Mode 7	73	83	509.2	708.2	1,546,100	952,300	0.9930	1.0614
Mode 8	73	93	773.0	426.4	1,546,100	619,800	1.0670	1.1029

Figure 10: Comparison between the existing model (Tian et al., 2012) and the proposed one for butt and fillet weld respectively (Gao et al., 2014).

Although this method uses Coffin Manson equation but it is applicable for high cycle fatigue (HCF) which is defined by the elastic part of the equation. However, the implementation requires special discretisation to divide the load history into finite cycles and integrate over the time period, the finite element implementation is detailed in [(Peerlings, 1999)ch (5)].

Validation

Peerling's model is capable of describing both fatigue and quasi brittle damage but here only the fatigue simulation is shown. A steel metal with notched geometry is axially loaded cyclically. The geometry, materials and boundary conditions are detailed in [(Peerlings, 1999)p86],the tested specimen is shown in figure 13L and the generated mesh is shown in 13R.

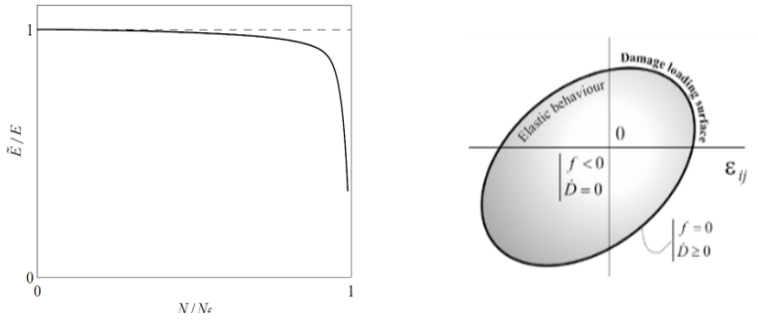

Figure 11:
R:Damage loading surface defined in strain space (Silitonga et al., 2013).
L:Elastic stiffness decrease in high-cycle fatigue (Peerlings, 1999).

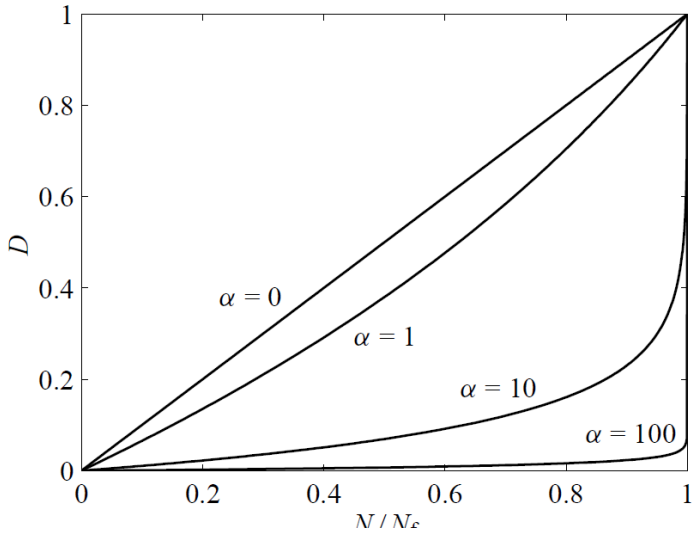

Figure 12: Damage evolution with cycles in Peerlings models. (Peerlings, 1999)

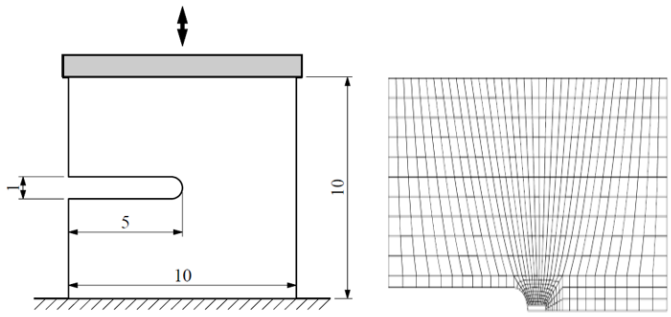

Figure 13: L:The studied geometry. R:Meshing and considering boundary conditions.

The model was not validated nor compared to experiment's results but still it is considered as good and easy tool to predict HCF damage evolution. However, the model shows good agreement with experiment conducted on concrete under monotonic bending loading.

2.9 Socie's proposal for HCF regime [So]*

In this model a linear combination of the shear stress τ_a amplitude and maximum normal stress $\sigma_{n,max}$ and the damage expression is given by:

$$D = \tau_a + k_2 \sigma_{n,max} \tag{35}$$

Where k_2 is material parameter identified from torsion fatigue data.
This fatigue life can be evaluated from the elastic part of the Coffin Manson given in (Dowling, 2012). but for shear loading instead of normal loading as follow:

$$D = \tau_a (2N_f)^b \tag{36}$$

The Rainflow counting [(Dowling, 2012)p(471)]should be applied on the shear strain τ_x and τ_y as shown in figure 14R.

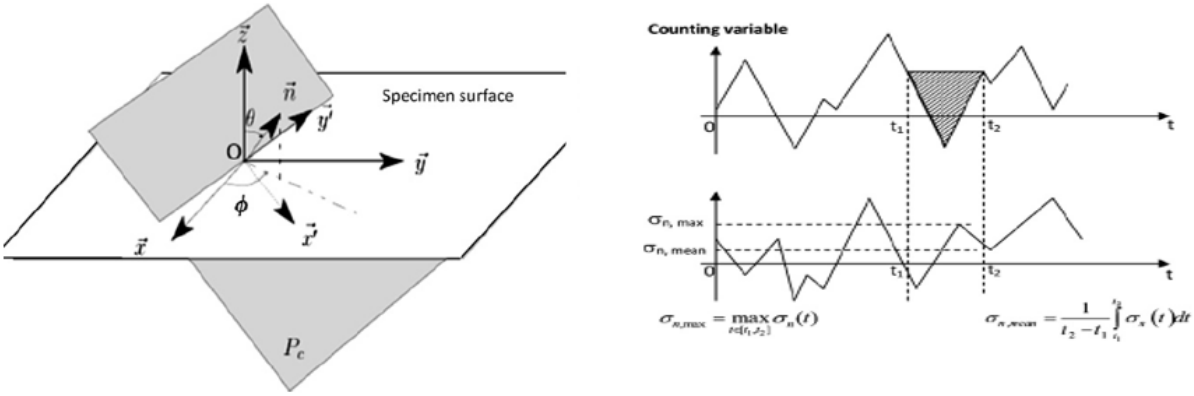

Figure 14: R: Definition of the mean and maximum normal stress during an extracted cycle (from t1 to t2) with the Rain Flow algorithm.(Aid et al., 2012) L: Critical plane definition (Aid et al., 2012).

This method is based on critical plane approach. All of the critical plane methods follow the same procedure as follow:

- Choosing the counting variable.In [**SO**] model τ_x and τ_y are the counting variables.
- Damage variable is chosen based on stress or strain quantities. In [**SO**] model D is given in equation 35.
- Evaluation of damage material on each plane; each plane is defined by it's normal vector $\overline{n}(\theta,\phi)$. As shown in figure 14R.
- To quantify the damage generated by each cycle identified with the counting algorithm it is necessary to exploit an equation relating the damage parameter to the number of cycles to failure N_f; which is given in equation 36. The details of this procedure can be found in [(Aid et al., 2012)p(21)]. The full Algorithm of this method can be found in (Banvillet, 2001).

2.10 A new modified model based on Xiao model*

Xiao model was mentioned before, and it was noticed that many parameters must be obtained and optimized. In this model the main concept of Xiao will be used but only one material parameter need to be evaluated. However However, the applicability of this model is limited to constant amplitude loading (**R** is constant). the concept is introduced in details in (Wang et al., 2016).
The damage evolution is given by the following relation:

$$\frac{dD}{dN} = \frac{\sigma_{eq,M}}{B(1-D)^{2q}} \tag{37}$$

B: A parameter depends on material proprieties and the stress ratio (R).
q: material constant.
The modified model has less fitting parameters and is accommodated to be integrated into finite element programs [(Wang et al., 2016)p (2)]. The model can be solved numerically in finite element routine as follow:

- For the first loading cycles the value of the damage variable D = 0.
- Stress field is evaluated and the damage evolution is studied using equation 37 for the most critical element (the most stressed one in tension).
- For the rest of the loading cycles for the critical element, the life increment is calculated according to:

$$\Delta N_i = \frac{B(1 - D_{i-1})\Delta D}{{\sigma_{eq,M}}^{2q}} \qquad N_i = \Sigma \Delta N \tag{38}$$

- For the rest of the elements the damage increment is evaluated according to equation 37 while ΔN is already evaluated in the previous step.
- Damage in other elements is evaluated from the accumulation of the increments.

Validation

The method was validation for pulsating loading (R = 0.1) for both notched and smooth Titanium specimens. The parameter B was not easy to be optimized since it was dependent on the experiment data so largely. This parameter will be determined from smooth specimen analysis and used in notched specimen analysis. The error percentage for the smooth specimen was found to be around 30 % While the notch specimen's overall lifespan predicted is at least one order of magnitude greater; so only the failure life of elements within 0.5mm from the notch region is taken into account to predict the fatigue life accurately (Wang et al., 2016).

2.11 Elemental stiffness reduction method*

Many of the the models discussed before like Miao model considers the damage through stiffness reduction this is also implemented in the given model. This is not strange since the elasticity is the main propriety that governs the material response among many proprieties (Poissson's ratio ν, Young's modulus E and yield strength σ_y). In high cycle fatigue no structural plasticity is considered so the use of yield strength as damage indicator is questionable and neither Poisson's ratio is not useful to be considered alone because this doesn't match with the physical behaviour but it can be used simultaneously with the yield strength reduction. This model is also usable for mulitaxial fatigue since it uses the Sine's multiaxial fatigue criterion to evaluate the the equivalent stress which will be an input for the S-N curve to evaluate the fatigue life of the structure.

The Sine multiaxaial fatigue criteria will be used to evaluate the updated elemental stiffness; which requires evaluating the material parameter C_s in the following equations:

$$\sigma_{eq} = \sigma_{VM} + C_s \times \sigma_{h,mid} \qquad E_{i+1} = E_i \times (1 - \frac{\alpha \times \sigma_{eq} - \sigma_{EN}}{\sigma_{el} - \sigma_{EN}}) \tag{39}$$

Where:
σ_{EN}: The endurance stress which if not exceeded no damage will be induced.
σ_{el}:The yield strength.
α: Factor to account for microcrack closure effect.
E_{i+1}, E_i: The current and precedence stiffness respectively.
σ_{VM},σ_h: The deviatoric and hydrostatic stresses respectively.

This model has the capability of describing the cycle fatigue problems if elastic material behaviour is assumed and the number of cycles required to cause stiffness reduction can be evaluated from the plugging the maximum equivalent stress in the Wöhler curve or by using the elastic part of Basquin equation.

E	σ_y	σ_u	K	n
72.5 GPA	290 MPa	337 MPa	440 MPa	0.08

Table 1: The mechanical proprieties for the Aluminum used for elemental stiffness and yield strength degradation described in sections 2.11 and 2.12.

The given model is capable of describing the microcrack closure effect due to less damaging effect in compression through the variable α which was suggested in the literature to be 0.1 (Bouchard et al., 2011) and this effect will be studied later. The material parameter C_s is chosen to be 0.42 for steel. Sine criterion is chosen but any multiaxial fatigue criterion can be chosen, e.g. DangVan.

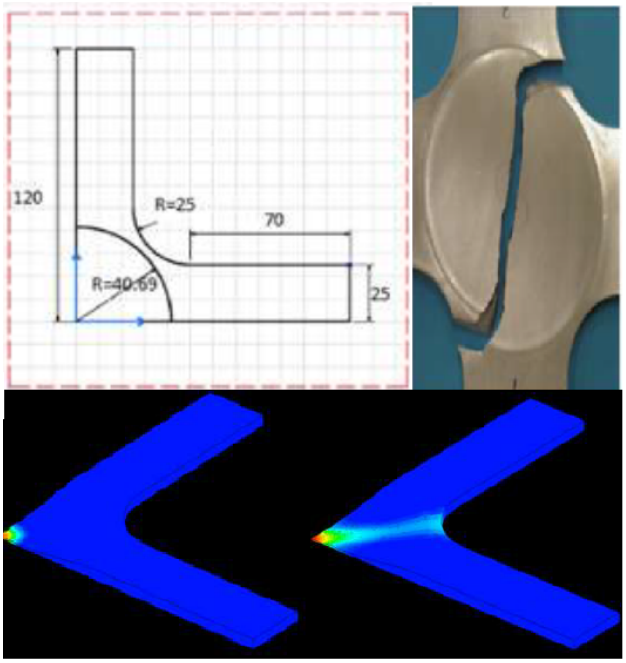

Figure 15: UL: The studied specimen considering the symmetry in both direction.
UR: The tested geometry.
L: The damage initiation and propagation(Asma Manai, 2017).

2.12 Yield strength reduction*

The given model describes the damage by the mean of plastic strain evolution but since in high cycle fatigue structural plasticity is not present,the damage can't evolve unless the yield strength is reduced. This reduction is taking place due to damage. Actually this reduction represents the microplasticity which takes place despite of structural elasticity which obeys Hooke's law. This representation is very explicit in this model more than the rest of the material degradation models due to elasticity reduction. However the raised plasticity isn't the microplasticity in one to one relation but it's related to it. Actually any damage model is useless if it can't describe the driving engine of HCF which is the microplasticity.

These two models (Elemental stiffness and yield strength reduction) were described and verified in (Asma Manai, 2017) for pulsating loading with stress ratio (R=0.1) on Aluminum alloy (Al-6082-T6). The mechanical proprieties of this material is described in table 2.11 as it's given in some literature (Shen, 2012) and (Asma Manai, 2017). The studied geometry is shown in figure 15. Notice that damage initiates from the center of the geometry and then propagate in 45 °angel. The given module expects a fatigue life of 1.5 $\times 10^5$ cycles which is close to the experimental life of 1.6 $\times 10^5$.

The common factor between both of these models is the use of jumping cycles technique. So, every degradation step is a result of a number of constant amplitude loading cycles to cause this degradation which makes the use of this method for variable amplitude loading questionable. However these methods uses different stress values to evaluate the fatigue life. The stiffness degradation uses the equivalent stress while yield strength reduction uses the yield strength value.

3 LOW CYCLE FATIGUE DAMAGE MODELS (LCF)

Low cycle fatigue is a phenomena where plastic distortions are induced which occurs when the driving force is high enough to exceeds the yield limit. Usually the number of cycles to cause LCF does not exceed 10^4 cycles. All of the following models must include the plasticity and cyclic loading material properties (kinematic and isotropic hardening) will be included.
Before getting started with LCF damage models some important terms must be defined:

The yield function

In LCF damage models, it is very crucial to introduce a criterion to differentiate elastic loading, plastic loading, elastic unloading and plastic unloading. this criterion is called *Yield function*. Usually this function is equal to zero in case of elastic loading. This concept can be found in (Runesson et al., 2006) with detailed application for perfect plasticity, hardening plasticity and visco-plasticity.

Backward Euler integration

In order to solve the differential constitute equation of the damage and strains equations numerically, implicit Euler (Backward Euler) can be a choice. briefly it can be defined as:

$$\text{If} \quad \dot{y} = f(t,y) \quad \text{Then y can be evaluated as follow} \quad y = y_{n-1} + \mu f(t,y) \tag{40}$$

where μ is the step size.
This method is the base for solving the plasticity evolution problems numerically.

3.1 Pirondi- Bonora model [PB]

A non linear continuum damage model based on **CDM** in which the damage evolution causes softening effect, this softening effect is counteracted by hardening effect due to plastic deformation. This model includes the triaxiality of the loading which means the capability to describe mulitaxial loading by dividing the stress into hydrostatic and deviatoric parts. The constitutive equations which include the strain and damage evolution are given in the following equations:

$$\dot{\epsilon_p} = \frac{3\dot{\lambda}(\sigma_{dev} - a_{dev})}{2\sigma_{eq}} \qquad \dot{a} = \dot{\epsilon_p} - \frac{3}{2}\dot{\lambda}\frac{a_{dev}}{a} \qquad \dot{h} = \dot{\lambda} \tag{41}$$

$$\dot{D} = \alpha \frac{\sqrt{D_{cr} - D_0}}{\ln \epsilon_{cr}/\epsilon_{th}} R_v (D_{cr} - D_0)^{(}\frac{\alpha - 1}{\alpha})\frac{P}{\dot{P}} \tag{42}$$

Where:
ϵ_p: The plastic strain.
a: The kinematic hardening strain.
h:The isotropic hardening strain.
λ: The plastic multiplier.
D_{cr}: Critical value of damage at failure.
D_0: Initial damage.
α: The damage exponent.
R_v The triaxiality function.
ϵ_{cr}, ϵ_{th}: The critical and the threshold strains respectively.

In this model the compressive loading doesn't cause damage evolution, this is implicitly included in the damage model through the triaxiality function; and since the model is based on stiffness modulus reduction due to damage the reduction must be limited to the tensile loading. as shown in figure 16R.

Validation

Notice that the model contains many material parameter to be fitted and optimized (α, D_{cr}, D_0,ϵ_{cr},ϵ_{th}). These parameters are evaluated through tensile test under displacement control; the

details of the tests are given in [(Pirondi et al., 2006)p (2156)]. Then equation 42 together with constitutive equations will be used to fit the plasticity parameter through optimization techniques(e.g Fmin search function in Matlab). The fitting curve is shown in figure [16L]. One of the drawbacks of this model is the absence method to find D_{cr}, D_0 so they were being assumed [(Pirondi et al., 2006)p (2162)]. Also the absence of the mean stress effect on the fatigue life is problematic.

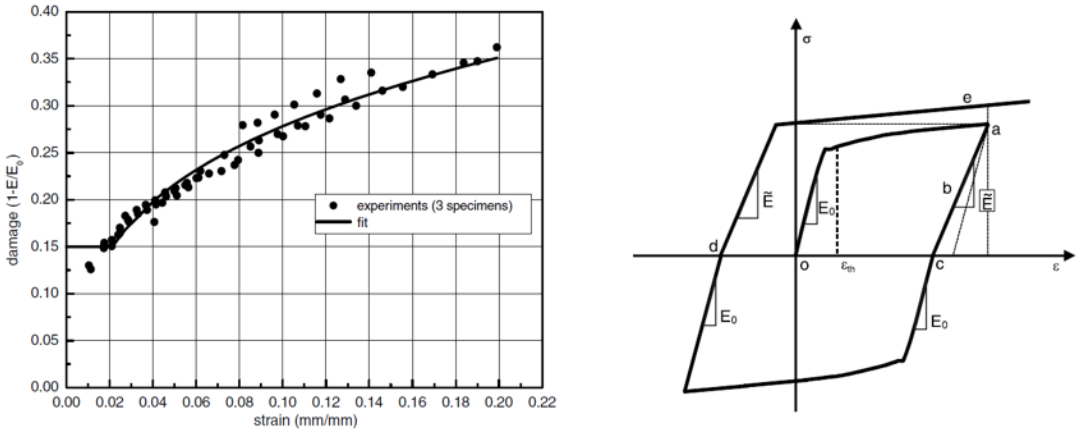

Figure 16: R:Tangent stiffness reduction in tensile loading.
L: Evolution of damage as a function of plastic strain (Pirondi et al., 2006).

Two experiments have been conducted for round notched specimens with different notch radius and different concentration factors. the test was conducted for both tensile and compressive loading and the following results had been found:

- The [**PB**] model is slightly conservative and predict damage evolution more than what was found in experiment as shown in figure 17d.
- The compressive loading causes slight damage which is not accounted for in [**PB**] model.

3.2 LPD model

This method was described in the same paper which [**PB**] model was described in. But the concept is completely different; [**LPD**] model is based on the theory of pressure dependent plasticity. An Important term used here to describe the damage is the void volume fraction (f) which is defined as the ratio of the volume of all cavities in a material element to its total volume (Pirondi et al., 2006).The evolution of f consists of void nucleation ($\dot{f}_{nuec}$)and void growth ($\dot{f}_{growth}$) which are given by the following equations:

$$\dot{f}growth = (1-f){\epsilon_{kk}}^{pl} \tag{43}$$

$$\dot{f}nuec = \frac{f_N}{s_N\sqrt{2\pi}} exp\left[-\frac{1}{2}\left(\frac{{\epsilon_{eq}}^{pl}-\epsilon_N}{s_N}\right)^2\right] \tag{44}$$

Where:
ϵ^{pl}_{kk}: The hydrostatic part of the strain $\epsilon^{pl}_{kk} = \mathrm{I}{:}\epsilon^{pl}$.
f_N: Volume fraction of void nucleating particles.
ϵ_N: The mean plastic strain value at void nucleation.
s_N: Standard deviation.
Where the damage variable f^* is defined as:

$$f^* = \begin{cases} f & \text{for} f < f_c \\ f_c + \kappa(f-f_c) & \text{for} f > f_c \end{cases} \tag{45}$$

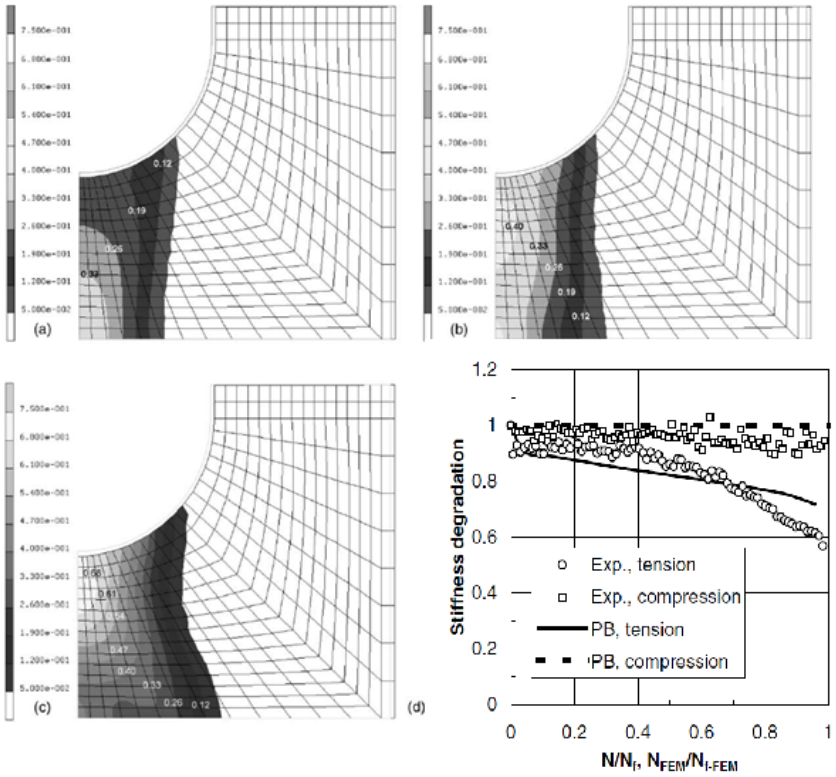

Figure 17: a,b,c: The predicted damage evolution contour (A. Pirondi, 2003).
d: experimental and **PB** predicted stiffness degradation (Pirondi et al., 2006).

where:
f_c: The critical void volume fraction.
κ: Damage acceleration factor.
This model is an extension for [**GNT**] model which accounts only for isotropic hardening while this model accounts for kinematic hardening by replacing the stress tensor by the difference between Caushy stress (σ)and back stress (α) and the yield function is defined by:

$$\phi = (\frac{q}{\sigma_0})^2 + 2q_1 f^* cosh(q_2 \frac{-3q_2 p}{2\sigma_0}) - (1 + q_3 f^{*2})) \tag{46}$$

where:
q: The deviatoric part of the difference between Caushy stress and back stress.
p: The hydrostatic part of the difference between Caushy stress and back stress.
q_1, q_2 and q_3: Material parameters affects the yield behaviour.
σ_0: Quantities result from a re- calculation of the homogenization problem for hardening material.

The backward Euler integration method can be summarized by the following equations[(Aravas, 1987)P(1406)]:

$$\sigma = -p : \mathbf{I} + \frac{2}{3} q \mathbf{n} \tag{47}$$

$$\Delta\epsilon^p = \frac{1}{3}\Delta\epsilon_p \mathbf{I} + \Delta\epsilon_q \mathbf{n} \tag{48}$$

$$\Delta H^1 = \frac{-p\Delta_p + q\Delta_q}{(1-f)\sigma_0} \tag{49}$$

$$\Delta H^2 = (1-f)\Delta\epsilon_p + \boldsymbol{A}\Delta\overline{\epsilon^p} \tag{50}$$

Where:
I: The idenity matrix n: Normal vector.
σ_0, $\boldsymbol{A}$: Are functions of the microscopic plastic strain ϵ^p.

Validation

Void nucleation can set to be zero; which means the growth of the voids is the prevailing damage mechanism. The material parameters f_0, f_c and κ are evaluated using monotonic tensile test.
The cyclic parameters were determined during the first cycles where the material showed strain hardening. In the contrary to the [**PB**] this method does not describe the damage through reduction of stiffness; but through the shrinkage of the yield surface with the increase of void volume fraction.

[**LPD**] model predicts smooth degradation in the stiffness and sudden abrupt reduction in the degradation trend [(Pirondi et al., 2006)p (2167)] as shown in figure [18L]. this model is non conservative contrary to the previous one by comparing figure [18R] with figure [17d].

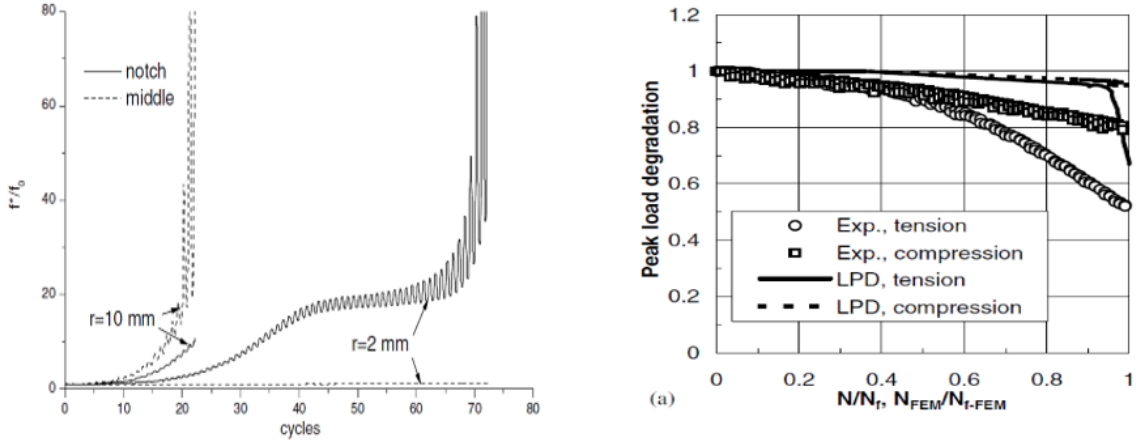

Figure 18: L: Experimental and **LPD** stiffness degradation (Pirondi et al., 2006).
R: Damage evolution predicted in **LPD** model showing the sudden increase in the damage at the end of the void propagation stage (Pirondi et al., 2006).

3.3 CDM for heat affected zone under LCF*

A new CDM model capable of describing damage evolution in the heat affected zone (HAZ) in welded joint which has a lower fatigue life than the base metal due to the weld defects (e.g undercuts). This damage accumulation model was purposed by Wang in (Wang and Lou, 1990). The damage model is given by:

$$D = D_c - (D_c - D_0)(1 - \frac{N}{N_f})^{1-\alpha} \tag{51}$$

Where:
D_c, D_0: The critical and initial damage values respectively.
α: A damage coefficient.

Validation

The coefficients D_c, D_0, N_f and α are determined by fitting and optimization of experimental data (by cyclic strain controlled test on smooth cylindrical fatigue specimen of low alloy steel) measuring the damage by alternating current potential damage measuring (ACPDM) method. Where the damage is identified experimentally as the drop of the potential:

$$D = 1 - \frac{V}{\overline{V}} \tag{52}$$

Where V and $\overline{V}$ the potential difference of the virgin and damaged materials respectively. The model shows a good agreement with the results as shown in figure 19. Notice how the damage evolve slowly at early stage and faster afterwhile.

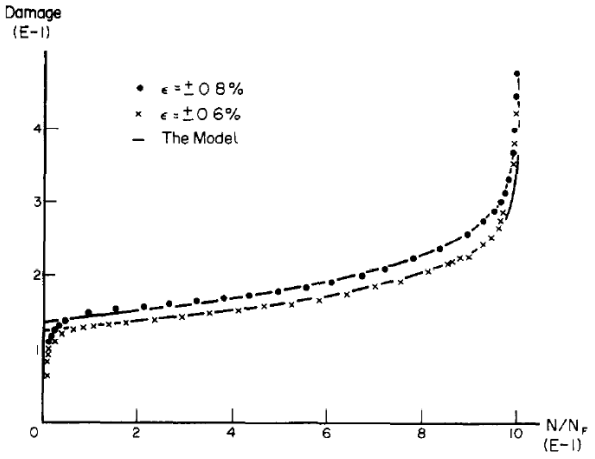

Figure 19: comparison of the Damage evolution with cycles by the proposed model and experimentally (Wang and Lou, 1990).

3.4 Ductility exhaustion model

During cyclic loading, the material absorbs energy and causes ductility degradation. Total energy required to cause fatigue fracture is then indicated by the area under this monotonic curve. This principle is given in details in(Cheng and Plumtree, 1998).
The damage accumulation model is very similar to the one proposed by Chaboche but critical value of damage is introduced to control the damage below one as the case for many engineering applications.

$$D = D_c \left(1 - 1 - \left[\frac{N}{N_f} \left(\frac{1}{1-\psi} \right) \right]^{\left[\frac{1}{1+\beta} \right]} \right) \tag{53}$$

The variable ψ in this model is defined differently than α in Chaboche model; here it represents the ductility while in Chaboche α is a function of the maximum, mean stresses and fatigue limits.

Validation

A fully reversed fatigue experiment was conducted on 16MnR steel as shown in figure 20 Alternating cyclic loading was applied for a given number of cycles and then monotonic tension was applied to fracture point; this is to allow the residual ductility to be measured (Cheng and Plumtree, 1998). The variable ψ, β and D_c are evaluated experimentally

3.5 Fatemi–Socie model [FS]*

This model is based on critical plane approach as defined in figure 14; so its based on the same principle of [**SO**] model discussed before. However, in this model the plastic part of Coffin Masnon equation is included. Also the counting variable this time is the shear stress amplitude [(Aid et al.,

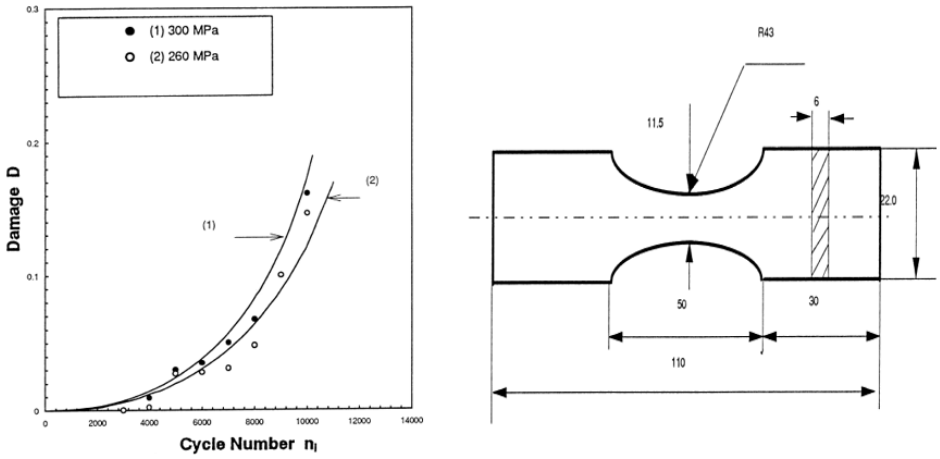

Figure 20: R:The tested notched specimen.
L:The damage evolution with cycles (Cheng and Plumtree, 1998).

2012)p(22)]. The damage variable for each loading cycle is defined as:

$$D = \gamma(1 + k\frac{\sigma_{n,max}}{\sigma_y}) \tag{54}$$

And the fatigue life can be evaluated using Coffin Manson equation on the shear stress:

$$D = \frac{\tau_f{}'}{G}(2N_f)^b + \gamma(2N_f)^c \tag{55}$$

G,c, τ_f and can be found in table 14.1 in (Dowling, 2012) with modification or from fitting data for torsional bending fatigue test. while (k) from simple static torsion test [(Aid et al., 2012)p (22)]. A conservative numerical value for k is equal to 1; and this value increases with increasing number of cycles as follow [(Schubnell et al., 2018)p (112-113)]:

$$k = (0.0003 \times HB^2 + 0.0585 \times HB)(2N)^{0.09} \tag{56}$$

Where HB is Brinell hardness.

3.6 Bannantine and Socie model [Ba]*

This model suggests using Smith Watson Topper (SWT) mean stress correction for LCF as a damage variable which is given by:.

$$D = \sigma_{n,max}\epsilon_{n,a} = \frac{(\sigma_f{}')^2}{E}(2N_f)^{2b} + \sigma_f{}'\epsilon_f{}'(2N_f)^{c+b} \tag{57}$$

So for each load cycle the normal strain amplitude is extracted as counting variable by rainflow counting.

3.7 Wang and Brown's model [WB]*

This model assumes the fatigue life is controlled by the maximum shear strain (similarly to the [**FS**]) model; so the accounting variables that should be extracted from rainflow counting approach are γ_x and γ_y.This method defines the equivalent strain as a combination of the shear strain and normal strain [(Aid et al., 2012)p (22)].

$$\gamma_a + S\Delta\epsilon_n = (1 + \nu_e + S(1 - \nu_e))\frac{\sigma_f{}' - 2\sigma_{n,max}}{E}(2N_f)^b + (1 + \nu_p + S(1 - \nu_p))\epsilon_f{}'(2N_f)^c \tag{58}$$

Where:
ν_e,ν_p: Elastic and plastic Poisson's ratios (0.3 and 0.5 respectively for steel).

S:A material parameter identified by fitting tension against torsion fatigue data.
γ_a: The shear strain amplitude.
$\Delta\epsilon_n$: Normal stress range.
Notice that the last four methods are applicable for constant strain amplitude since they are built on Coffin Manson equation. So in order to apply these methods for variable amplitude loading, they must be divided into blocks and Miner's rule (or similar) is used for accumulating their fatigue damage.

The Coffin Masnon equation constants for axial strain and shear strain can be translated to each other as follow (Schubnell et al., 2018):

$$\sigma'_f = \sqrt{3}\tau'_f \qquad \gamma'_f = \sqrt{3}\epsilon'_f \qquad b \approx b_{\gamma_f} \qquad c \approx c_{\gamma_f} \tag{59}$$

For many steels b ≈ -0.09 and c ≈ -0.06. σ'_f and ϵ'_f could be also evaluated in terms of Brinell hardness (BH) as follow (Schubnell et al., 2018):

$$\sigma'_f = 4.25BH + 225 \qquad \epsilon'_f = \frac{0.32BH^2 - 487HB + 191000}{E} \tag{60}$$

Validation

[**SO**], [**FS**], [**Ba**] and [**WB**] models were tested to see how much their results match the experiments; so three experiment were conducted to construct three S-N curves as shown in figure 22.

- $\tau_{-1}(N)$ Fully reversed torsion test (R=-1).
- $\sigma_{-1}(N)$ Fully reversed tension test (R = -1).
- Pulsating tension test (R = 0).

The tests were conducted on low-carbon steel cruciform specimen shown in figure 21.

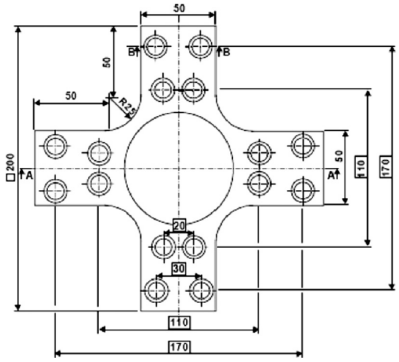

Figure 21: Cruciform specimen descriptions.

[**WB**] model show always non conservative results while [**SO**] model for HCF is very Conservative and could lead to over-sizing if it's used for design. [**Ba**] and [**FS**] are the closest to reality; notice how close are they to 45°line in the experimental/models comparison figure 22.

3.8 Ductile damage model in Abaqus*

As it's described in Abaqus user manual ductile damage initiation criterion is a model for predicting the onset of damage due to nucleation, growth, and coalescence of voids in ductile metals. The model assumes that the equivalent plastic strain at the onset of damage is a function of stress triaxiality η and strain rate ϵ_p (Hibbitt et al., 2001). In this method a variable Δw is defined as state variable and it increases monotonically with the increase of plastic deformation and it's calculated by equation:

$$\Delta w = \frac{\Delta\epsilon_p}{\epsilon_D^{Pl}(\eta, \dot{\epsilon_p})} \tag{61}$$

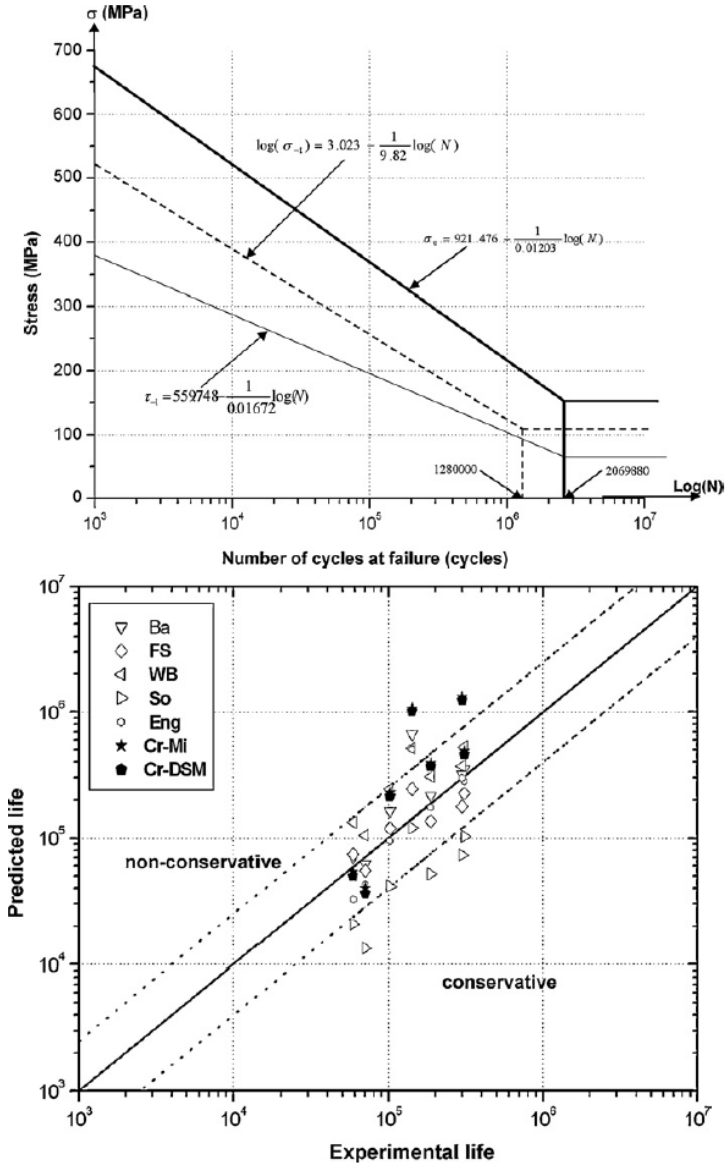

Figure 22: U:The obtained S-N curves. L:Models experiment's comparison (Aid et al., 2012).

3.9 Damage coupled with plasticity*

Constitutive modeling can be very beneficial to define the damage when it's coupled with plasticity, this works in parallel with effective stress concept. One of the facilitates of this model is the capability to describe both isotropic, kinematic hardening or mixed hardening; the following procedure is mentioned in (Runesson et al., 2006).

- for a given stress state $(\epsilon_n, \sigma_n, \kappa_n, \alpha_n, d_n)$ the trial stress for the next time step is calculated as

$$\epsilon_{n+1} = \epsilon_n + \Delta\epsilon \qquad \sigma_{tr} = \sigma_n + E \times \Delta\epsilon \tag{62}$$

- Check the elastic/plastic status of the updated solution by evaluating the yield function ϕ where ϕ is calculated as:

$$\phi = \sigma - \alpha - \kappa - \sigma_y \tag{63}$$

If $\phi \leq 0$ then the trial value of stresses is true and should be considered for the next time step. Otherwise,then the load is plastic loading which requires defining the plastic modulus(h):

$$\hat{\sigma} = c_1\hat{\sigma_{tr}} + (1 - c_1)\alpha_n \qquad \kappa = \kappa_n + rH\mu \qquad \alpha = c_2\hat{\sigma_{tr}} + (1 - c_2)\alpha_n \tag{64}$$

Where:

$$c_1 = 1 - \frac{E\mu}{(\sigma_{tr} - \alpha_n)(1-d)} \qquad c_2 = \alpha_n \frac{(1-r)H\mu}{\sigma_{tr} - \alpha_n} \tag{65}$$

r: Parameter to control the relation between isotropic and kinematic hardening where it's equal to zero in case of pure kinematic hardening and equal to one in case of pure isotropic hardening.
d: The damage variable.
μ: The plastic multiplier.

- The damage then can be evaluated using a nonlinear solver or simpler procedure is to exploit that the damage is limited between zero and one then keep squeezing this until the convergence is reached to solve the following equation:

$$y(d) = d - d_n - \mu \frac{\hat{\sigma}}{2ES(1-d)^m} \qquad S = \frac{1}{2} m s \sigma_y \epsilon_y^2 \tag{66}$$

Where:
m: The damage exponent which governs the rate of damage development.
s: The ductility measure which is in the range of 100-200 for ductile damage and 1-2 for brittle damage.(Runesson et al., 2006).

This requires small time step. Otherwise **d** can't be found between the maximum and minimum values as shown in figure 23. The details for this squeezing technique are given in [(Runesson et al., 2006)P (154)].

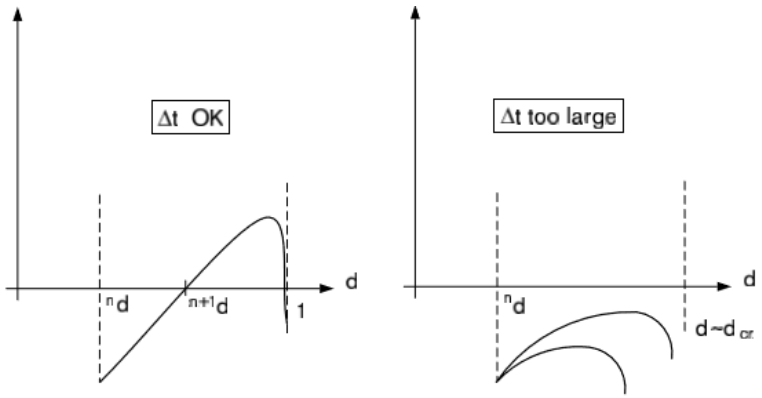

Figure 23: The illustration for squeezing technique for damage evaluation (Runesson et al., 2006).

This method can be used to assess the low cycle fatigue damage when the plasticity is very pronounced. One of the drawbacks of this model is the correlation between damage and plasticity; which means that elastic loading doesn't induce any damage which doesn't match with the results.

4 METHODS

This study will be limited in implementing different methods described in the previous chapters. No experimental work will be conducted here, despite of the need for test results for the sake of comparison of the studied damage models. But since this work won't be conducted, numerical and analytical studies of the fatigue life will be compared. So any description appears in the results section would be flawed or limited and misses the comparison to the test results.

Many damage accumulation techniques will be studied analytically without need for any numerical approximation since their expressions are very straight forward. So only the stress field is needed to be evaluated numerically and Matlab would be used for their implementation. Numerical solution would be also necessary to introduce the damage into the stiffness matrix, that would be difficult trick to do in Abaqus. The finite element routine would be built using Calfem toolbox with the help of mesh reader (D.Floros, 2018). That enables the user to conduct elastic and elastoplastic analyses with the ability to adjust the matrices which would be important for many methods (e.g Miao model).

The use of numerical methods for solving nonlinear equations would also appear in implementing the critical plane methods, for example Newton Raphson method is used for Fatemi Socie model and this will be shown in details in the following chapters. Besides, Iterative process is required to implement the squeezing technique which is less accurate and easier than Newton method. This method was described in the last chapter when isotropic kinematic hardening model was discussed.

All the finite element analyses are linear; except the ductile damage model in Abaqus. This is because the post failure behaviour is not interesting for crack initiation phase. However in the ductile damage model linear analysis would creates numerical problem. Both elastic and elasto-plastic analyses will be used to cover the damage models and to study miscellaneous topics like overloads and underload effects, residual stresses and notch effects.

FE-Safe software is an extension for Abaqus and allows for conducting fatigue analyses with the use of strain life equation and Neuber's rule. In addition it enables for defining mean stress correction algorithms and different roughness coefficient. One more useful application connected to Abaqus is Abaqus welding interface (AWI) which provides an easy way to simulate welding process and the residual stresses obtained from it.
The following diagram explains the used methods for the studied fatigue damage model:

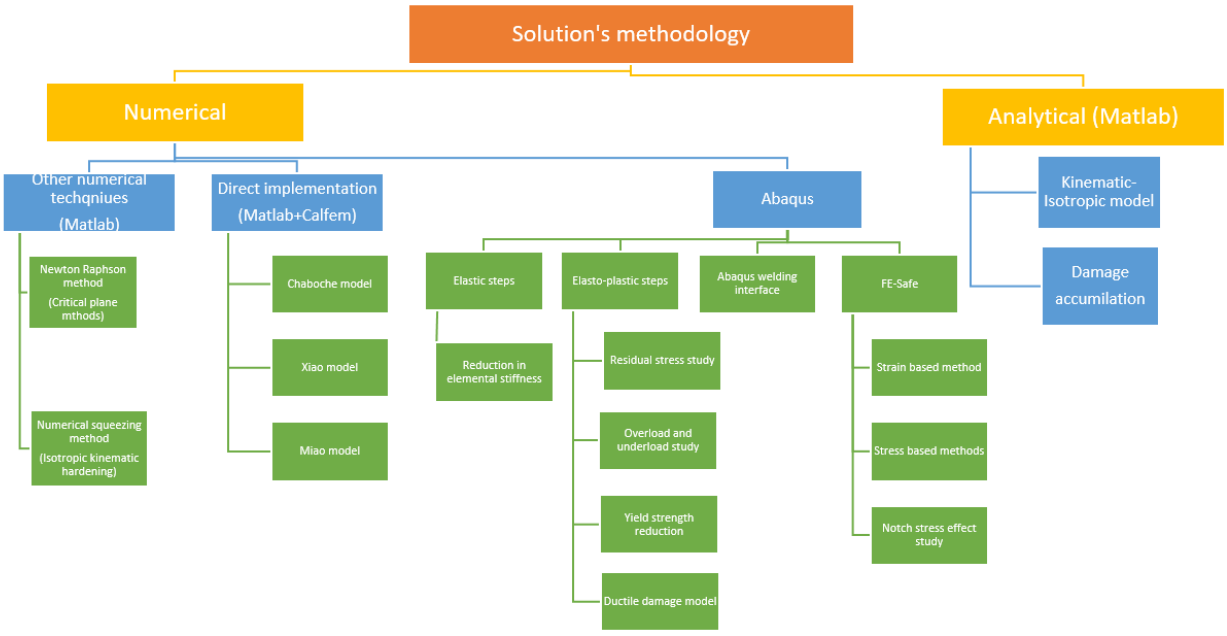

Figure 24: The used methods to identify the fatigue damage.

5 RESULTS

In this chapter different methods will be used to quantify the fatigue damage. Some of them were introduced in chapter 2 while some of them were implemented in FE-Safe program; they will be mentioned briefly in this chapter. For more details regarding FE-Safe fatigue models the readers are referred to (Corp, 2017) which is the user manual for the mentioned software.

In order to conduct the comparitve study, the specimen should be unified for all of them. This applies for the material parameters, boundary conditions and applied loading. The material used is given in table 2 and the specimens and boundary conditions are shown in figure 25; notice that this is a tensile specimen and the symmetry is considered in both directions. The loading applied is alternating loading of 105 MPa applied on the right edge of the specimen. In order to control the mesh around the notched area the specimen is cut there so the mesh size is minimized there.

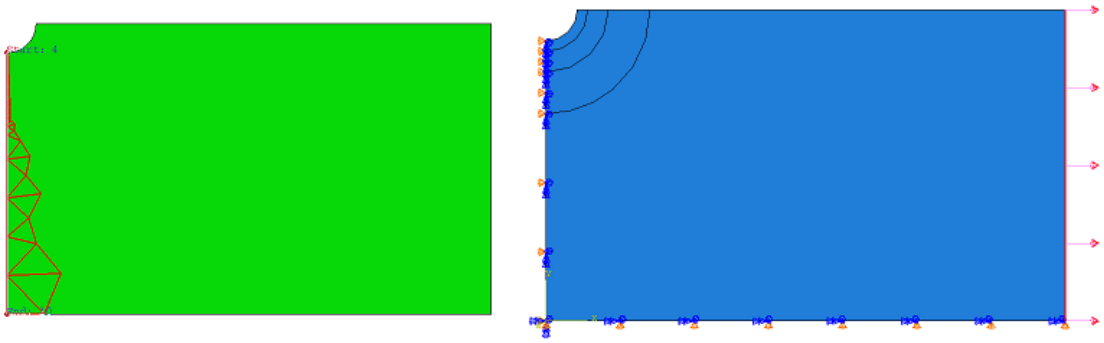

Figure 25: L :The studied path for comparing stress based methods.
R :The studied geometry, boundary conditions and applied loading

Another welded specimen will be used for the sake of residual stress simulation using Abaqus welding interface, it will be also used in studying the FE-Safe welding toolbox. The studied geometry is a full penetration butt weld shown in 26. And the thermal material properties used are given in the appendices.

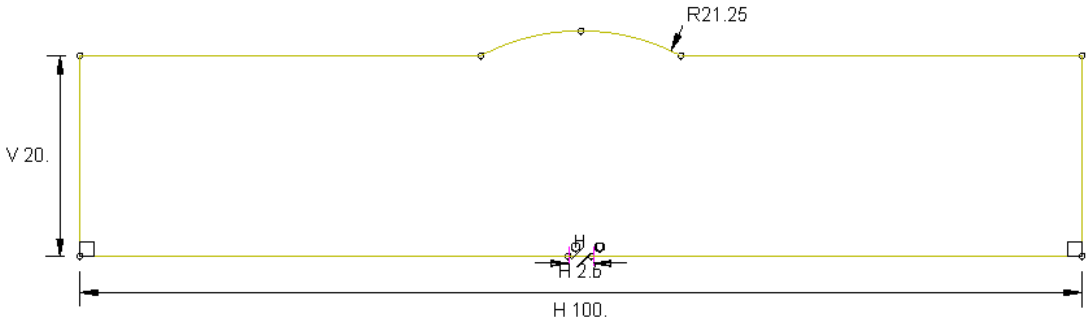

Figure 26: The partial penetration butt weld used in AWI analysis.

5.1 FE-Safe damage models

FE-Safe is specialist software for fatigue assessment, different algorithms are defined for calculating the fatigue life; many of them are based on strain life (Coffin Manson) equation. What is uniquely special about this software is the ability to import the stress and strain datasets from the finite element processor and to conduct the fatigue analysis and export the results (damage, the fatigue life and other field outputs) to the same FE-software.

The propriety	The value	The unit
The elastic modulus	210	GPa
The Hardening modulus	2100	MPa
Poisson's ratio	0.3	-
The Yield strength	355	MPa
The ultimate strength	400	MPa
The fatiuge limit	40	MPa
The length	50	mm
The width	30	mm
The notch radius	3	mm
b	-0.138	-
c	-0.513	-
ϵ'_f	0.439	-
σ'_f	1020	MPa

Table 2: The geometric and material proprieties of the studied specimen

Elastic and elastoplastic analyses

The analyses done by FE-Safe can be classified to two different categories, Elastic and elastic plastic analyses. The former imports the elastic dataset only; so it is capable of performing stress based (high cycle fatigue) analysis. There are two possibilities to do that either by importing all stress datasets from finite element analyzer for all cycles or by importing only the first cycle and define the amplitude in FE safe solver. The later (elastoplastic analysis) import the stresses and strains from FE analysis, and the amplitude should not be defined in FE -safe; this can be replaced by elastic analysis with Neuber's rule. However, the results are not satisfactory as shown in figure 28 which shows a compassion between elastic and ealstoplastic analyses results.

5.1.1 Elastic block models

Different algorithms are defined to calculate the fatigue life and the damage (by Miner rule), these methods are given in table 3; these methods were studied for the following geometry in figure 25. and the material proprieties used are shown in table 2.

These methods were studied with elastic dataset applying Neuber's rule for plasticity correction; the damage was extracted on the red path shown in 25 for these methods; the damage dispersion is shown in figure 27R. Brown Miller algorithm was found to be the most accurate one for ductile materials while normal, uniaxial stress and Von mises models show bad estimation and deviate from the true solution (Corp, 2017); these methods are only applicable in elastic block analysis.

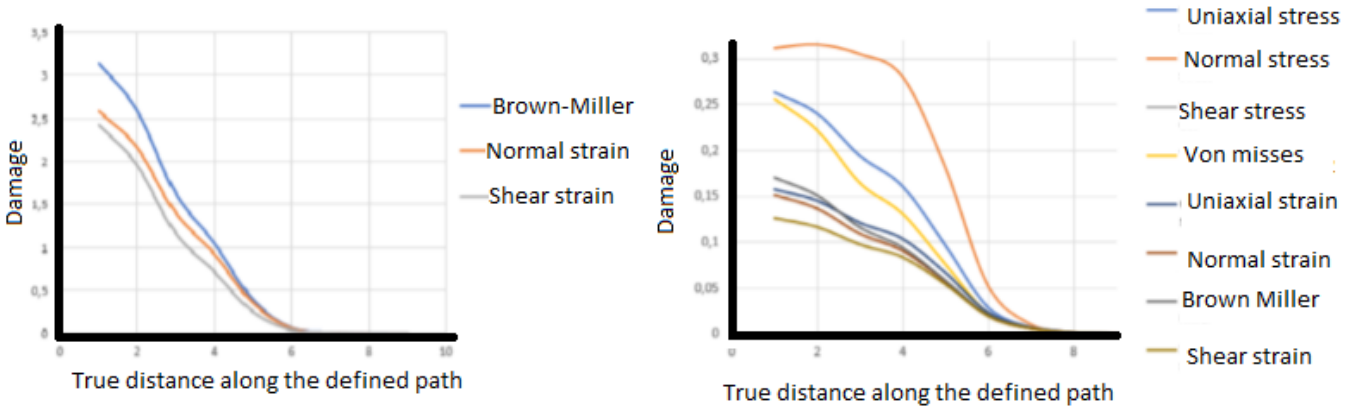

Figure 27: L: Damage on the red path given in figure 25 by stress-strain blocks algorithms.
R: Damage on the red path given in figure 25 by stress blocks algorithms.

5.1.2 Elastic plastic block

There are only three algorithms in FE-Safe can take elastic plastic block and they are Brown Miller, shear strain and normal strain. These methods were compared for the same geometry described before in 25L and the comparison is shown in figure 27L. Notice that the strain life analysis (which is conducted on the imported stress strain blocks) is more determintal and damaging than elastic blocks even with Neuber's plasticity correction; that's also confirmed by the analysis given by (Kariyawasam and Mallikarachchi, 2015). The elastic block with Neuber's correction shows good agreement with the plastic block in case of elastic loading (loading doesn't exceed the yield limit) as shown in figure 28. On the other hand, in case of plastic loading the plastic block shows more damaging values than elastic block even with Neuber's correction; that was expected since the stress and strain concentration factors are equal in elastic loading and the strain values can be easily detected from elasticity theory but they will be deviated from each other in accelerating manner, this will be further explained in section 5.3.

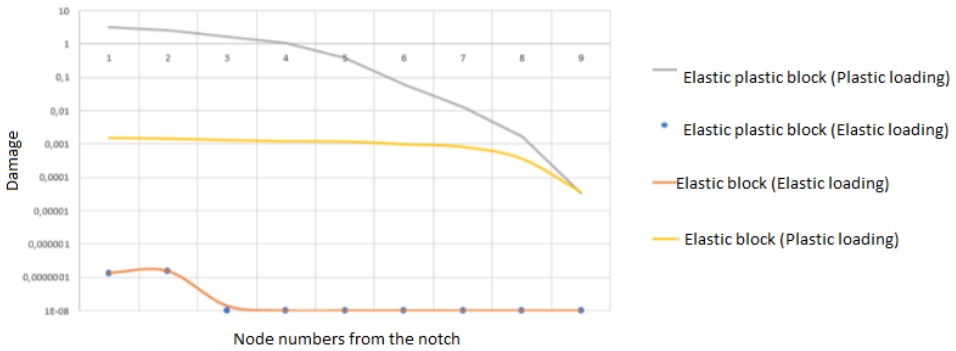

Figure 28: Comparison between stress and strain based fatigue in FE-Safe for
L: Elastic loading R: Plastic loading.

5.1.3 Other features in FE-Safe

FE-safe also provides the used with the ability to conduct simple low cycle fatigue assessment without even the need for finite element simulations if the strain values are obtained from test at specific point by an extensometer; the applied strain cycles are to be given for the software in a table format. Then the material, the desired mean stress correction algorithm and the stress concentration factor is defined (because it's for low cycle fatigue so the stress and strain concentration factors won't be the same). Then the software will run a very quick analysis and gives five outputs:

- The Rainflow counting for the given the strain history; this will be given as three dimensional histogram with mean and stress range in the X and Y plane and the frequencies of each cycle in the Z axis.
- Damage range mean histogram, which is simmilar to the previous item but with the damage on Z axis instead of cycles frequency. Both of these results are shown in figure 29.
- The largest stress strain hysteresis loop which is shown in figure 30.
- The signal input file with time. Which is actually an input but it's considered as an output
- Time correlated damage file; this one is simmilar to the previous item but damage value on the Y axis. Both of these items are shown in figure 31.

All of the generated files are done for a strain history which is displayed in figure 31U. and the studied material proprieties are shown in table 2.

It worths mentioning that all the analyses conducted before were done with no mean stress correction and smooth surface finishing conditions, both of these factors can be changed by selecting a mean stress correction techniques and changing the surface finishing conditions respectively.
This methodology is straight forward and suitable for expecting the low cycle fatigue damage for

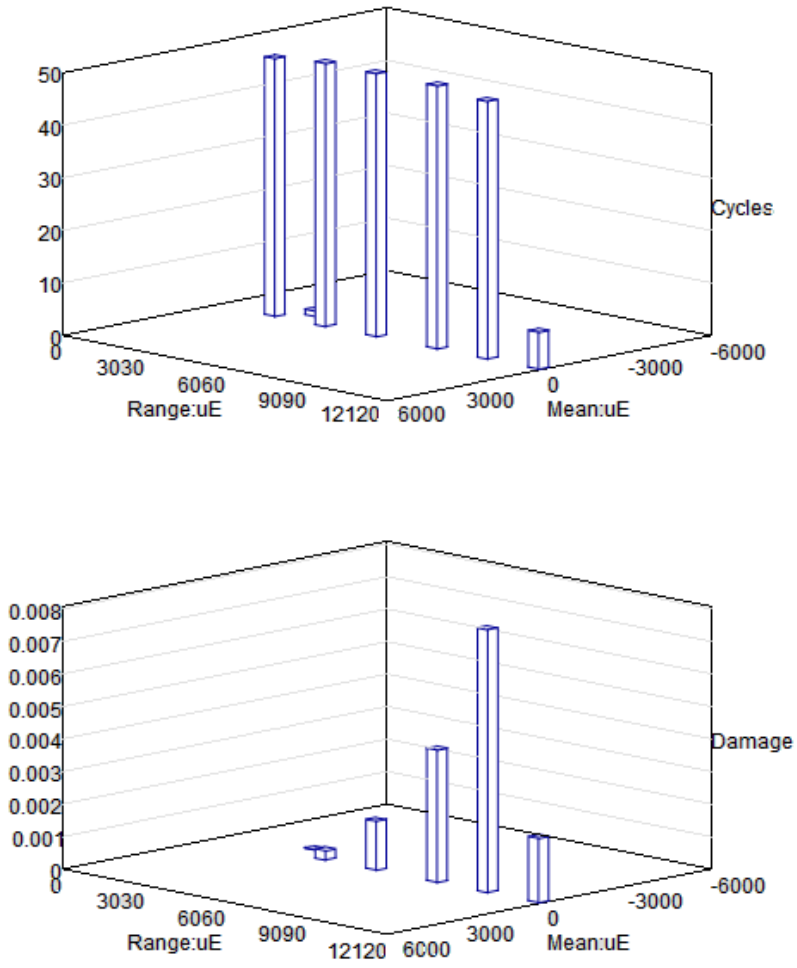

Figure 29: U: Rainflow cycles histogram. L: The damage histogram.

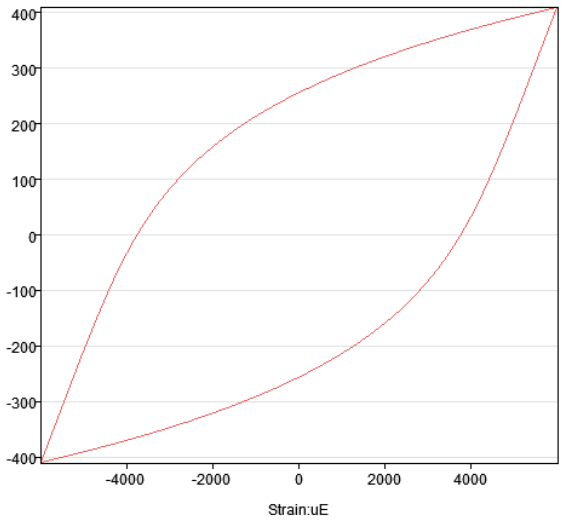

Figure 30: Stress strain hysteresis biggest loop

by measuring only the strain. However, this is limited for only one node so the damage contour can't be plotted or the damage pattern can't be extracted.

The conducted work was for a uniaxial loading; However FE-Safe is also capable of conducting gauge fatigue analysis on multiaxial loading, but this requires a definition of strains in three

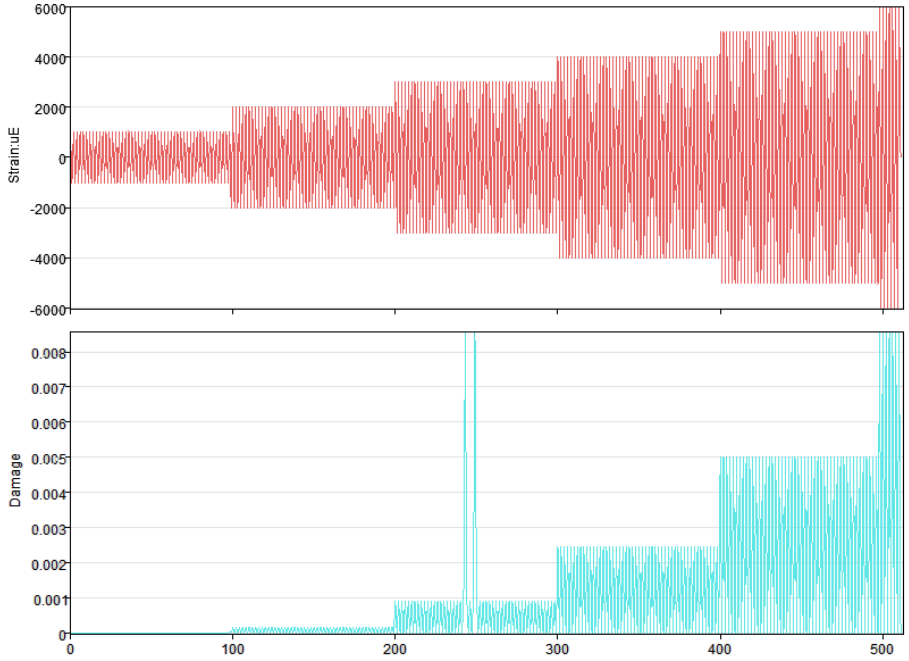

Figure 31: U:The applied strain history (in μ m/m) . L: The time correlated damage.

directions and they are necessarily perpendicular to each others (they can be oblique). One additional feature of FE-Safe is the ability to quickly calculate the fatigue life for a constant amplitude strain by defining only the maximum and minimum. Then the software uses the strains to calculate the fatigue life with or without mean stress correction (Only SWT algorithm is available in this option) .However, this won't have any effect since the loading applied in figure 31U is alternating loading (R=0). This quick analysis is doable for both steel specimens and welded joints, the only difference will be that in welding joints its possible to input either stress or strain. Besides, the welding type and the design criteria are additional inputs to be defined.

FE-Safe provides the ability to conduct high cycle fatigue life evaluation for welded details. This is because different S-N curves for different welded details are defined as shown in figure 32U. This is similar to the S-N curves defined in the Euro-code and and FAT curves in international institute of welding. This is tested for the butt weld shown in figure 26 with the same material parameters defined before for thermo-mechanical analysis. The selected design criteria is **0** as shown in figure 32L and the design curve is **W** and subjected to repeated to alternating constant amplitude loading of 105 MPa (R=-1), the results are presented in 33; the results fulfills the expectations since the damage initiates from the weld toe and the fatigue life for the critical section is found to be 125000 cycles. This option is only available for high cycle fatigue problems where no plasticity is induced since the strain life equation's parameters will not be used.

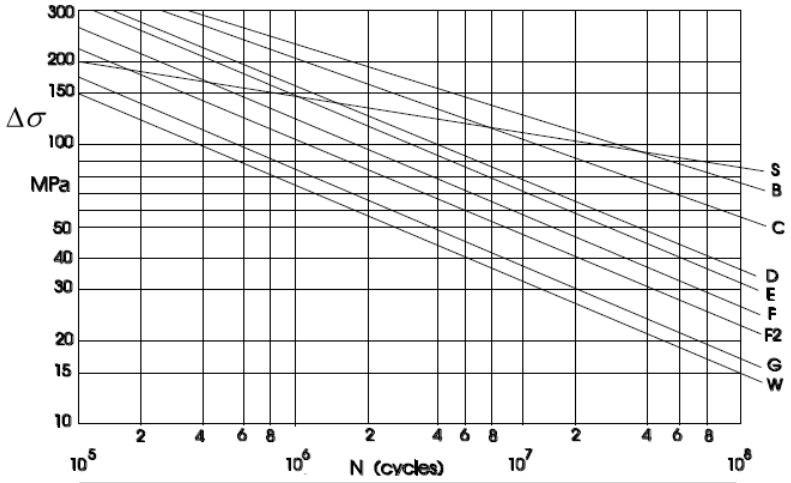

Design criteria	Probability of failure before the calculated life (%)
0	50
-2	2.3
-3	0.14

Figure 32: U: The S-N Curves defined in FE-Safe database.
L: The different design criterion's probabilities of failure before the calculated life (Corp, 2017).

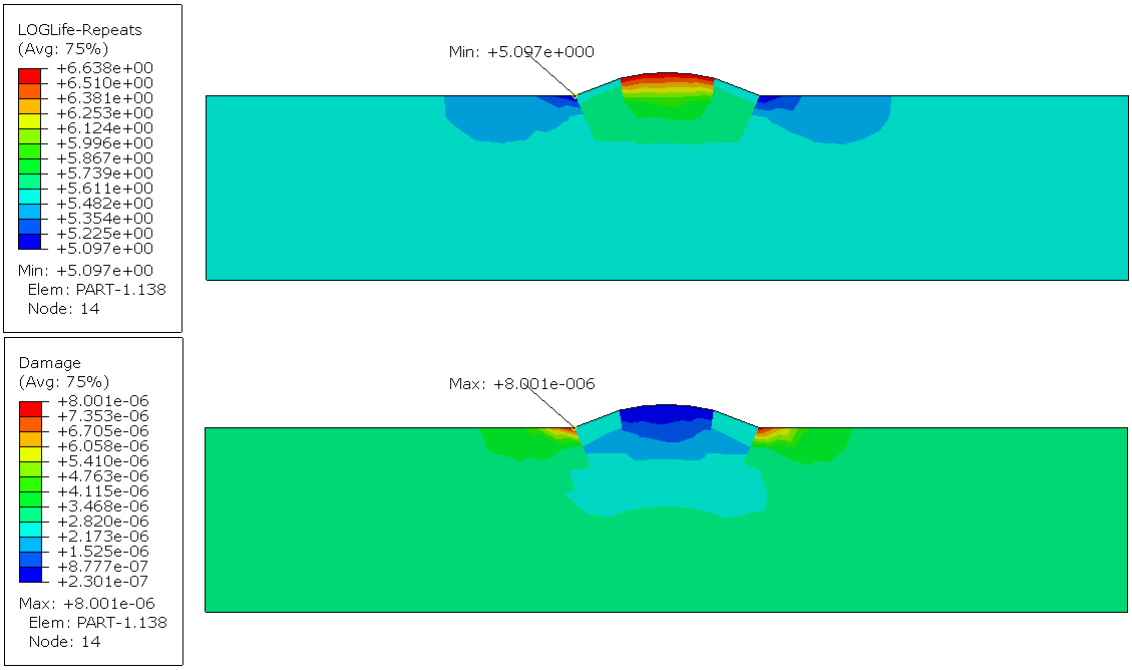

Figure 33: The fatigue life and damage contour found using S-N curve defined in FE-Safe.

5.2 Damage accumulation techniques

In this section different damage methods will be compared and examined for different types of loading. Matlab codes are provided in the appendix to see the mathematical implementation for these methods. Miner, S-N, modified damage, HAZ, Peerlings and Henry methods are to be compared for the following loading configuration as shown in figure 34:

The model	fatigue life equation
Uniaxial strain life	$\Delta\epsilon/2 = \frac{\sigma'_f}{E}(2N_f)^b + \epsilon'_f(2N_f)^c$
Uniaxial stress life	$\Delta\sigma/2 = \sigma'_f(2N_f)^b$
Normal stress life	$\Delta\sigma_1/2 = \frac{\sigma'_f}{E}(2N_f)^b$
Normal strain life	$\Delta\epsilon_1/2 = \frac{\sigma'_f}{E}(2N_f)^b + \epsilon'_f(2N_f)^c$
Brown Miller	$\Delta\epsilon_n/2 + \Delta\gamma_{max}/2+ = 1.65\frac{\sigma'_f}{E}(2N_f)^b + 1.75\epsilon'_f(2N_f)^c$
Maximum shear strain	$\Delta\gamma_{max}/2 = 1.3\frac{\sigma'_f}{E}(2N_f)^b + 1.5\epsilon'_f(2N_f)^c$
Von Mises	$\Delta\epsilon_{eff}/2 = \frac{\sigma'_f}{E}(2N_f)^b + \epsilon'_f(2N_f)^c$

Table 3: The elastic algorithms defined in FE safe.

- High load followed by low load cylces.
- low load followed by High load cylces.
- Constant amplitude loading (equivalent loading).

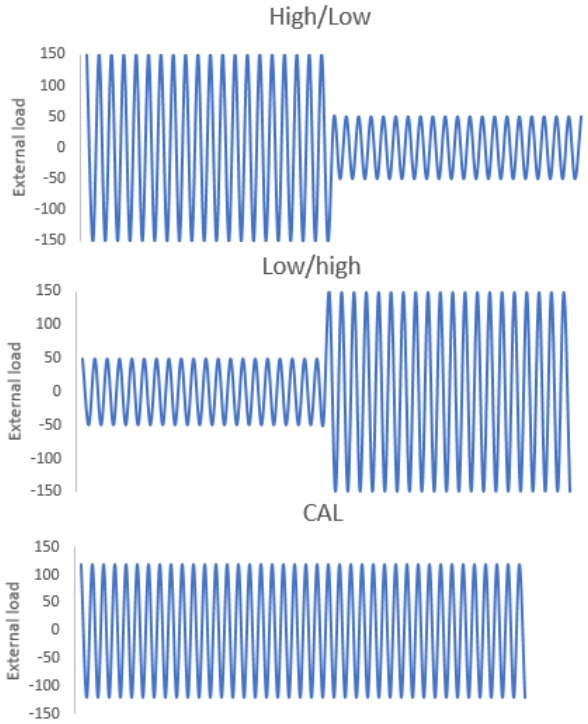

Figure 34: The applied loading for stress based method analyses.

The damage is calculated for each block and then the damage accumulation method will be used to evaluate the damage; that means separate finite element analyses are performed for the high loading (150 MPa), for the low loading (50 MPa) and for the equivalent constant amplitude loading (120 MPa) which is uniquely special for S-N curve's slope of 3. The stress values will be used to evaluate the damage. The results are shown for different methods in figures 35 and 36.

The geometry used for these analyses is shown in figure 25. The geometry was partitioned at the notch area to control the mesh size to capture the steep variation of the filed outputs (stresses and strains) at the critical area; that an easy technique to capture the localization of stresses

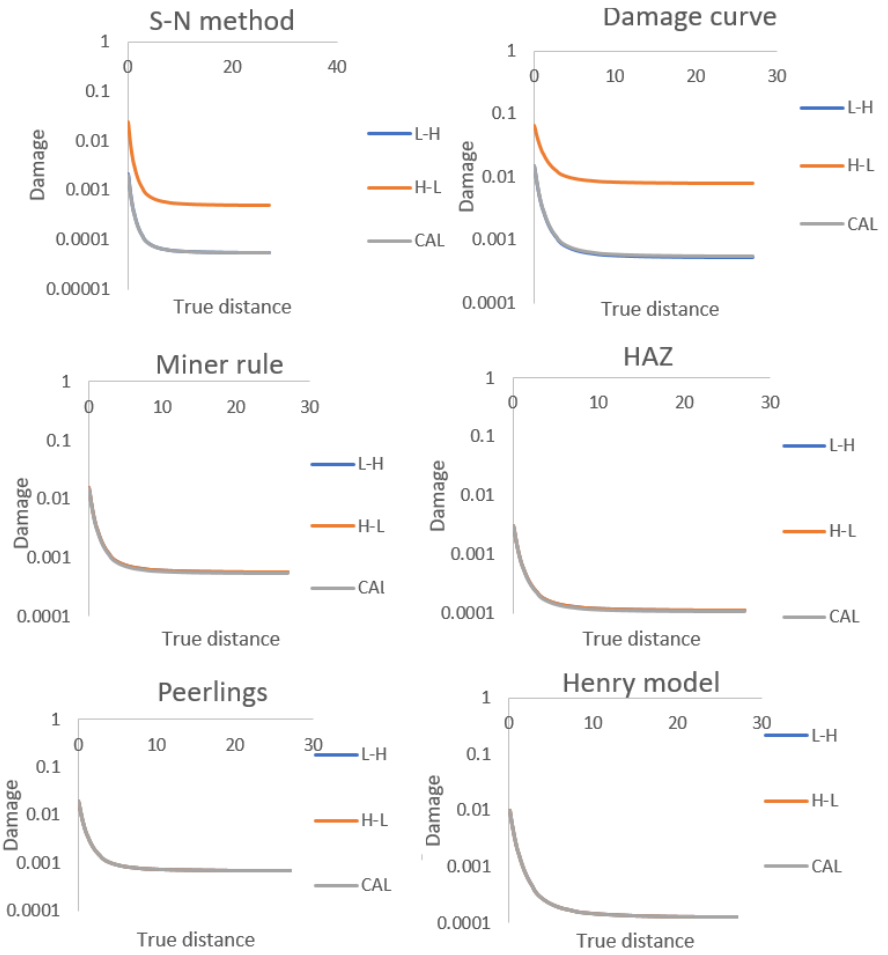

Figure 35: Damage distribution in the studied path shown in figure 25.

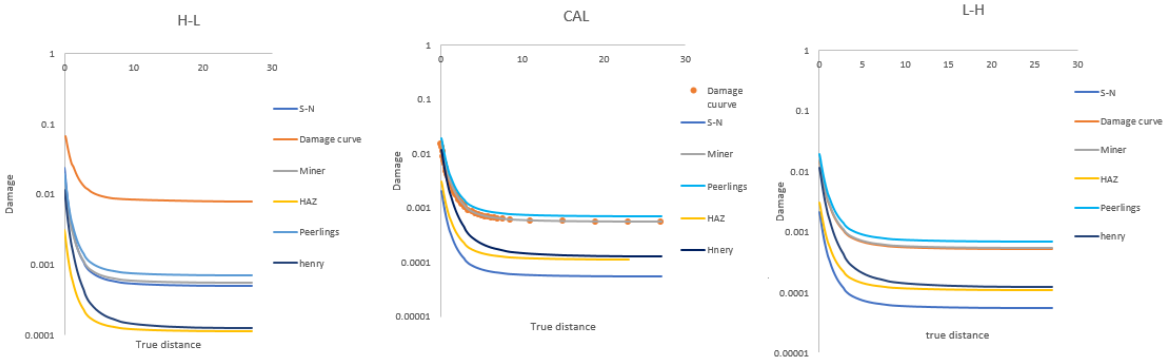

Figure 36: Comparison between different accumulation techniques.

around the notch. The left edge of the specimen will be used for predicting the damage. The material and geometric proprieties are shown in table 2.

Since the applied loading is uniaxial, it's wise to use σ_x to estimate the endurance (from the S-N curve defined by the material proprieties σ_f and σ_u). The S-N curve is defined according to the procedure given in [(Dowling, 2012) chapter (10.7)]. If the Mises stress is used instead of σ_x, the damage distribution will differ if residual stress is introduced since the Mises stress is in maximum value at notch tip while σ_x will not have the maximum value at the same node; this is shown in figure 37. This concept will be explained in details in section 5.3.

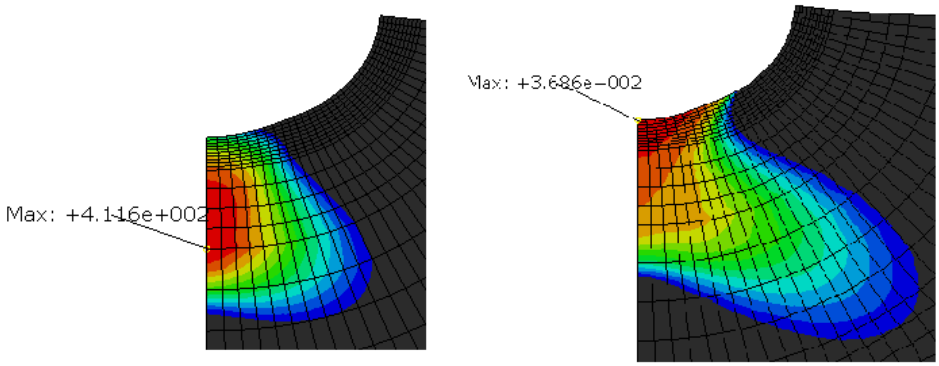

Figure 37: The difference between the stresses mises and stress in x directin distributions
L: σ_x R: σ_{mises}

Miner, Peerlings, Henry and HAZ models do not consider the load sequence effect which makes all the curves for these models identical in figure 35. That does not agree with the test results (Carlson et al., 1991); since the early overloading shows higher damage than equivalent constant amplitude loading. On contrary S-N and modified damage curve approaches consider the load sequence effect which makes the early overloading more damaging than late overloading as shown in figure 35.

In the case of induced plastic deformation there will always be history effects. The presumption in linear accumulation is that these deformations are small and can be discarded if the load is fairly regular; this should be reasonable since it will be close to shakedown (elastic or plastic) at the point of damage initiation.

The comparison between the studied methods is shown in figure 36. Damage curve approach is overestimating the early overloading effect when compared with the rest of the methods; while S-N method underestimates the damage ; Both of these methods don't require any material parameters except the S-N curve while Peerlings and HAZ methods requires some parameters which makes the damage estimation require further tests to quantify these parameters.

As mentioned earlier, Peerlings model includes the damage acceleration effect by introducing the parameter α as shown in figure 12. HAZ model requires the D_c, D_0 and α. D_c and D_0 were set to be 1 and 0 respectively. α effect in both of these models were studied in figure 38. Notice that these parameters are so decisive and influential so these methods are not recommended to be used before the evaluation of α.

The damage accumulation per cycle (instead of per block) could be more interesting if elatoplastic material model is assumed; since the history of the plastic deformation has an effect. However, if elatoplastic material model is used the damage will be underestimated since the stresses will be less than the elastic stresses as shown in figure 39.

The material model used for these analyses is liner elastic, when compared to elastoplastic material model (which represents the true behaviour of material) the elastic material behaviour results in higher damage; that is explained by the lower endurance due to higher stresses exceeding the yield limit; this concept is shown in figure 39. However the use of S-N curve is uniquely use for stress based fatigue design (Dowling, 2012). And the plastic loading is assessed with the strain life equation which will be used in later sections.

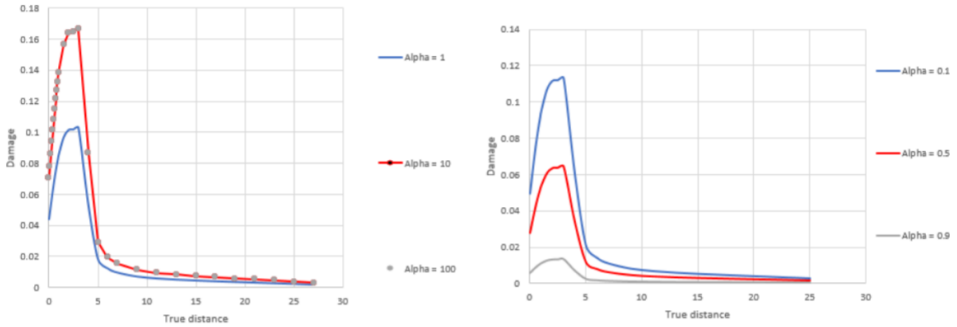

Figure 38: Sensitivity analysis for α factor in peerlings and HAZ methods respectively

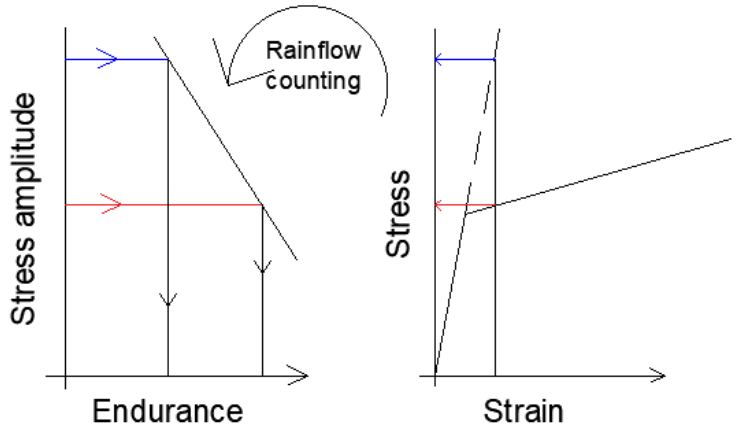

Figure 39: Illustration shows why the elastic analysis is more conservative than real stress analysis

5.3 Notch stress effect

The elastic stress concentration factor may be employed to characterize the severity of the notch as follow:

$$K_\sigma = \frac{\sigma}{S} \qquad K_\epsilon = \frac{\epsilon}{e} \qquad k_t = K_\sigma = K_\epsilon \tag{67}$$

Where **S** and **e** are the nominal stress and strain respectively and σ and ϵ are the notch stress and strain respectively, this concept was introduced in (Dowling, 2012). This concentration effect has the same influence on stresses and strain if the external force does not cause plasticity, once the plasticity is induced the strain concentration increases up to specific value (k_t^2) and the stress concentration decreases down to 1 according to (Dowling, 2012); However these results were not totally confirmed when they were studied as shown in figure 40; notice in the left figure k_ϵ can be as large as 90 which exceeds k_t^2=14. In addition the stress concentration k_σ starts to decrease when the plasticity is induced but when the load increases k_σ increases again 40R. But the general trend is that k_σ decreases while k_ϵ increases.

Since the strain concentration would be larger than stress concentration so it would be expected that strain based fatigue will give lower estimation of the endurance and overestimation of the damage. Besides, the damage distribution will be different because the early loading would cause plasticity at the notch end and induce compressive residual stresses but this stresses wouldn't be enough to shift the maximum damage from the notch edge which is highly concentrated because it was evaluated using strain based methods. However in stress based methods the stress concentration under plastic loading is smaller which means the stress distribution when combined with residual stresses will yield maximum tensile stress away from the notch edge, this is shown in figure 43. Neuber rule which states that the geometric mean of the stress and strain concentration

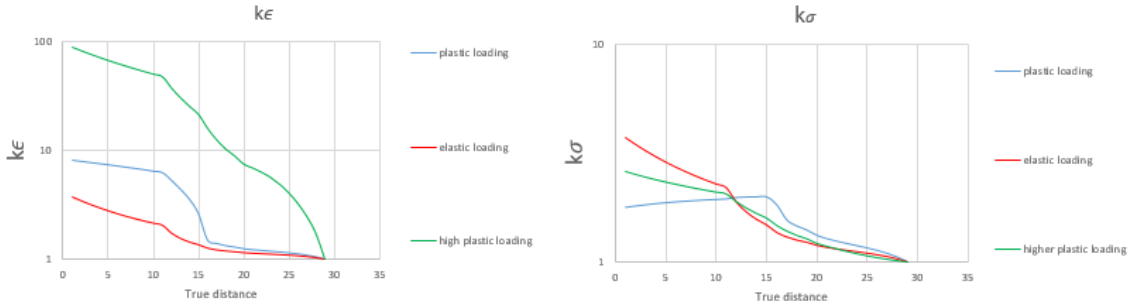

Figure 40: Stress and strain concentration for elastic and plastic loading along the studied path for different loading conditions.

factors remain equal to the elastic concentration factor as follow:

$$\sqrt{k_\sigma \times k_\epsilon} = k_t \tag{68}$$

Though this rule would be applied for stress based algorithms in FE-Safe but this wouldn't be enough because it assumes the maximum strain concentration does not exceed k_t^2 which was shown not to be accurate in figure 40; so for $k_\epsilon = 91$ and $k_\sigma = 2.6$ which yields according to Neuber's rule $k_t = 15.4$. This is four times larger than the the elastic concentration factor which will be used in FE-Safe $k_t = 3.7$.

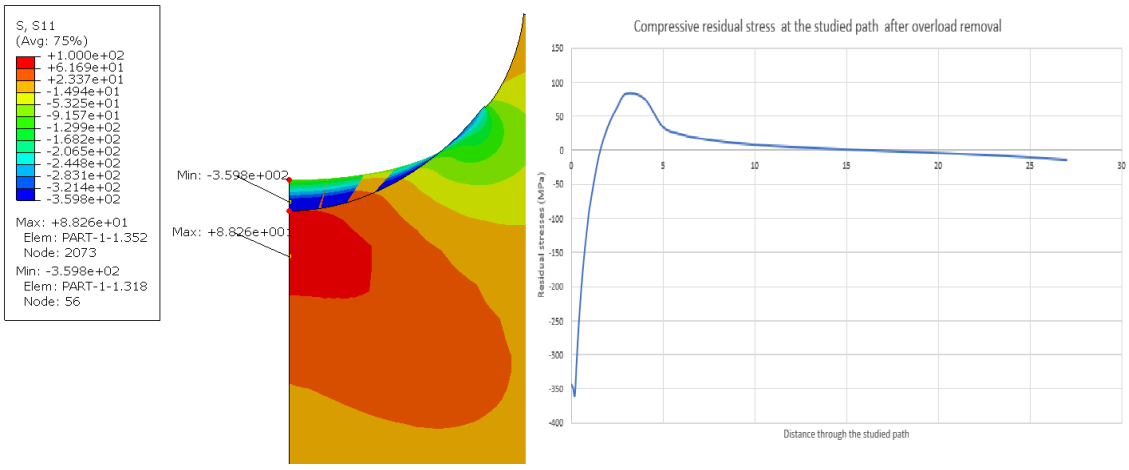

Figure 41: Tensile and compressive residual stresses along the studied path after overload of 250 KN removal

It's noticeable that in the case of absence of plastic matertial model the damage will be maximized at the notch tip which fulfills the expectations since there is no damage retardation due to overloading which causes plastic compressive residual stresses. On contrary, this residual stresses raises in case of initial overloading as shown in figure 41.

This kind of residual stress distribution which is self balancing (the area under the x-axis and over it in figure 41 are equal) when combined with later tensile loading will cause the maximum damage not to be at the notch tip. That makes the damage distribution for overloading to be different than the CAL; that is not to be confused with the figure 35; that figure shows the effect of the overload under elastic material model due to the load sequence effect without any mentioning to the residual stresses; these stresses will will appear only if elastoplastic material model is used. The comparison of different FE-Safe models was discussed earlier in section 5.1 and it is out of the scope of this section which aims to throw a light on the stress and strain concentrations and the validity of Neuber's rule; this rule is found to be approximate and does not hold always. Neuber's rule applies when yielding is limited to a small volume of material at the stress concentration but

it doesn't hold when general plasticity is reached.

The four stress based methods (S-N, Damage curve, Peerlings and HAZ) and Coffin Manson

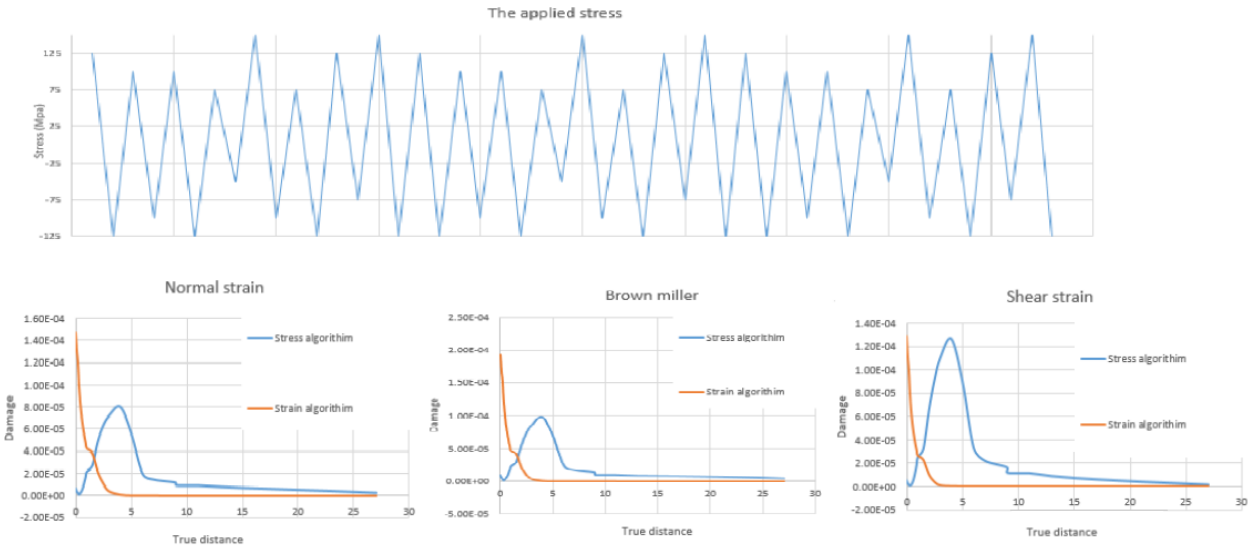

Figure 42: U: The applied loading for the study in section 5.3.
L: Different FE-Safe models considering stress (blue curve) and stress-strain block (orange curve).

equations model which is implemented in FE-Safe were studied in these sections and compared for two geometries with stress concentration. The simplicity of implementation is the main feature for all of these models since they do not require many material proprieties which makes the comparison easier.

5.4 Residual stresses application

One intelligent way to introduce the residual stresses is by applying plastic stresses and then remove the effect of this stress; this would generate plasticity during loading but during unloading the stress won't reach the plasticity limit in compression (if the applied loading is tensile) or tension (if the applied loading is compressive). This principle is shown in figure 44 for both overload and underloads to create beneficial stress (e.g HFMI) and detrimental stresses (e.g The welding stresses) respectively.

These stresses will influence the later cyclic loading through their self balancing forces or displacements components on the following equations which will influence the evaluation of the displacement field which affects the strain evaluation and the stresses afterwhile using Hooke's low.

$$K \times (a_{RS} + a) = f \qquad \text{or} \quad K \times a = (f + f_{RS}) \tag{69}$$

Where:
K: The stiffness matrix.
a: The displacement degrees of freedom due to cyclic loading.
a_{RS} : The residual stress displacement field.
f: The nodal force vector.
f_{RS}: The nodal forces generated by the residual stresses.

The self balancing nature of these stresses can be checked in different methods; one of them is already mentioned in the previous chapter by checking the area under the curve shown in figure 41 but this was an easy check since this geometry and boundary conditions are simple. In case of more complicated geometries and boundary conditions. The reaction forces which are an external reaction for the internal forces must be also self balanced as shown in figure 45. The summation of these forces in X and Y directions are equal to -14×10^{-3} and -17×10^{-3} respectively, these small difference are just numerical approximation errors.

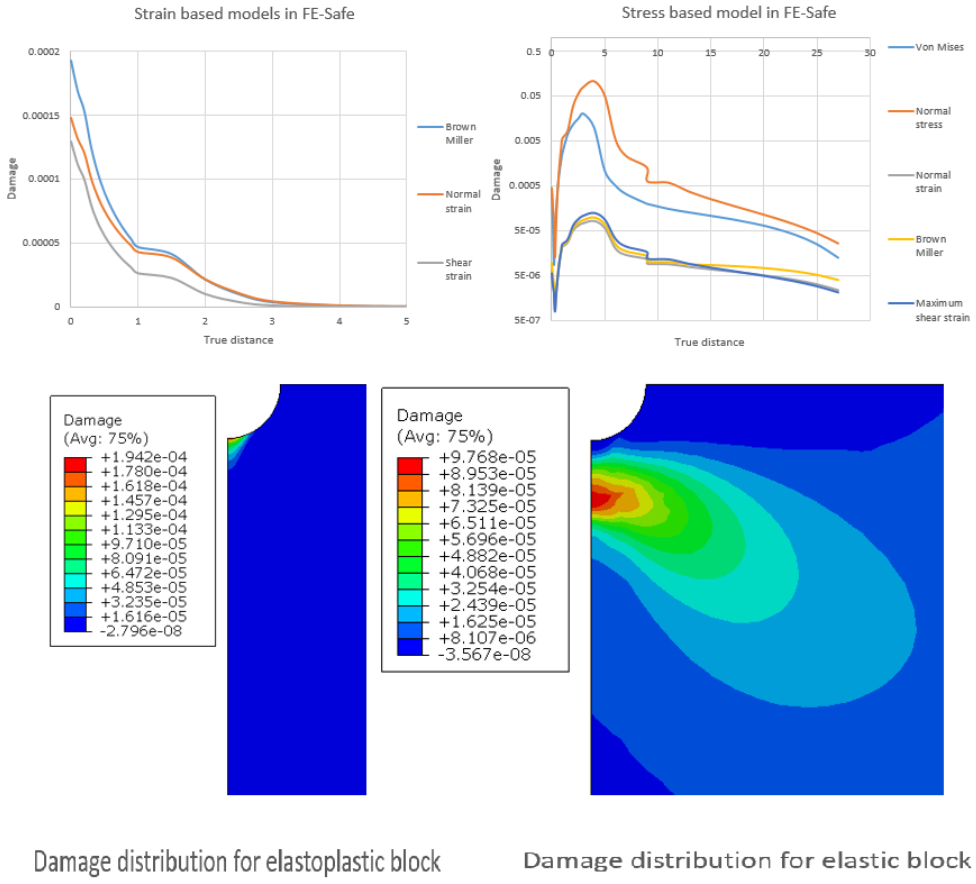

Figure 43: FE-Safe results for the given geometry in figure 25.
U: Comparison between plastic and elastic block results in FE-Safe.
L:Contour maps for the notched area for plastic and elastic blocks in FE-Safe.

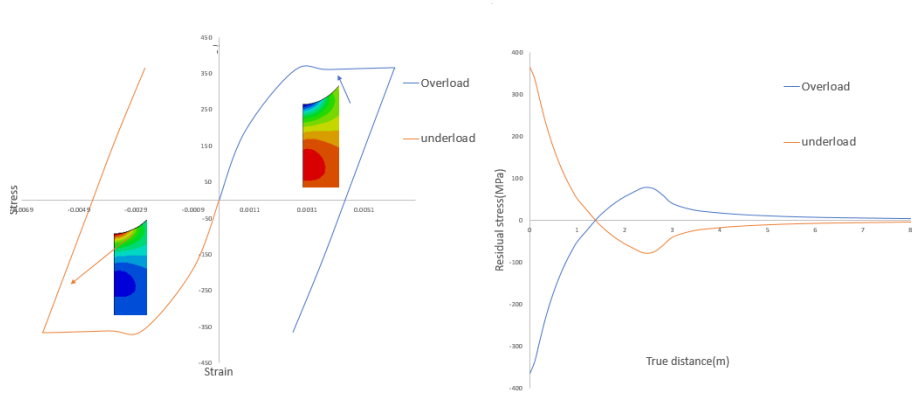

Figure 44: R: Over and underloading residual stresses
L:Over and underloading residual stress on the defined path in figure 25.

Welding heat energy introduces tensile residual stress at the welding zone and compressive stresses to counteract the tensile one, this effect is due to the thermal load applied from the welding gun; this can be simulated using high plastic underloading. On the other hand, the mechanical treatment by inducing compressive residual stresses which would be equilibrated with tensile ones; This is simulated by applying an overloading. In reality it's not only a simulating technique but also it's one of the weld improvement methods.

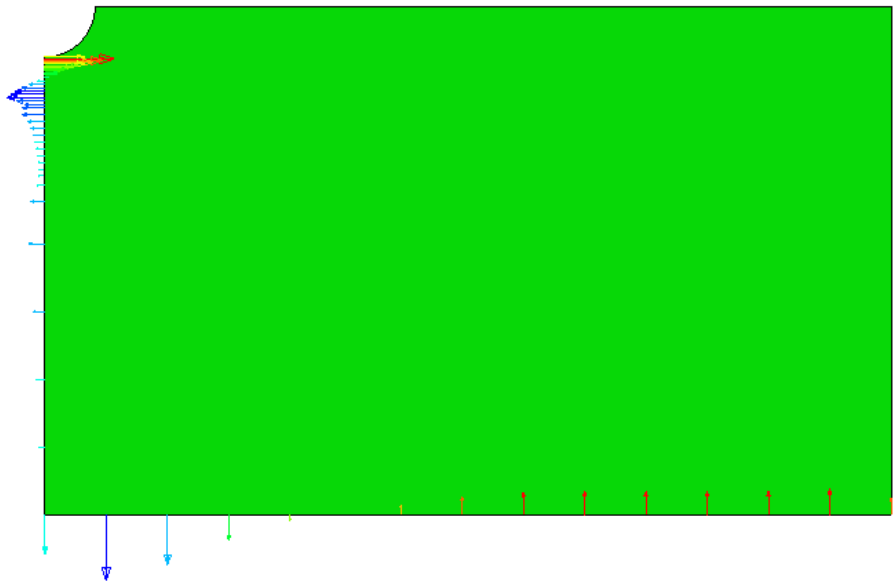

Figure 45: The external reaction forces due residual stresses results from overloading

One problem associated with this way of defining the stresses is that the stress wouldn't be evaluated actively. So many tensile external load must be applied to reach the desired residual stress distribution. Besides, The stress distribution can't be found identical. However, the residual stress distribution is hard to be measured for the whole geometry so only the limited zone can be measured and the rest can be evaluated numerically.

Another way of defining the residual stress is by defining an initial stress field; this would allow for assigning the maximum value of stress generated by mechanical impact or by the heat due to welding without iteration; however the profile of the residual stress is not as smooth as overloading or underloading. see figure 46 with red and blue contour represent tensile and compressive residual stresses respectively. This distribution is not realistic due to the presence of sudden change in the stress sign within few nodes; which doesn't confirm with the true distribution given in the literature as in (Björn åkesson, 2013).

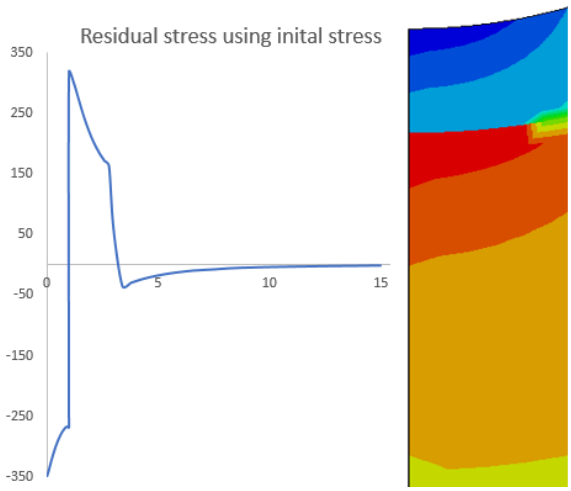

Figure 46: Residual stress distribution below the notch edge defined by initial stresses

A predefined temperature field can also be used but this requires a definition for the thermal expansion coefficient. Predefinition of stress or temperature fields will allow for conducting elastic analysis without an initial step for the elastoplastic analysis to create residual stress. However for

all of the analyses done before containing residual stresses; these stresses are define by mean of overloading or underloading.

The best way of simulating the residual stress due to welding is by conducting thermo-mechanical analyses; this was tested for a butt welded connection subjected to the thermal loading due welding. The specimen is shown in figure 26. This requires two kind of steps; the first one is thermal with one degree of freedom (temperature) so a special shell element is needed to be defined. In this analysis 5 steps will be defined in Abaqus. In the first step the weld bead is removed but it will be reactivated in the fourth step. The temperature will be increased to 1500 °C to simulate the heat introduced by the weld. The temperature is kept for sometime to allow the heat to propagate in the steel body. Finally a cooling step would be important to allow the thermal exchange process to end.

Special film conditions must be defined to the outer edges to simulate the surrounding temperature. This can be found in the interaction module. In this module bead's removal and reactivation also can be found. See figure 47. The thermal conductivity for steel of 40 W/mK, Thermal expansion coefficient of steel 11 $\times 10^{-6}$ and heat capacity of steel is equal to 0.12 KJ/KgK are required in the material model.

The temperature distribution field (NT11) will be extracted and used for the stress analysis as

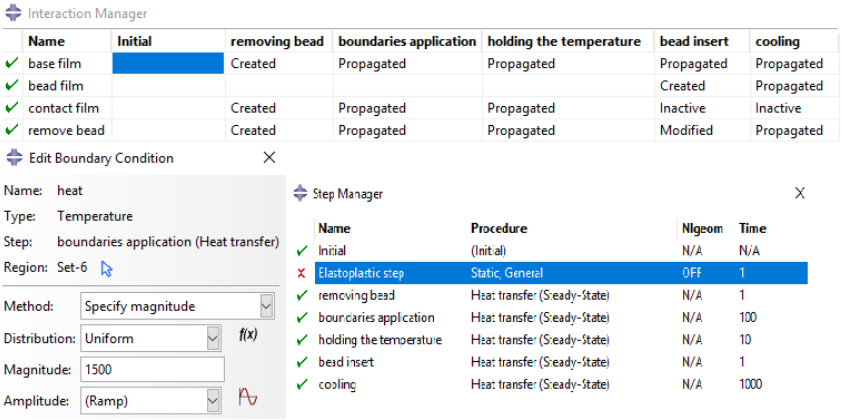

Figure 47: U: The interaction module in the thermal analysis.
LL: The applied temperature definition.
LR: The thermal steps definition

predefined field which will create residual stresses. The temperature and stress distributions are shown in figure 48 accompanied with the boundary conditions in the first and second steps. The light green colour is the weld body while the dark one stands for the welded steel. The figure also shows that the simulated part consider the symmetry around the Y-axis as a boundary condition.

A dynamo-thermo-mechanical analyses is required if the mechanical impact to generate compressive residual stress at the stress concentration zone is to be simulated; However this is very computationally demanding and out of the scope of this study so the overloading is enough to simulate the mechanical impact treatment. This process seems to be very time consuming since it requires the definition of 5 steps for each welding pass from bead insert to cooling step and the same for the structural model which will follow the thermal one; Thats why a new tool will be used for the sake of defining the residual stress resulted from the welding process more accurately and precisely. This tool allows the definition more complex welding pass geometries. This will be detailed in the next section.

5.5 Abaqus welding interface (AWI)

AWI is beneficial tool to simulate more complex welding geometries and detailed the welding passes regardless to their numbers. Abaqus welding interface**(AWI)** is a set of Python scripts for thermal and structural steps used to form an integrated application. This application provides a model-tree based approach to defining all aspects of the weld model such as weld beads, weld passes, film

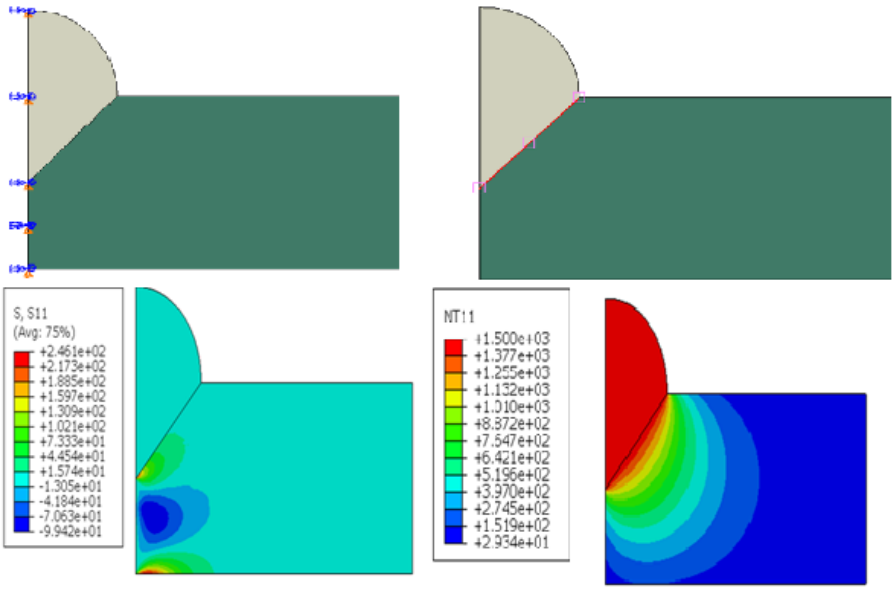

Figure 48: U: Deformation and thermal boundary conditions
L: Residual stress (σ_x) and temperature fields

loads, radiation (Simulia learning community, 2017).

The same methodology used in the previous model to simulate the residual stresses will be used here but in automatic manner. The same butt weld will be analyzed but in an interactive way, this time it's a full penetration weld. This method requires detailed definition of thermal and mechanical material proprieties as before. And these proprieties should be a function of temperature because similarl to stress problems the behaviour of the material changes when the degrees of freedom goes to its extreme. So when the strain exceeds a specific value the behaviour changes from elastic to plastic, that applies also for temperature fields. When the temperature reaches high values (e.g 1500 °C) the expansion coefficient, the heat capacity, the elasticity and plasticity and other material proprieties change completely. These mechanical and thermal proprieties are given in the appendix which is taken from the model defined in the workshop (Simulia learning community, 2018).

The procedures to build up such model are listed as follow:

- The activation of (**AWI**) from the drop in down item Plug-in.
- The definition of parts, material proprieties, sections and assemblies, while it's preferable to have two materials for welding and the base metal even if they have the same proprieties.
- From the (AWI) initial parameters are required (e.g Initial temperature, thermal constants); and it is preferable to define the welding regions in sequential manner so it's better to start from the first bead to be inserted during welding process. In the studied case 10 beads are defined sequentially as shown in figure 49.
- The number of passes can be controlled. However one pass is only considered for each bead. Also the sink temperature can be adjusted to control the minimum (The ambient temperature) the structure can reach after long term cooling, that requires the definition of film coefficient which was set to be $0.025\text{mJ}/mm^2/\text{K}$.
- The thermal and structural job can be created in (AWI) and this will allow for interaction, step and loading modules to consider the previous steps in Abaqus graphical interface.
- The jobs then can be submitted in sequence since the structural job requires an output thermal value from the thermal job.

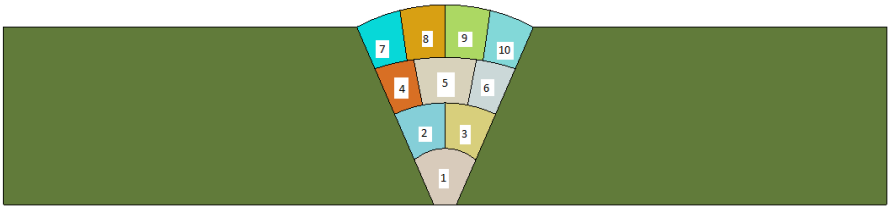

Figure 49: The sequential application of the welding beads.

- In the structural analysis, additional mechanical boundary conditions are required to be defined to avoid rigid body motion and in order to allow the residual stresses to raise. The type and location of this boundary condition will define the distribution of the residual stress.

The temperature steps results are shown in figure 50. Notice that temperature develops during heating but shrinks during cooling process. The described figure doesn't show all the passes so only each layer is shown and that explains why the thermal load is shifted to the right since the left bead is inserted before the right one. The temperature distribution is a function of many factors, The material parameters, The cooling period, The beeds distributions, The number of passes, the geometry and the ambient and torch temperatures.

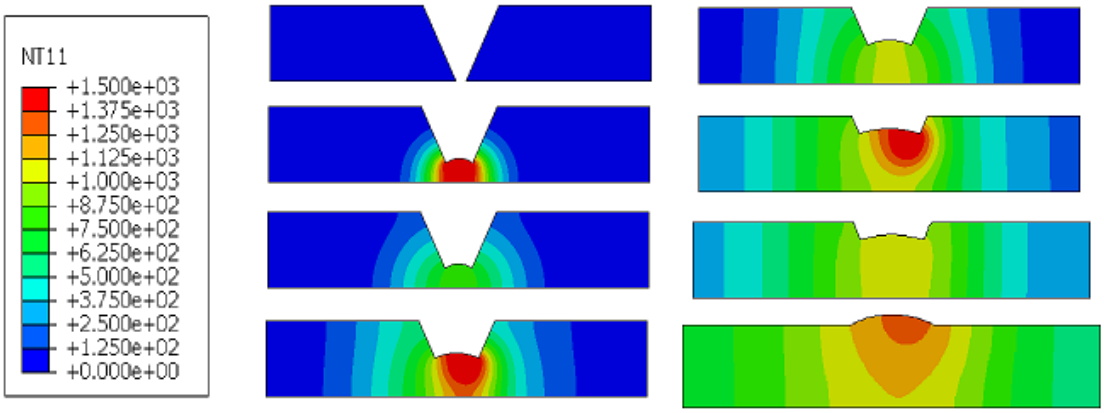

Figure 50: Temperature development during welding process including cooling steps

The residual stress resulted from such analyses can be also evaluated. However, this would be a tricky part since the distribution will differ with the boundary condition considered in the analysis. The self-equilibrated stresses will be achieved on these boundary lines as shown before in figure 48 which shows the concentration of these stresses around the boundary which was the X-symmetry line on the left edge of the studied geometry.

Different boundary conditions have been studied but the one will be displayed is the the full constrain of all the edges in the body except for the weld body edges. The results for this type of boundary conditions are displayed in figure 51 which shows the Mises stress distribution.

Since there are many mechanical boundary conditions so it's not easy to check the residual stress through the stress distribution. Instead, the reaction forces can be used to check the balance of these stresses. That is shown in figure 52; the summation of reaction forces in X and Y directions are -1.01kN and 0.0071kN respectively; which are almost zero and these small deviation is due to numerical approximation error.

Notice that all of the thermal steps discussed before are transient analyses which make the analyses very sensitive and difficult to achieve convergence if extremely fine mesh is used. The steps for each

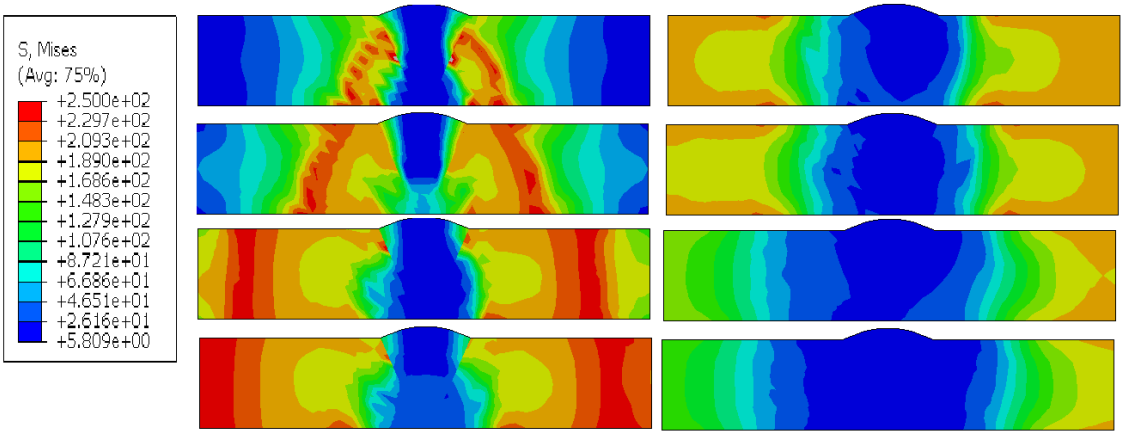

Figure 51: The Mises stress development simultaneously with the temperature development during heating and cooling steps shown in figure 50.

bead in the thermal analysis starts with bead removal followed with heating the bead boundary and then the the heat is kept for a specific time, then the element can be reactivated and finally the bead is cooled down. However this sequence will change in the structural analysis which has static general steps with no loads except the predefined temperature fields which causes stresses due to thermal expansion and shrinkage. The heat will be imposed from the thermal analysis and then the beads are removed and then it can be reactivated and finally the structure is left for cooling period.

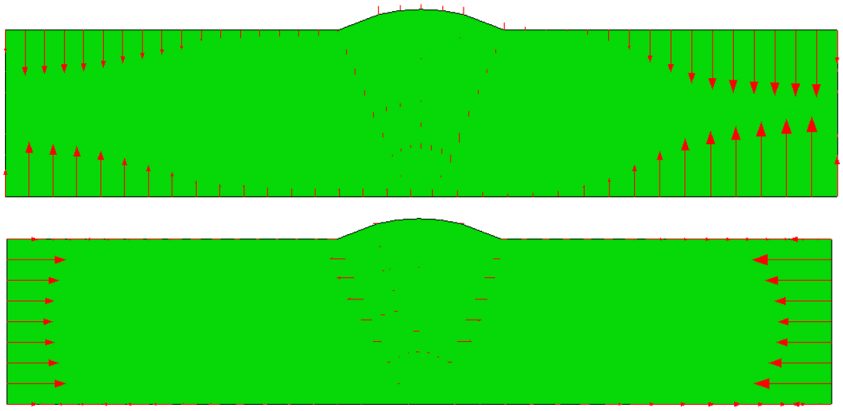

Figure 52: The reaction forces in Y and X directions respectively of the residual stresses

5.6 Residual stress relaxation

As it was stated before, residual stress is self balancing force which (in some cases like welding treatment by the mean of mechanical impacts) is considered as defense mechanism which the structure uses to defend itself against loading so the relaxation of residual stress is one form of the damage. The fatigue damage in principle is a combination of formation slip bands, movement of dislocation and the formation of intrusion and extrusion formation. The compressive residual stress can be understood as hydrostatic pressure acting on the grain boundaries which makes the three mentioned driving forces (slip band, movement of dislocation and intrusion and extrusion formation) harder to occur and require more energy.

Actually, there are two philosophies to study this influence; the first one is that damage won't initiate until all of these residual stresses are relaxed. Then the driving force can afterwards act on the grain instead of being resisted by the residual stress. By this way of thinking no damage is initiated unless all residual stress relaxes completely then the micro plasticity which is formed

by these forces can take place which cause high cycle fatigue after given number of cycles being exceeded, a complete residual stress relaxation means it reaches a level that gives tensile (or shear) stresses of a magnitude low enough to generate microplasticity.

There is also another philosophy which state that the fatigue damage and relaxation can work simultaneously, this is because the residual stress relaxation (or the removal of the compressive hydrostatic pressure as it was stated earlier) is the result of the movement of dislocation, which gives the possibility of the damage accumulation before the relaxation of all of the residual stresses. This means that microplasticity is possible despite of the existence of the compressive residual stress; That might sound odd however it's capable of explaining the residual stress relaxation as a result of damage.

Microplasticity is the result of small loading cycle which doesn't cause yielding, these loadings are usually variable in amplitude, the VAL can be replaced with an equivalent constant amplitude loading but this will kill the loading sequence effect. However, this effect can be neglected here for the sake of simplicity. So any damage model used in the following section used for high cycle fatigue simulation is the representation of these micro stresses on the macro scale. Of course this problem can be studied on the microscale but this is unpractical and computationally very demanding and required the definition of grain size and imperfections and boundaries and the inclusion and extrusion which are outside the scope of this study.

In case of presence of overloads and underloads among the applied loading cycles; these cycles are usually not so many which means they won't cause considerable damage accumulation. However they influence the residual stresses which causes a shift in the mean stress field as shown in figure 53. The effect of microplasticity in this case will be pronounced in the fatigue damaging but it will not be considered in the residual stress relaxation; That's of course a simplification but it's a valid one since this micro plasticity will cause the relaxation over high number of cycles while overloads cause instantaneous change in these residual stresses. For steel bridge girders, these overloads will cause the large portion of residual stress to relax within short time in service due to overloading (e.g Trucks passing on the bridge).

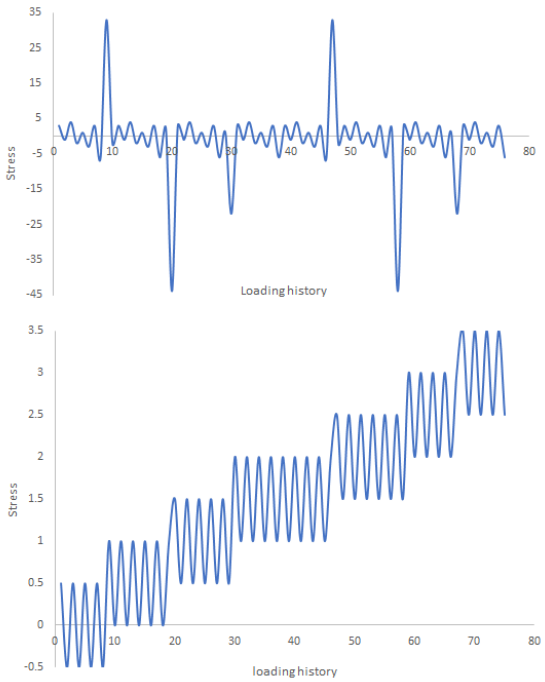

Figure 53: U: The applied loading including loading cycles in presence of residual stresses.
L: Treatment of the elastic loading as constant amplitude loading shifted due to presence of residual stresses

.

The methodology defined before requires categorization of the stress in the loading history into overloads and normal loading. The dividing line should be assigned for the tension and compression sides; this is a trail and error iterative problem. An example of this iterative procedure is shown in figure 54 which shows the compressive residual stress removal under different level of overloads, this was conducted on the geometry shown in figure 25. Applying a nominal stress of σ_y (355 MPa) doesn't cause full relaxation; this is evident by the existence of these stress after loading which means that the stress mean value will be higher up as shown in figure 53, that means the upper bound of the dividing line mentioned before is higher than σ_y. It worths mentioning here that locally (at the notch where residual stresses exist) the stresses (and strains) exceed the elastic values, which is the effect of stress concentration. The figure shows that applying an external load of $1.1\times\sigma_y$ (380 MPa) will cause the complete relaxation so by this the upper bound of overloading is determined. The lower bound is determined with the same iterative methodology. Once these bounds are calculated the equivalent loading can be evaluated and the mean stress can be calculated. To solve the problem of residual stress relaxation coupled with damage, the following procedures can be helpful:

1. Determine the upper and lower bounds separating the overloading from the normal loading.
2. Determine the equivalent loading for each loading between the overloads using the formula given in (Björn åkesson, 2013) or by another method.
3. Determine the relaxation of residual stress due to overloading and find the new mean stress and shift the next equivalent loading up or down depending on the resulting residual stress field.
4. Ignore the relaxation due microplasticity or the equivalent amplitude loading.
5. Evaluate the damage for each block of loading using one of the methods (e.g Miner rule).
6. Find the total damage using one of the accumulation methods.

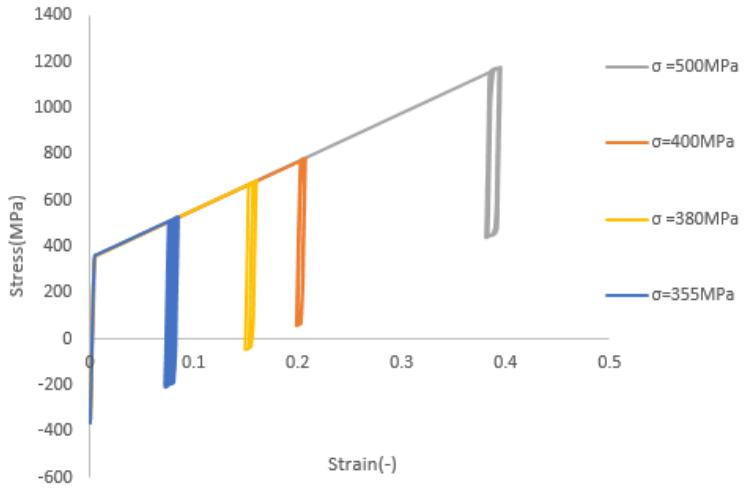

Figure 54: Iterative cyclic plasticity analyses to find the upper bound σ_y

The second step in the given recipe is very important since the evaluation of the equivalent stress plays a vital rule for the further steps. The simplest method is by using the formula found using Miner's method and this is given by:

$$\Delta\sigma_{eq} = \left[\frac{\Sigma_{i=1}^{k}(n_i\Delta\sigma_i^m)}{\Sigma_{i=1}^{k}n_i}\right]^{(1/m)} \tag{70}$$

Where:
m: The slope of S-N curve.
n: The number of cycles.

$\Delta\sigma_{eq}$: The equivalent stress range.
σ: The stress range of the ith cycle.

This equivalent stress is the stress range which gives the same damage Miner's rule gives. However this might be developed to be closer to reality by reshaping the variable amplitude load mentioned in the second step using Foruir's series, then the resulting different loads from different terms in the mentioned series will be imposed on the structure as a loading amplitude in an elasto-plastic step. Then the equivalent loading can be evaluated from any mulitaxial fatigue criterion (e.g. Sines criteria). This stress can be representative to the equivalent load instead of Miner's rule equivalent stress.

The residual stress can also be studied to relax cycle by cycle regardless to the amount of the cyclic loading but that requires a detailed finite element analysis which must cover the whole loading spectrum and this is demanding job. This can be used as prior step to verify this method by experimental tests.

5.7 Ductile damage model in Abaqus

Damage by definition can not be initiated in elastic material behaviour since elasticity unlike plasticity or hardening is not energy dissipation phenomena; this is shown mathematically with details in (Runesson et al., 2006). However, that doesn't mean that under elastic loading plasticity can not be induced in the micro scale. This micro plasticity is the driving mechanism for high cycle fatigue. Therefore it's important to differentiate between plasticity at micro scale and that at the structural scale. However, some damage models describe the damage by plastic strain accumulation on the structural scale. PB, LPD and ductile damage model in Abaqus which has been described in sections 3.1, 3.2 and 3.8 respectively are few examples. The ductile damage model described in Abaqus was studied and the results for constant amplitude pulsating and alternating loading on the same specimen shown in figure 25 were compared. In addition the effect of initial overloading will be studied. The loading conditions and material constants used are shown in table 4. The damage model was described in section 3.8.

It is possible to extract two important field outputs in Abaqus when ductile damage model is used, DUCTCRT and SDEQ. The former describes the damage criterion; when this variable is equal to 1 it means the damage has initiated but DUCTCRT can also be used as a damage indicator. This variable is directly proportional to the plastic strain ϵ_p. The later variable (SDEQ) describes the reduction in the stiffness; when it reaches 1 this means the member is completely damaged; these two variables are displayed in figure 55 for alternating loading with initial overloads.

The initial overloading of 250 MPa is very influential and introduces the plastic strain which will be imposed to the later constant amplitude loading. That makes the damage criterion for the pulsating and alternating loading (Yellow and grey curves) 10 times higher than it without overloading. Another observation is the concentration of damage around the notch area which contradict with the damage distribution shown in figure 43. That can be explained wih the same argument presented in figure 40 regarding the difference between stress and strain concentration under plastic loading.

5.8 Miao model implementation

The model described in section 2.6 is solved numerically using Matlab. As stated earlier, this model doesn't give a damage variable. Instead it gives the fatigue life using equation 21 though a predefined damage increment is set by the user. The magnitude of ΔD is defined depending on the convergence of the fatigue life. This convergence study is shown in figure 57 for Miao and Xiao models. Notice that higher damage increment leads to non conservative endurance which means that the use of very fine increment size to capture the true endurance.

The method is tested for the same geometry shown in figure 25 but for triangular elements instead of quadrilateral ones. Different material parameters are required for the numerical implementation

The Propriety	The value	The unit
The elastic modulus	210	GPa
The Hardening modulus	0.26	GPa
Poisson's ratio	0.3	-
The Yield strength	275	MPa
Fracture strain	0.1167	MPa
Stress triaxiality	1/3	MPa
Strain rate	0.02	MPa
Displacement at failure	0.2	m
The loading history	max _ min (MPa) number of cycles	Initial overloading (MPa)
Loading condition 1	210_0 (50)	0
Loading condition 2	105_-105 (50)	0
Loading condition 3	210_0 (50)	250
Loading condition 4	105_-105 (50)	250

Table 4: The material properties and the loading history for the studied ductile damage model in Abaqus

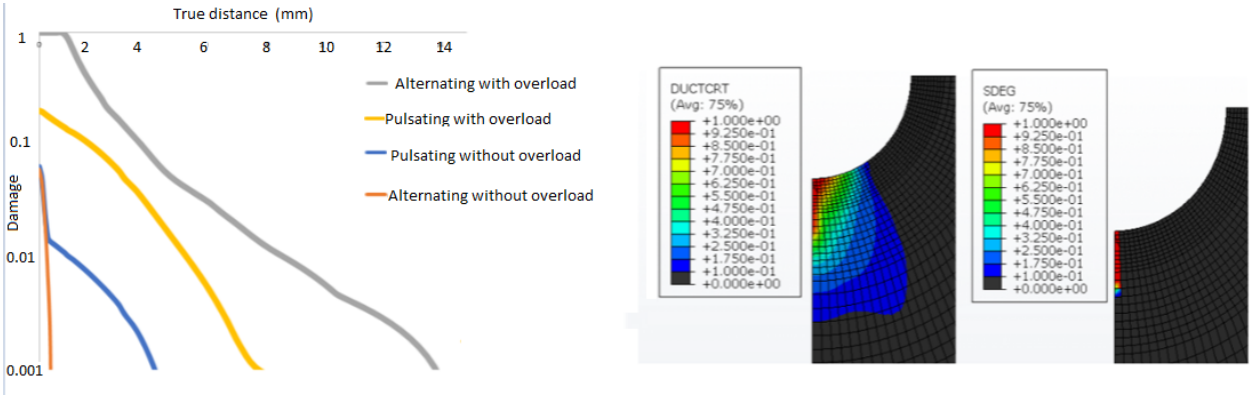

Figure 55: L:Comparison of DUCTCRT for different loading conditions described in tables 4.
M:DUCTCRT distribution for loading condition 4.
R:DUCTCRT distribution at the after 90 cycle for loading condition 4.

and they are described in the same paper in which the model was described in (Zhang et al., 2010).

Although this model is suitable for elastic material behaviour only but it is capable of considering the effect of load sequence as shown in figure 56. A constant amplitude alternating tensile loading of 105 MPa (30 cycles) is applied on the left edge; this load is preceded and followed by an overloading of 250 MPa as shown in figures 56L and 56R respectively. It's obvious in figure 2.6 that the early overloading is more damaging and cause lower fatigue life.

Notice that compressive stresses has the same damage as tensile ones according to this model; so the initial overloading which creates compressive residual stress doesn't cause a change in the distribution as the case described in figure 37, so it's wiser to use σ_{Mises} instead of σ_x to predict the damage.

5.9 Xiao model implementation

Similarl to Miao models, Xiao model doesn't give the damage value but it gives the damage distribution as an eigen vector without defining the amplitude of the vector, so the damage increment must be defined by the user for the most stressed element and the rest of elements will follow according to their stress values. As mentioned in section 2.10 this method is capable of describing the damage only close to the stress concentration nodes; this locality of damage is confirmed in figure 58. The study was conducted to the same geometry described before but under five cycles

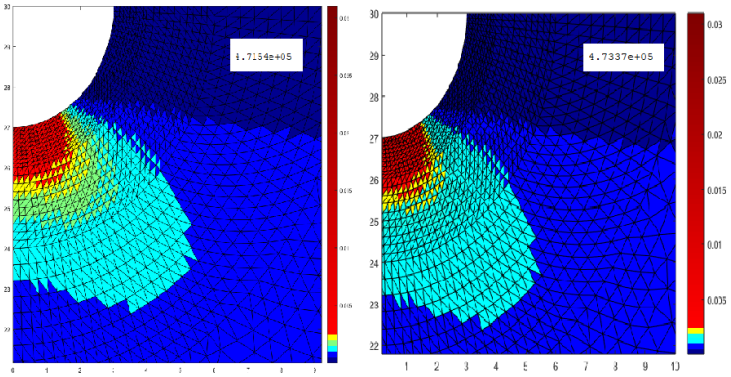

Figure 56: Comparison between early (left) and late overloading (right) and the fatigue lifes are shown for each case.

only of 105 MPa (for the sake of capturing the locality of damage but the comparison will be done later for more number of cycles). The implementation is given in a Matlab code in the appendix. The original Xiao model described in section 2.3 requires many material parameters which were not identified in the literature so the simplified version of the model is used instead.

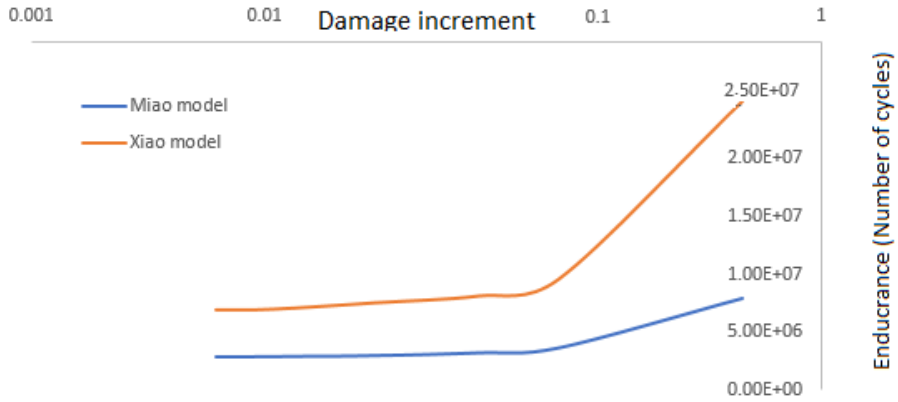

Figure 57: Convergence study describes the damage increment effects on the endurance

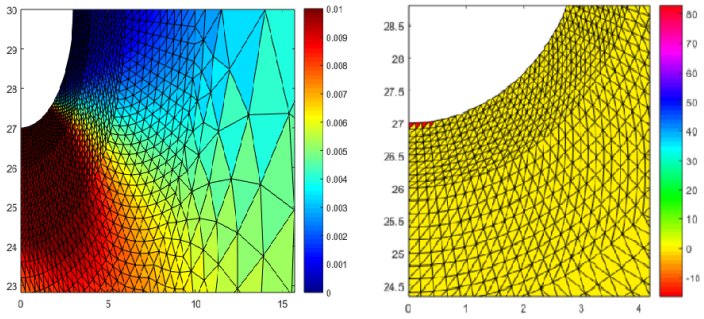

Figure 58: The locality of damage given by Xiao model Vs The damage dispersion in Miao's model

5.10 Chaboche model implementation

As shown in figure 59 which is the result of 1000 cycles of 105 MPa nominal stress on the same specimen described in figure 25. Here the damage is not localized like in modified Xiao model as

shown in figure 58. The values in figures 56 and 58 and 59 are not comparable since different damage increment and loading conditions were used in each of them since the reasons of studying each of them are not the same. The comparison between these three models can be made if the loading

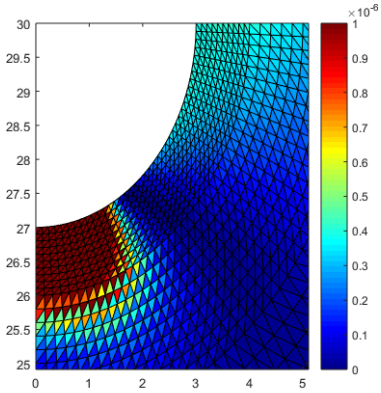

Figure 59: Damage distribution in Chaboche model

conditions are perfectly the same but this is not doable since Chaboche model requires an initial damage definition so it was put to be 1×10^{-15} which is negligible difference. A constant amplitude alternating loading of 105 MPa with a stress ratio (R=-1) is applied and the damage evolution and the endurance is evaluated for each model. Chaboche shows an endurance of 1.03×10^{6} while Miao shows an endurance of 2.83×10^{6}. Xiao shows very unconservative life of 6.9×10^{6}, The damage distribution for these three models is shown in figure 60.

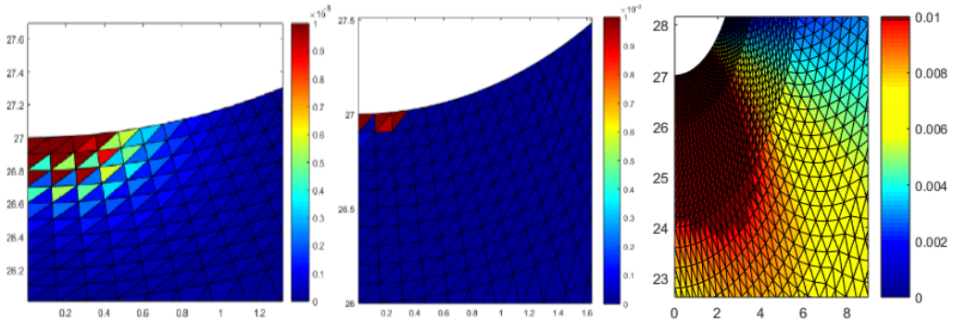

Figure 60: Chaboche, Xiao and Miao model comparison under 105 MPa alternating loading.

5.11 Critical plane method

Different critical plane methods were discussed in chapter 3. Since these methods are based on Coffin Manson equation that makes the comparison of these methods doable using FE-Safe, that applies for [**Ba**] which is SWT mean stress correction of the strain life equation. It applies also for [FS] model but the parameters must be operated to include the coefficient (k) in equation 54. Besides, [**SO**] can be easily implemented by putting the plastic part parameters (c, ϵ_f) to be zero. On the other hand, [**WB**] is hard to be implemented even though it's based on strain life equation. So all the methods will be studied numerically in Matlab.

The parameters and loading conditions are described in table 4, these are to be used here but without any fracture strain or stress triaxility definition in the material model. A comparison between between [**FS**], [**SO**], [**WB**] and [**Ba**] models will be conducted under constant amplitude alternating loading (R =-1) and maximum stress of 105 MPa; this makes the comparison of [**SO**] model which is meant to treat high cycle fatigue with [**FS**] or [**Ba**] possible.

Fatemi Socie modle

Fatime Socie [**FS**] model equation will be solved numerically to find the root of the following equation which gives the out of balance force g(N):

$$g(N) = \gamma_a(1 + k_1\frac{\sigma_x}{\sigma_Y}) - \frac{\tau_f}{G}(2N_f)^b - (2N_f)^c = 0 \tag{71}$$

where the Jacobian matrix which gives the derivation of the out of balance force is given by:

$$J(N) = \frac{dg(N)}{dN} - 2b\frac{\tau_f}{G}(2N_f)^b - 2c(2N_f)^c \tag{72}$$

Then J(N) and g(N) will be used to evaluate close solution as follow:

$$N^{i+1} = N^i - \frac{g(N^i)}{J(N^i)} \tag{73}$$

Where:
i: The iteration's number.
k_1 will be set to be 1 as recommended in (Aid et al., 2012) for steel.

Bannantine and Socie model

[**Ba**] also will be solved using the Newton's method as described in previous section. This method doesn't require any material parameters except the Coffin Manson equation parameters.

Socie model

This model doesn't require nonlinear solution since it can be solved for the number of cycles as follow:

$$N = \frac{1}{2}(\frac{\tau_a + K_2\sigma_{max}}{\tau_{max}})\frac{1}{b} \tag{74}$$

The parameter k_2 wasn't found in the literature for steel; so it will be set to be unity (K_2= 1).

Wang and Brown's model

Similarl to [**FS**] and [**Ba**], this method will be solved numerically using Newton's method. But this method requires a material parameter (S) in equation 58 which wasn't found in the literature. The parameters k_1, k_2 and S in equations 54, 35 and 58 respectively control the contributions of the normal stress; so their values couldn't be more than one since the shear is the driving force in fatigue initiation but since these values are not described in the literature they will set to be unity, which means that the normal stress/strain causes and contributes in the damage initiation with the same magnitude to the shear stress/strain.

The fatigue life estimated using [**FS**] was found to be 7.57 $\times 10^6$ which is close to the estimation described in section 3.7; while [**SWT**] and [**WB**] are less conservative and yield life of 9.10 $\times 10^7$ and 4.35 $\times 10^7$ respectively. On the other hand [**SO**] was too conservative and results in a life of 4.41 $\times 10^4$.

It's hard to say whether the results fulfill the expectations or not since there is no available test results. However [**SO**] is very conservative model as described in section 3.7. Besides, it was described in the literature that [**FS**] is close to reality while [**WB**] is underestimating the damage as described in section 3.7. On the other hand [**Ba**] was described as realistic while here it underestimates the damage.

[**FS**], [**WB**] and [**SO**] are based on the combination of the shear and normal stresses/strains which makes the maximum damage shifted toward the maximum shear location which is a few millimeters from the notch tip; this doesn't match with the damage distribution found in the other methods.

These models are mainly used for constant amplitude loading but they can be also extended for variable amplitude loading if they are combined with one of the damage accumulation models described before. However, these models lack the ability of modeling the beneficial or detrimental residual stresses.

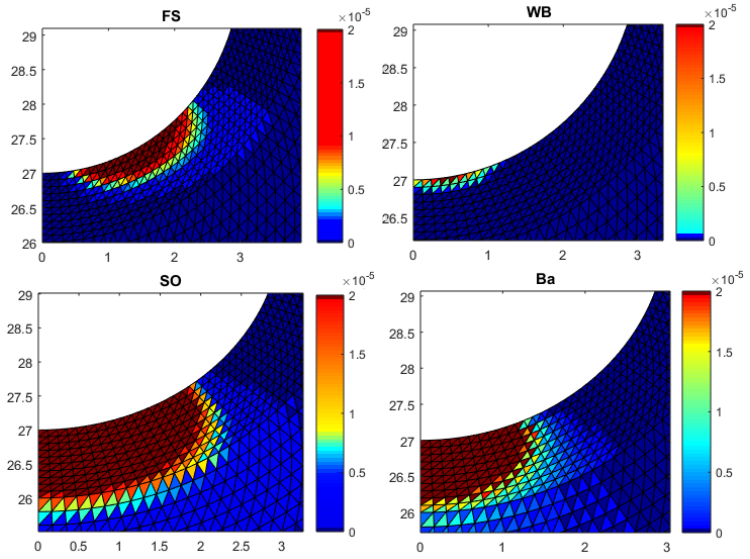

Figure 61: Comparison between different critical plane methods

5.12 Model describing the damage due to reduction in yield strength

Describing the damage by the plastic strain is not a new concept; it was described in section 5.7. But the concept is different in this model. Reducing the yield strength with increase number of cycles would allow for plastic strain to raise even for stress lower than the material yield strength (Asma Manai, 2017).

The plastic strain will be used as a damage indicator which will accumulate due to plastic deformation of new element due to shrinkage of yield function which is for uniaxial loading given by:

$$\phi = \sigma - \sigma_y \tag{75}$$

where:
ϕ: The yield function which indicates the plasticity if greater than zero and elasticity otherwise. This yield function will be used as damage function also, which shrinks with cycle accumulation. This damage accumulation is studied for constant amplitude loading with and without precedence overload which creates residual stresses. Seven increments of yield strength's reduction were considered and the maximum plastic strain (The damage indicator) is given in table 5.12. Part of these increments are shown in figure 62.

It's possible to determine the number of cycles required to drop the yield strength from σ_{y1} to σ_{y2} using Basquin equation which defines the S-N curve [$\sigma_y = A(2N_f)^b$]. Where σ_y is the yield strength at the second elastic phase.

The number of cycles will continue to accumulate until the plastic strain reaches the ultimate strain (0.1167 in this analysis) which means the strain shown in figure 62 doesn't cause complete damage and further cycles can be applied to the structure. And further reduction in yield strength can be conducted to reach the ultimate value. The damage initiates when the plasticity is reached. However a threshold value can be set to be any other value than ϵ_p=0.

There are mainly two flaws in this model:

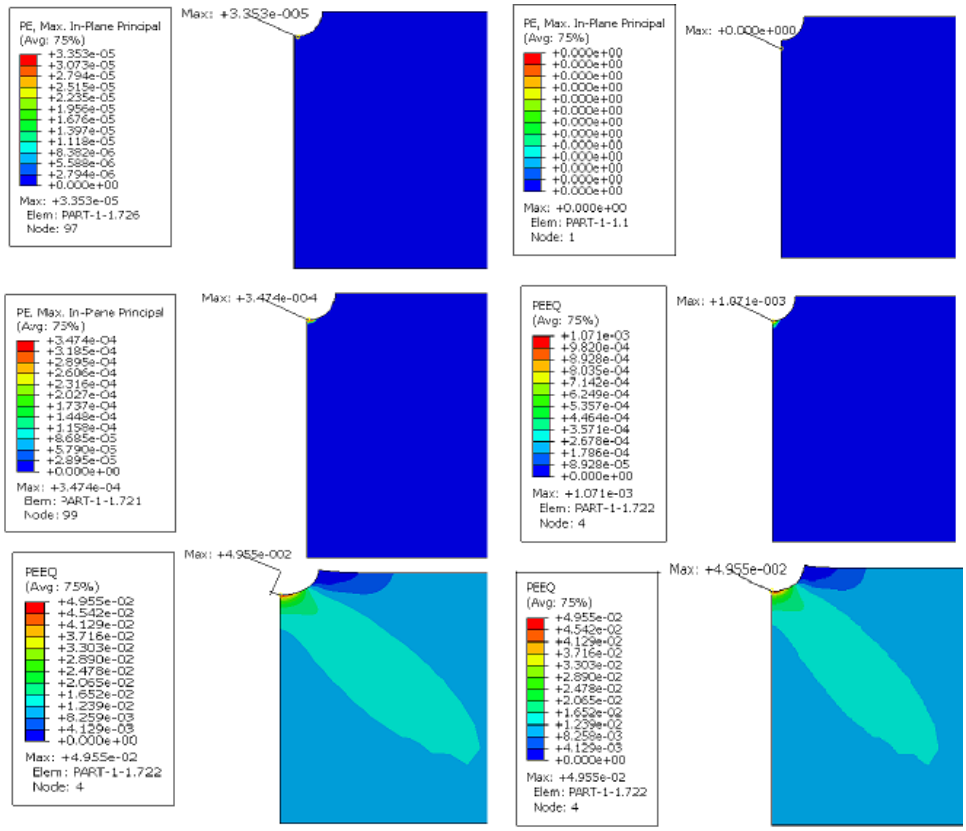

Figure 62: Equivalent plastic strain (Damage indicator) when the yield strength is 350, 280 and 50 MPa with and without overloading respectively.

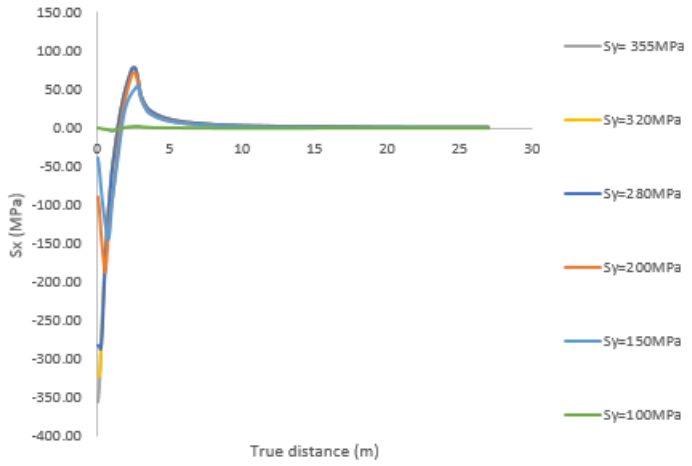

Figure 63: Relaxation of residual stresses with yield strength degradation

- It's limited only for CAL and becomes more difficult for implementation for variable amplitude loading (VAL). This is because the degraded value of the yield strength is obtained from jumping cycles.
- It causes general structural plasticity which doesn't match with test results which shows continuation in elastic behaviour away from the stress concentration zone.

On the other hand, the method is capable of describing the relaxation of residual stresses caused by early overloading as shown in figure 63; the distribution of early overloading is similar to the one shown in figure 41. That's physically appealing since the residual stress is expected to be lost

The yield strength (MPA)	$\epsilon_p$with Overloading	ϵ_p Without Overloading	Number of cycles(cycles)
350	0.00007122	0	-
320	0.0002182	0	2.2×10^3
280	0.0002797	0	5.8×10^3
200	0.0007139	0.001071	6.7×10^4
150	0.0005933	0.0003234	5.4×10^5
100	0.01833	0.01751	1.0×10^7
80	0.01732	0.01733	5.1×10^7
50	0.04955	0.04955	1.5×10^9

Table 5: Maximum damage expressed by the plastic strain for 2 load cases

when the yield strength is reduced due to cycle accumulation; the initial residual stress defends the structure against the cyclic loading but this defensive energy will be depleted when the number of cycles reaches specific values. However, the statues of the residual stress will not be changed as self equilibrating force.

The analyses were conducted in Abaqus where the applied load is pulsating with stress ratio R=0.1. Each step's last increment is saved to be imposed and used for the next step. While each step represents a jumping cycle with further reduction in yield strength; fatigue damage is considered to have initiated when the plastic strain is reached. For R =1, the endurance is less than 6.7×10^4 cycles while it was evaluated for alternating loading for the same loading of (105 MPa) is less than 5.4×10^5.

Notice that in comparison with many models mentioned above this method is too conservative. This is because the damage initiation criterion is set to be the attainment of the plastic strain, this is very conservative presumption since the plastic loading isn't necessarily correlated to damage. So a damage threshold can be set to be 0.0015 can raise the life estimation to 10 millions cycles.

Unlike Chabooche, Miao and Xiao models, this method doesn't require reduction in strength element by element. The yield strength is reduced for all of the elements; Then it doesn't require special definition of material property change due to damage.

One of the criteria that governs the choice of the model is the capability of describing the effect of both beneficial and detrimental residual stresses especially for weld study. The problem with this model is the ambiguity of the threshold which if set to be zero, the damage commences directly when the welding is applied and the cyclic loading causes just propagation and intensification of the damage. Then the choice of the threshold value of damage is so decisive and that is one of the drawbacks of this model.

5.13 Model describing the damage due to reduction of elemental stiffness

Similarl to the previous model, this model describes the damage through material proprieties degradation but for this model, the stiffness is reduced instead of yield strength(Asma Manai, 2017). But this requires defining the stiffness for each element which is possible in Abaqus through the following procedure:

- Define the section by inserting this line in the keyword in the **section** field
  ***Solid Section, elset="The name of the set ", material="The name of the material"**
- Define a distribution pattern and set the element to be the target of the distributed filed.
- Set the field to be the elasticity modulus and Possion's ratio.
- Define the default value of the elastic modules and Possion's ratio; this value will be used for the elements which haven't taken a stiffness value (the default stiffness).
- Define the stiffness and Possion's ratio for each element.

An example of the material model definition by the mean of defining distribution of the element's stiffness is shown in figure 64.

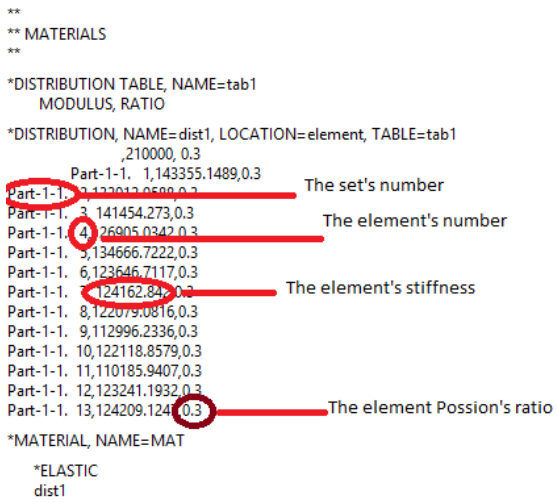

Figure 64: The definition of the material model by the mean of distribution

For the given geometry, the hydrostatic stress at the notch will be negative due to initial overloading. However if α is chosen to be unity which means that negative and positive stresses will cause the same damage which makes the damage initiates from the notch as shown in figure 65; which displays the damage distribution for three sequential jumping cycles . 3.38 $\times 10^5$ jumping cycles of 105 MPa alternating loading are required to cause the damage level to reach 99.5 %. Notice that in order to elevate the damage value to 100% (which represents crack initiation) more number of cycles are required.

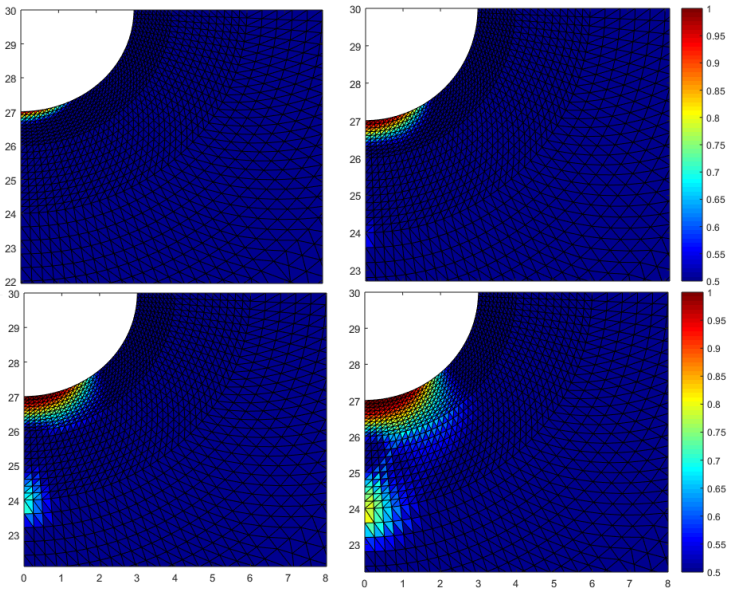

Figure 65: The damage evolution in figure 25 according to the stiffness method for $D_{max} = 0.92$, 0.95, 0.98 and 0.995 respectively

Repetitive loading causes higher damage in tension than compression because compression causes the closure of existing microcracks and microvoids which gives larger resistance to the damage; the mircocrack closure effect is examined by comparing the damage when $\alpha = 1$ and 0.1. In the left part of figure 67 this effect was ignored which makes the damage initiation possible

in the compressive stress zone and since the compressive residual stress is higher than the tensile stress as shown in figure 41. However, the crack closure effect makes the damage initiates from the tensile zone, the crack closure effect is a conservative assumption since the value of α is material parameters and there is no consensus on it's numerical value. Lemaitre suggests to use 0.2 for steel (Bouchard et al., 2011).

The damage starts to appear in the notch tip where the Mises stress value is highest. Then the tensile residual stresses at the left edge starts to play a vital rule and causes damage as shown in the third picture in figure 65. Finally the whole area will be damaged due to the drop of stiffness (in the tip due to Mises stress and in the left edge due to tensile stress), then the connector area will be loaded, this principle is very similar to the plastic redistribution in indeterminate beams.

If there is no overload applied the damage will certainly starts from the notch and propagate in the same manner of the plastic strain distribution shown in figure 62.

In comparison with the previous method, the damage distribution follows the von Mises stress pattern if $\alpha = 1$ and the stress in x direction if $\alpha = 0.1$ while using the plastic strain as a damage indicator makes the damage distribution follow the Mises stress distribution which makes the current method superior to the previous one in term of the ability to include the crack closure effect.However, this method is more computationally demanding since it requires special definition of the stiffness for each element while the previous one reduce the material yield strength for all the whole structure.

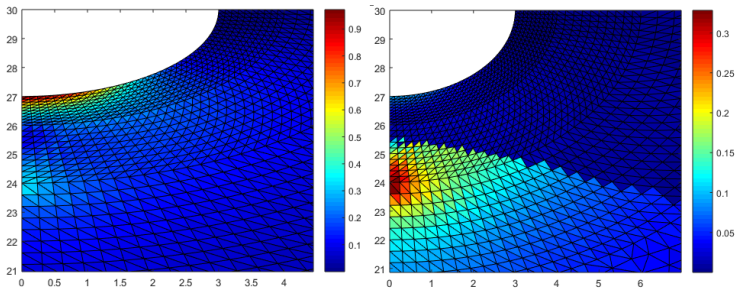

Figure 66: Microcrack closure effect for $\alpha = 1$ and 0.1 for the right and left figures respectively

Studying the overloading effect is more pronounced in the previous model since the yield strength is chosen to determine the number of cycles that makes the comparison straight forward; while in this method the maximum equivalent stress which is a result of the post processing will be the input for the Wöhler curve; so the comparison can't be made in the same systematic way.

The model is also capable of describing the relaxation of the residual stress (e.g HFMI). This is done by applying the residual stress degradation on elasticity and predict the new elastic modulus fields and apply this new filed on the residual stress (the plastic cyclic overloading which creates these stresses as mentioned in the previous section); this was studied and shown in the figure 67.

In comparison with the relaxation achieved in yield strength degradation shown in figure 65 the given relaxation shows a shift in the maximum tensile residual to achieve the equilibrium; that wasn't the case in yield strength degradation method because the mechanical propriety's reduction (yield strength) was on the whole structure but in the current model the stiffness is reduced element by element. There is a need for test results to decide which of them is closer to reality; since both of them are physically acceptable.

Similarly to the previous model, this model is deficient to describe the effect of the detrimental stresses introduced by welding and if the same methodology is followed, this residual stress will also relaxed due to stiffness degradation as shown in figure 68.

Studying residual stress relaxation according to this model and the previous model is done by jumping cycles because studying this effect cycle by cycle is very computationally demanding. However, this is doable theoretically and the effect of one pulsating loading cycle of (105 MPa) is

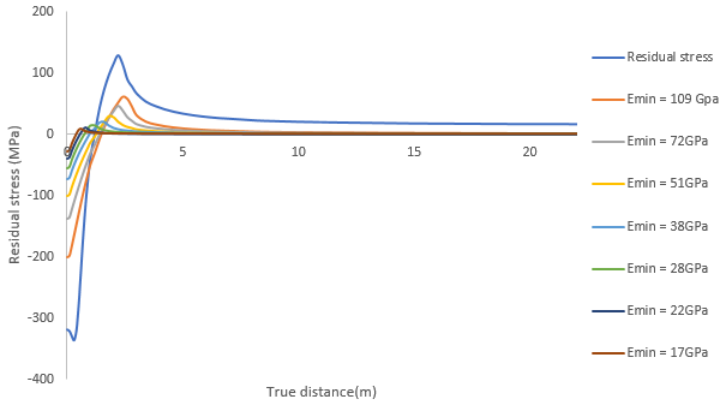

Figure 67: Compressive residual stress relaxation due stiffness degradation

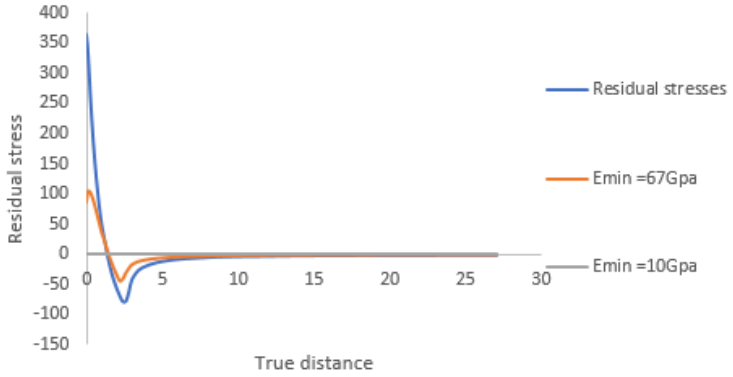

Figure 68: The deficiency of stiffness degradation model to simulate detrimental residual stresses effect.

shown in figure 69R. It's interesting that the relaxed stress in compression is more noticeable than tension. One more observation is the relaxation behaviour starts stronger in the first loadings than the later ones which confirms the results found in the literature as shown in figure 69L.

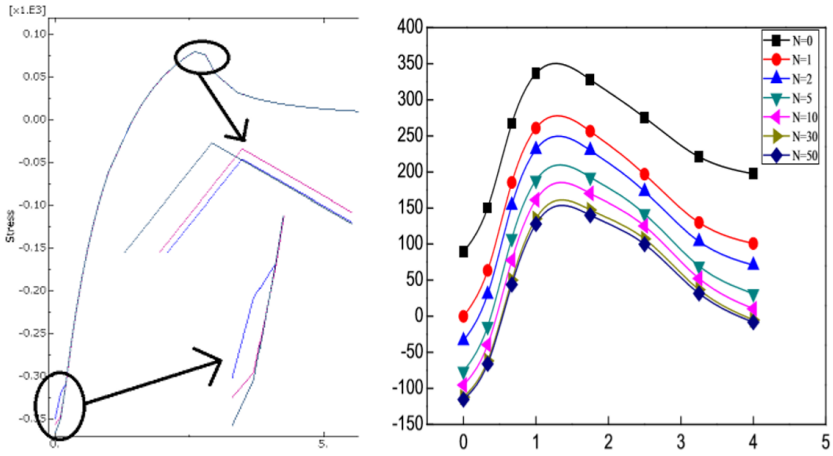

Figure 69: R: The relaxation of residual stress under two loading cycles.
L: Residual stress relaxation under 50 cycles given by (Xie et al., 2017).

The single loading relaxation can be adjusted to include the effect of more loading cycles using the residual stress formula (Leitner et al., 2017). but that requires one material parameter for

fatigue damage softening β which was found to be -0.004. The residual stress due to 100 cycles is examined and shown in 70.

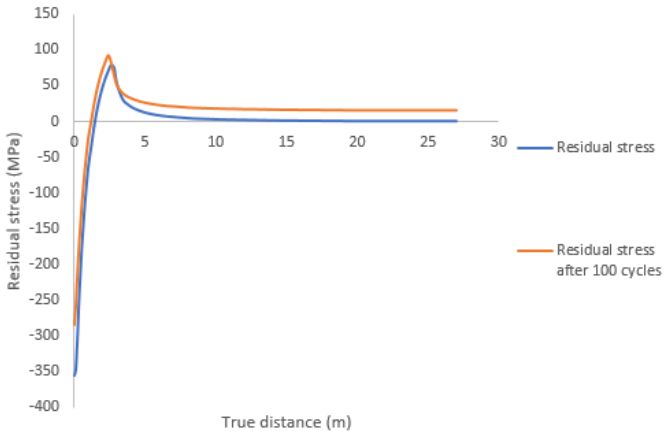

Figure 70: The residual stress relaxation after 100 cycles using the given formula in (Leitner et al., 2017).

5.14 Damage coupled with plasticity

This model was described in section 3.9. the model is tested for constant amplitude 100 cycles with a strain amplitude for each of them equal to 0.003 which exceeds the yield strain of steel 0.0021. The model requires some parameters (m,s) in equation 66. The ductility measure (s) is assumed to be 200 since there is an ability to undergo some plastic deformation prior to the failure, while the damage exponent (m) is assumed to be one.

One of the benefits of this model is to study the effect of the hardening model. It's obvious in figure 71R that the isotropic hardening (R=1) is less damaging than the kinematic hardening (R=0) which sounds physically correct since in kinematic hardening the yield surface is shifted in the stress space while in isotropic hardening it remains the same shape but only with expansion due to the increase in stress.

The effects of the damage exponent (m) and the ductility measure (s) are shown in figure 72. It's obvious in the mentioned figure that the ductile damage has more detrimental effects than the brittle one and the damage exponent has an inverse relation to the damage.

Final notes about this models is that it doesn't differentiate between loading in tension and compression as long as they cause the plasticity and the shape of the damage evolution curves take the shape of staircase; this is because during elastic unloading no damage is accumulated.

5.15 Finite element tricks

In this section some finite element techniques which is used in this study to reduce the running time and increase the results accuracy are presented. This techniques are doable in commercial software (Abaqus); these techniques are adaptive mesh refinement and finite element sub modeling.

5.15.1 Adaptive mesh refinement

This concept is described in Wikipedia as "a method of adapting the accuracy of a solution within certain sensitive or turbulent regions of simulation"; this turbulence in fatigue takes place in the highly concentrated plasticity zone at the notch tip; especially when nonlinear geometry effect is activated like in ductile damage model. It can be adjusted in the step module in Abaqus.

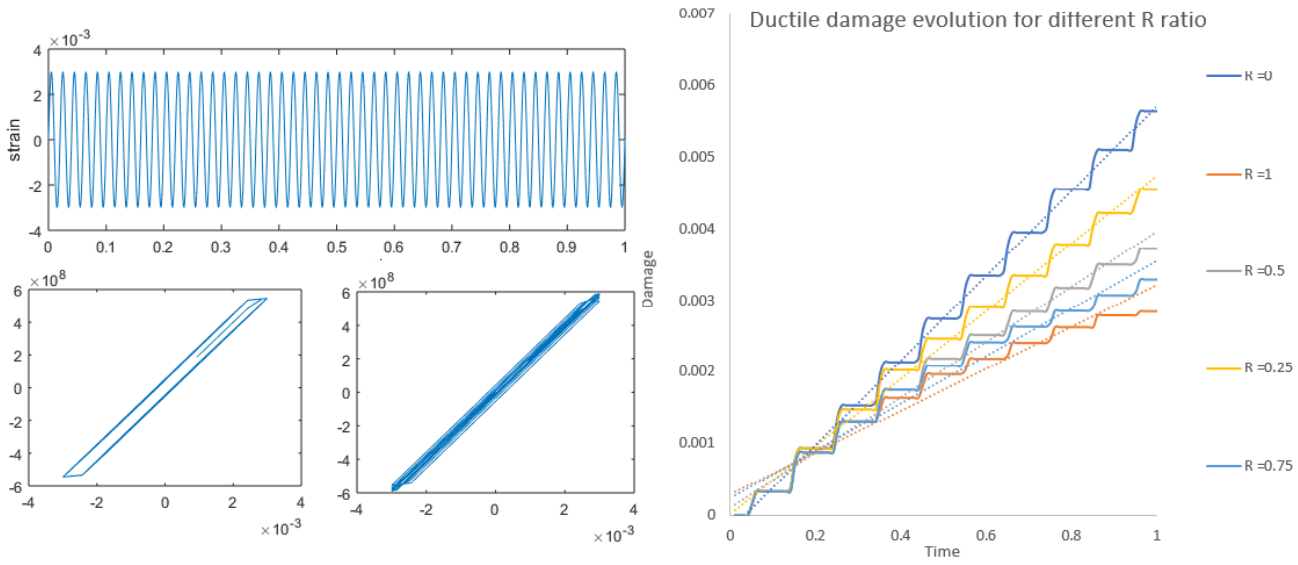

Figure 71: L-U: The loading history.
L-L: The mechanical behaviour for isotropic and kinematic gardening respectively.
R:The damage evolution with time for different R ratios.

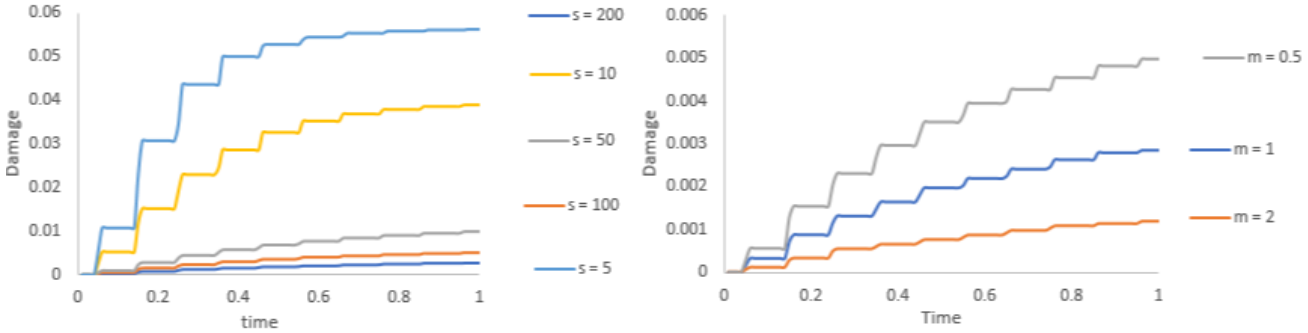

Figure 72: The effect of damage exponent(m) and ductility measure(s) .

5.15.2 Sub modeling

The geometry in hand is notched specimen which makes the interesting area for fatigue study limited around the notch; that was controlled before using the cutting tool to refine the mesh in that area. An efficient alternative technique which is less computationally demanding is to conduct two analyses as shown in figure 73: One global analysis with coarse mesh to study the general behaviour and intensified mesh on the interesting area which reads the results from the first analysis and conduct detailed finite element simulation on the notched zone. In this case the stiffness matrix size would be smaller and the running time to solve the fundamental finite element equation ($K \times a = f$) becomes shorter. This technique wasn't necessary in many analyses since nonlinear study wasn't used except in ductile damage model.

This technique can be achieved in Abaqus by copying the global model and edit the attributes in the copied model to read the data from the global job. This might requires changing the boundary conditions and applied loading position. Notice the difference the refinement in the obtained results with lower computational time in figure 73.

This idea would be very fruitful if the microscopic scale is to be studied which can be a necessary technique to identify the damage in high cycle fatigue due to microplasticity which won't be captured by macroscale. Making a very fine mesh going deep to the grain size in the sub-model and relate that to the global model using the technique described would be good. However that

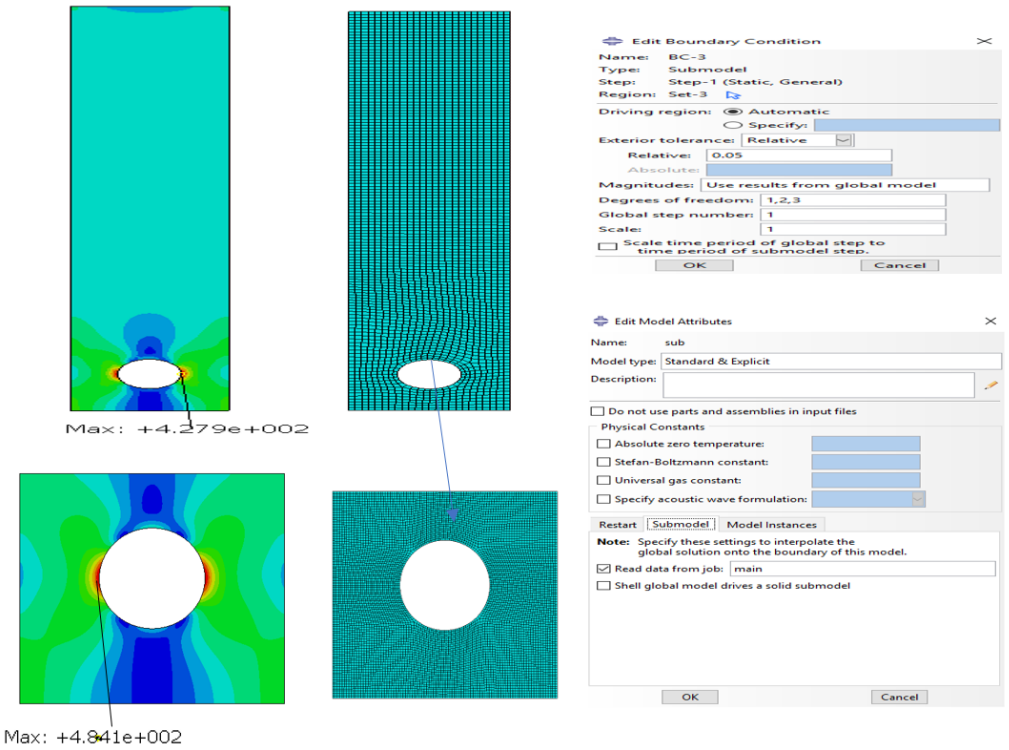

Figure 73: L: Sub modeling effect on the Mises stress distribution with a global mesh size of 2mm and sub model mesh size of 0.5mm R: required steps to create the sub model.

doesn't represent the true grain distribution.

6 DISCUSSION

Most of the damage models described and implemented in the previous section were suitable to be used for high and low cycles fatigue and this is the scope of this study; However plasticity plays a vital rule in the case of welds. Different load histories were applied for different methods but for the sake of comparison an uniaxial alternating loading of 105 MPa will be applied and the endurance will be estimated and compared in table 6. The damage accumulating methods were discussed in section 5.2.

Starting with the damage accumulation models; these models aim to give better approximation for the damage than Miner rule. Miner rule was based on the linear accumulation assumption disregarding any loading sequential effect; which is covered by two models, S-N curve model through the damage transfer concept and damage curve approach through the exponent (α). It was found that applying the high amplitude cycle earlier is more damaging than if it's applied later. Also no considerable difference was found between case where the low amplitude cycles were applied first followed by high ones and the equivalent loading cycles.

FE-Safe models are simple for implementation and can be easily used for judging the stress ratio effect; since many mean stress correction techniques are defined: SWT, Morrow, modified Morrow Gebro and Goodman. Also, the software gives the chance to define user defined mean stress correction algorithm by defining a relation between the mean stress and stress amplitude.

Keeping the track with FE-Safe, stress based algorithms were found to be accurate for high cycle fatigue when no plasticity is induced while the strain based algorithms are inevitable if plasticity starts to appear somewhere in the structure. Strain based algorithms allow for evaluating the damage when local yielding is evolved around the notch. Employment the stress strain curve is uniquely used for strain algorithms while S-N curve accompanied with geometrical stress concentration are used for stress algorithms.

Critical plane methods are very effective to evaluate the fatigue crack initiation because they are usable for both high and low cycles fatigue regardless to the mechanics behind the fatigue type. However they could be very expensive computationally because of the necessity to solve the nonlinear problem for evaluating the fatigue life.

Many damage models were presented in the first and second chapter but due to the lack of test results for steel for the given geometry they won't be studied because of the need for their parameters, only three of them will be studied in detail. However, they give different results but they in general were more conservative than the strain based methods. That is expected since the stress concentration remains the same in these elastic methods while it's supposed to drop down when the local plasticity is reached.

Damage in fatigue problems as any damage phenomena can be understood as material degradation. This degradation can be performed to any property which is related to the mechanical performance (stress and strain); elastic modulus, Poisson's ratio and yield strength are just examples. This degradation is questionable physically since the reduction don't impact one property only. However they give good approximation for the fatigue damage in term of the endurance and the relaxation of compressive residual stresses. They require detailed steps in yield strength or stiffness reductions to get the exact fatigue life; course steps in yeild sterngth reduction would approach the fatigue life from the safe side. The same trend was found for the stiffness reduction method.

Since the studied geometry is of two dimensions and subjected to uniaxial loading, then the stress is almost uniaxial loading and using Dang Van, Sines or Crossland criterion would be more accurate than σ_x but the difference is not considerable (though the stress state is not uniaxial because of the notched geometry). So in most of the studied stress based methods the stress in X direction would be more efficient.

From physcail perspective, the compressive loading is less damaging than the tensile one; that's

due to microcrack closure effect. That effect can be simulated using many methods; stiffness degradation and Chaboche and reduction of yield strength are examples of these methods which all take into consideration the microcrack closure effect. However, in order to compare the different methods including the ones that don't consider that effect the crack closure effect wouldn't be considered.

The relaxation of beneficial residual stresses is very comprehensive and physically acceptable. On the other hand; the detrimental thermal stress can also be dissipated with compressive stress cycles. This requires strengthening the material property with cycles which wasn't described in the given literature of these methods (Asma Manai, 2017).

Both of the material degradation methods (Elasticity and yield strength reduction) when used to simulate the relaxation of residual stresses must regain their virgin properties after the lost of the residual stress (or at least part of it); that sounds odd for the first glance but it's explainable physically; though the residual stress loss is due to damage introduced by cyclic loading but the damage initiation won't commence unless the defence mechanism (residual stress) disappear. That leads us to two different nomenclatures of damage, the first is the loss of defense mechanism which protects the structure from the fatigue damage while the other is the degradation of the material due to cyclic loading.

The coupling between fatigue damage and residual stress relaxation is a debatable issue as to whether damage and relaxation work simultaneously or in sequence. Both of these philosophies have their own advantages and drawbacks which makes the question debatable till now, since it deals with crack initiation phase which is still not been clarified enough.

This misunderstanding would raise if and only if the residual stresses are beneficial. However, if these stresses are detrimental (e.g the stresses introduced by welding) this misconception won't exist since the degradation of the material properties commence from the beginning. However this applies only in the crack initiation zone.

The damage initiation can be understood as an intermediate step between plasticity and the crack initiation. The response starts to be elastic then it enters the plasticity zone (on the macro-scale) then it reaches the damage initiation which is governed by the damage models described before then the damage propagates to cause crack initiation. Once the damage reaches the critical value (unity for example) which indicates crack initiation. Then the crack propagates and finally it reaches the fracture when the structure is not being able to undergo further plastic deformation.

This consequence of deterioration is measurable from the elastic stage to failure with extensometers or strain gauges. However the trickiest stage to be measured is the damage which needs a potential difference measurement as mentioned in section 3.3.

Damage itself is not an interesting term for studying since it's a vague term which can mean many form of material degradation or energy dissipation. However, the interesting term in fatigue is the life of the structure; this life is composed of two terms; crack initiation and crack propagation. However, no light were thrown on the propagation stage models.

Deciding which method is the best to evaluate the damage depends on the usage of this model; if material parameters are available Miao model is the best to be used since it's described the damage through reduction in the stiffness matrix; so it can be used in coordination with finite element and this is describes in the basic literature of continuum damage mechanics (Lemaitre and Chaboche, 1994). However this method requires many material parameters and wasn't described for different welding configurations;also it doesn't consider the microcrack closure due to compressive cycles. If no material data is available then basic mechanical properties degradation σ_y or E is a good choice.

The residual stresses are self equilebrated stresses introduced due to different reasons. Non stressing strain like thermal strain is one of that reasons. The removal of plastic loading is also another reason. Different methods were used to introduce these stresses like initial overloading or underloaing. Introducing compressive/tensile stress at specific regions will be also useful to create this distribution. But the best method despite of its price is the true simulation of the phenomena that

The method	The endurance	Suitability	Crack closure	Parameters
Miao model	2.83×10^6	HCF	-	α_k, m_k
Xiao model	6.9×10^6	HCF	-	q, B
Chaboche model	1.03×10^6	HCF	✓	α, β, a
Fatemi Socie model	7.57×10^6	HCF-LCF	-	$\epsilon_f, \sigma_f, b, c, k_1$
Socie model	4.41×10^4	HCF-LCF	-	$\epsilon_f, \sigma_f, b, c, k_2$
Bantiene model	9.10×10^7	HCF-LCF	-	$\epsilon_f, \sigma_f, b, c$
Wang and brown model	4.35×10^7	HCF-LCF	-	$\epsilon_f, \sigma_f, b, c, S$
Stiffness reduction	$\geq 3.38\times 10^5$	HCF	✓	-
Yiled strength reduction	$\geq 5.4 \times 10^5$	HCF-LCF	-	-
From S-N curve	4.35×10^7	Depends on the curve used	-	-

Table 6: Fatigue crack initiation life for different models

creates these stresses. Welding process was simulated and the results were presented in the last chapter. The importance of the true residual stress evaluation is important to study the relaxation problems which is coupled with the fatigue damage.

The geometry in hand is very simple and it's straight forward to control the mesh size in different stress concentration zone. However finite element sub-modeling technique can be used also for more complex geometries to reduce the running time by reducing the stiffness matrices size (mesh size). One more beneficial technique to enhance the accuracy is to use the adaptive mesh refinement, this will allow for regenerating the mesh once the distortions starts to appear in the notch-elements which gives better capture for the local plasticity in this region. Disregarding this option gives conservative estimation in all low cycle fatigue analyses.

When the damage model is to be used from Abaqus or the stress field would be extracted from the program, it's highly recommended to use the adaptive mesh, especially when distortions are expected to occur at the notched area. That would allow for the stress field to be more realistic instead of having raw data from the numerical simulations. The difference can be very influential especially in ductile damage model defined in Abaqus.

7 CONCLUSION

A comparitve study between different fatigue damage models has been conducted to see the benefits and drawbacks of each model. So they can be used later for further studies regarding fatigue and fatigue life improvement.

Different accumulation techniques for variable amplitude loadings (composed of different constant amplitude loading blocks) were studied along with different damage models. The accumulation techniques are also considered as damage models and they use the S-N curve as material model accompanied with the material elasticity.

The S-N curve method is very effective and suitable to be used for variable amplitude loading because of its capability to capture the sequence effect. That makes the high-low loading more damaging than the low loading followed by high amplitude. In addition to that it does not need any material parameters which can be expensive since these parameters must be identified for the base metal, HAZ and the weld material. Already the method was used and verified for both fillet and butt joints. Besides, it's capable of describing the effect of load interaction. Modified damage curve approach is also capable of including load sequence and load interaction effects but the error margin is relatively big. It results in more conservative and shorter fatigue life. This can be accepted for design purposes but not for assessment. The concept of these two methods are similar but the latter is more conservative than the earlier.

The rest of the accumulation methods do not include the load sequence effect. They will be (similarly to Miner's rule) conservative in low-high loading and less damaging in high-low loading. So Miner's rule can be used if no material parameters are available. In case of their availability they would lead to more accurate evaluation.

Chaboche is very simple model and gives an explicit damage formula. This formula includes the effect of mean stress and the residual stresses without referring to different S-N curves for different stress ratios. However it covers the micro-propagation which is beyond the objective of the study. Xiao and Mioa models do not offer explicit damage expression. So the damage increment should be specified for the critical element then the life consumed ΔN is evaluated for that element, then the rest of the elements damage is evaluated for ΔN. All of these three models require material parameters by data fitting. However Zhang can be superior to other models because of its capacity to include the plasticity and hardening effects but it wasn't studied because of the absence of the experimental results and lack of material parameters for welding and even for steel. On the other hand Miao, Xiao and Chaboche were studied numerically in Matlab and using the material parameter in their literature and they yield completely different damage distribution and different fatigue initiation life in the order of 10^6.

Four critical plane models were presented. All of them use coffin Mason equation (or at least part of it) for describing damage when they accompanied with Miner's accumulation rule if the load history varies in amplitudes. The main advantage of such methods is the availability of the strain life equation's parameters for both shear and normal loading. [**FS**] and [**Ba**] show best matching with experiment while [**SO**] found to be conservative as expected.

Two damage coupled with plasticity models were presented however they were used for different purposes. The latter (which was described in (Runesson et al., 2006)) was used to see effect of the type of hardening on the damage evolution and throw a light on the ductility effect on the damage. However, the former is the ductile damage model defined in Abaqus which correlates the damage with plastic strain evolution.

The relaxation of residual stresses is studied through another two methods. During this relaxation process equilibrium is preserved. In stiffness reduction model this equilibrium is preserved by shifting the peak tensile value while in yield strength reduction this shift is not required. Also the welding residual stress is simulated using different methods. The most effective one among them was the thermo-mechanical analysis which ease the process. However, its still computationally demanding. So overloads and thermal predefined field can also be representative of these

stresss. Two methods defines the fatigue damage through the degradation of material proprieties, reduction in stiffness and yield strength are used. And one from of damage is studied through the dissipation of compressive residual stresses and both of them were able to describe it. The following diagram concludes the methods and the topics discussed in this study.

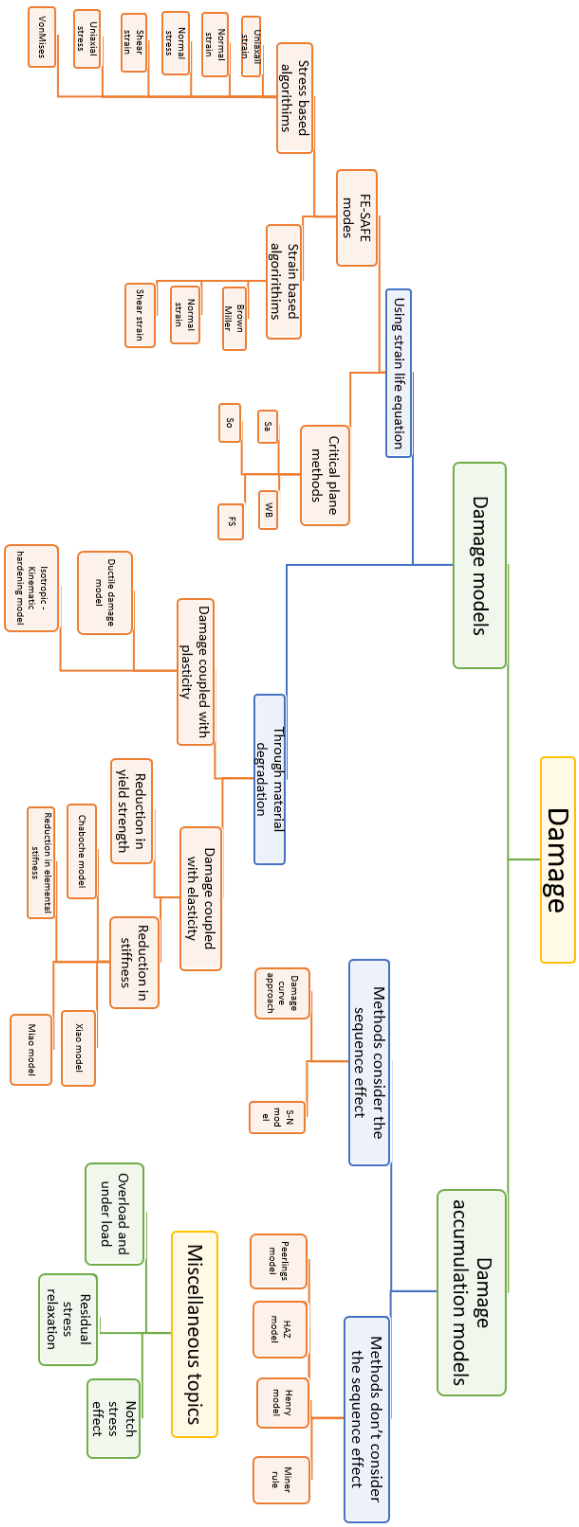

Figure 74: Hierarchy shape showing the damage models described in the study

8 APPENDIX A: MATLAB CODES

8.1 The main code used for Miao, Xiao and Chaboche models

These two codes are used to implement the three damage models using CALFEM finite element tool which can be found online for free.

8.1.1 Main code

```
% PURPOSE
% This code is the main code to be used for Chaboche , Miao and Xiao
% fatigue damage models.
%
clc
clear all
close all
%Calling the mesh  used in Abaqus to be used in Matlab
[ Edof, Dof, Coord, Ex, Ey, NoDofs, NoNodes, NoElem, Enode ] = ...
           AbaqusToFEMGeneral('detailed.inp', 'linearTriangle') ;
%

F =[ 105e6  ]*ones(10,1);% size(F) = Number of cycles
type = 'Alternating'      ;% Specfify the type of the
%loading(Pulsating,Alternating)
NOcycle = length(F)     ;% The number of applied load cycles
D =0e0*ones(NoElem, 1)  ;% Iniatiating an inital value for the damage
Nm = 0*ones(NoElem, 1)  ;%
N = 0                   ;% Initaing fatigue life
dD_max = 0.1;           ;% The damage increment and this is to be studied to
Number =1/dD_max        ;%
%
%This for loop is to loop over all the loading cycles
for i = 1 :Number
L = 105e6% This is the applied alternating loading
% If pulsating load is to be used , then the mean stress
%correction is required.
[dD,dN_max ,dN] = coding1( D, CONSTANTS ,L  ,type);
D= D+dD' ;  % Accumulating the damage
dN_max;
N =N +dN_max ;% Calculating the number of cycles required to caise this damage
% This will be stopped when the damage value reaches D=1.
end

%Plotting the damage contour
figure
fill(Ex',Ey',D')
```

8.2 Finite element implementation code

```
% This code works in parallel with the main code to solve the
% elasticity problem and introduce the damage into the stiffness
% matrix.
%
function [ dD,dN_max,dN] = coding1( D, CONSTANTS ,F ,type )
%The dimension of the plate (to be used in setting
%the boundary conditions and the loads)
 L = 0.03;% Length of the specimen
 B = 0.05;% Width of the specimen
 b = B   ;% The width are expressed in different terms
```

```
%
%Definition of the important matrices to be used in Calfem
[ Edof, Dof, Coord, Ex, Ey, NoDofs, ~, NoElem, ~ ] = ...
           AbaqusToFEMGeneral('detailed.inp', 'linearTriangle') ;
v = 0.3 ;      % poisson ratio
E = (210e9)*ones(NoElem,1); % Elastic modulus
ep = [ 1 1 ];  % plane stress 2D problem
[ex,ey]=coordxtr(Edof,Coord,Dof,3);% extracting the elemental nodes coordinate
b= max(max(Ex));
%
%LOADS AND BOUNDARY CONDITIONS LOCATING MATRICES
RE=  [] ;
LE = [] ;
LN = [] ;
RN = [] ;
%
%LOAD AND BOUNDARY CONDITIONS
% Boundary conditions if-statements
for i = 1 : length(Edof)
   if (Ex(i,1) == b && Ex(i,2) == b )||(Ex(i,3) == b &&
   Ex(i,1) == b)||(Ex(i,2) == b && Ex(i,3) == b)
       RE = [RE ;Edof(i,1)] ;
       if Ex(i,1) == b && Ex(i,2) == b
       RN = [RN ; Edof(i,[2 4])];
       elseif Ex(i,2) == b && Ex(i,3) == b
       RN = [RN ; Edof(i,[4 6])];
       elseif Ex(i,1) == b && Ex(i,3) == b
       RN = [RN ; Edof(i,[2 6])];
       end
   end
   if (Ex(i,1) == 0 && Ex(i,2) == 0 )||(Ex(i,3) == 0 &&
   Ex(i,1) == 0)||(Ex(i,2) == 0 && Ex(i,3) == 0)
       LE = [LE ;Edof(i,1)] ;
       if Ex(i,1) == 0 && Ex(i,2) == 0
       LN = [LN ; Edof(i,[2 3 4 5])];
       elseif Ex(i,2) == 0 && Ex(i,3) == 0
       LN = [LN ; Edof(i,[4 5 6 7])] ;
       elseif Ex(i,1) == 0 && Ex(i,3) ==0
       LN = [LN ; Edof(i,[2 3 6 7])] ;
       end

   end
end
%
 Right_node = round(RN/2) ; Left_node = round(LN/2) ;


k = zeros(max(max(Dof)));
Kd = zeros(max(max(Dof)));
  for i =1 : NoElem
%The stiffness matrix for each element
DE =  (E(i)/((1+v)*(1-2*v)))*[ 1-v  v 0 ; v 1-v 0 ; 0 0 0.5*(1-2*v)];
% Ready made function to evaluate the stiffness value.
[ke ]=   plante( Ex(i,:), Ey(i,:),ep,DE );
% Reducing the stiffness due to fatigue damage
[Ked]= D(i)*ke ;
%Ready made functioin to assemply them in one matrix
[Kd] = assem (Edof(i,:),Kd ,Ked );
```

```
[k  ] =assem (Edof(i,:),k ,ke );
  end
%
 %Force vector
  f = zeros(NoDofs,1);
 % Removing the repeated elements in the BC
  number_right = length(unique(Right_node));
  f(unique(Right_node) )= F%*L/number_right;
 %Boundary conditions
  LN1  = Left_node(:);
  BC1 = unique(LN1);
  BC = [BC1   zeros(length(BC1),1) ]  ;
 % This is a Calfem ready made function to solve the equation K*a = f
  a = solveq(k-Kd,f,BC);
  EDX  = [ a(Edof(:,(2:7)))];
 % Extracting the degree of freedom values
 %to be used later for the stress analyses
 % To draw the deformed shape
  Ed=extract(Edof,a);
% figure(2)
% plotpar=[  1, 1, 1]  ;
% sfac = 1000 ;
%  eldisp2(Ex,Ey,Ed(:,:),plotpar,sfac)
%
 str = zeros(3,1);
 STR = zeros ( NoElem ,3);
 strain = zeros ( NoElem ,3);
% Looping over the element to calculate the elemental stresses and strains
 for i = 1 : NoElem
% This is a Calfem ready made function for triangular
%elements stresses and strains
 [es,et]=plants(Ex(i,:),Ey(i,:),ep,DE,EDX(i,:));
STR(i,:) = [es];    % Locating value for the strain matrix
strain(i,:) =[ et]; % Locating value for the stress matrix
 end
 %
%STRESSES
  strx = STR(:,1);% The stresses in X direction
  stry= STR(:,2); % The stresses  in Y direction
  strxy = STR(:,3);% The shear stresses
  smises = (strx.^2+stry.^2+3*strxy.^2-strx.*stry).^0.5 ;% Von Mises stress

%   figure(3);
%   fill(Ex',Ey',strx');
%  figure(4)
%  fill(Ex',Ey',stry');
%  figure(5)
%  fill(Ex',Ey',strxy');
 [ dD,dN_max,dN ] = Miao( strx  ,D) ;
%[ dN_max,dD ] = xiao( smises  ,D) ;
%[ dD,dN_max ] = XXX( strx  ,D , type) ;
%[ Nf, D  ] = XX( strx  , type )
end
```

8.3 Miao , Xiao , Chaboche models implementation

8.3.1 Miao's model

```
function [ dD ,dN_max , dN] = Miao( strx  ,D )
```

```
% Model parameters
D0 = 0.04971 ; m0 = 1.83898 ; alpha0= 0.0765159 ;
Kt = 2.90999 ; k2 = 1.44831 ; mu = 0.111908 ;
lamda = 0.954223 ; t = 0.101213 ; Sth0  =0 ;
dD_max = 0.005; E=210e9 ;
% The stress in X-direction will be used for damage evaluation
S_k0_max = strx ;
e_th_k0 = Sth0/E ;
e_k0_max = S_k0_max./E ;
%The evolution of strain due to damage.
e_th_kD=  e_th_k0./sqrt(1-D) ;
e_kD_max=e_k0_max./sqrt(1-D);
%These equations are described in the literature
a_k = alpha0*exp(lamda*(Kt-1)) ;
m_k = m0*exp(t*(Kt-1)) ;
Sth_km = Sth0*exp(1-D0)*exp(-mu*(Kt-1));
%
strxmax = strx(find(strx == max(strx))) ;
max_index = find(strx == max(strx)) ;
e_kD_max_max = max(e_kD_max);
dN_max =(1/a_k)*((1-D(max_index))
./abs(max(e_kD_max)-max(e_th_kD))).^(m_k)*dD_max ;
%
for i =1 : length(strx)
        dD(i) = a_k*(abs(e_kD_max(i)-e_th_kD(i))/(1-D(i)))^(m_k)*dN_max ;
        dN(i) =(1/a_k)*((1-D(i))./abs(max(e_kD_max)-max(e_th_kD))).^(m_k)*dD(i) ;
        end
end
```

8.3.2 Xiao's model

```
function [dN_max ,dD ] = xiao( smises  ,D)
% The model parameters
B = 6e43 ; q = 2.1927;
dD_max =0.005;% Converengce study is required
%
dN_max = abs(B*(1-max(D))^(2*q)./((max(smises).^(2*q)))*dD_max) ;
    for i =1 : length(smises)
    dD(i) = abs((smises(i)^(2*q)./(B*(1-D(i))^(2*q))))*dN_max ;
    end
end
```

8.3.3 Chaboche's model

```
function [ dD ] = XXX( strx  ,D , type )
%
%Model parameters
beta = 1.581 ; a = 0.6861 ; M0 = 3.91e5 ;
b1 = 0.0024 ; b2 = 0.0001098 ;
%
S_ = 40e6  ;% Fatigue limit ;
Su = 420e6 ;% The ultimate strength
%
M = M0*(1-b2*Sm/Su) ;
Sf = S_* (1-b1*Sm/Su) ;
%
dD_max = 0.2;

X = max(Smax)-max(Sm)/(Su-max(Smax));
    if X >0
        alpha = 1 -a*X;
    else
        alpha =1;
    end

dN_max = ((1-(1-max(D))^(beta+1))^(-alpha)*
((Smax(i)-Sf(i))/(M(i)*(1-max(D))))^(-beta))*dD_max ;

%


for i =1 : length(strx)
 X = (Smax(i)-Sm(i))/(Su-Smax(i)) ;
    if X >0
        alpha = 1 -a*X ;
    else
        alpha =1 ;
    end
 dD(i) = (1-(1-D(i))^(beta+1))^(alpha)* ((Smax(i)-Sf(i))/(M(i)*(1-D(i))))^(beta) ;

end
end
```

8.4 Critical plane methods

This code shows the implementation of the four critical plane methods in one code.

```
clear all
close all
clc
type = 1 ;
[ Edof, Dof, Coord, Ex, Ey, NoDofs, NoNodes, NoElem, Enode ] = ...
           AbaqusToFEMGeneral('residu.inp', 'linearTriangle') ;
ex0  = zeros(NoElem,1) ;
ey0  = zeros(NoElem,1) ;
ex0  = zeros(NoElem,1) ;
s0 = zeros(NoElem,1) ;
% The values of shear and normal strains and stresses
%must be extracted from Abaqus and read on excel files on the given lines.
%overload strain
%
 ex1 = xlsread('book1.xlsx','Sheet1','C1:C2960') ;
 ey1 = xlsread('book1.xlsx','Sheet1','D1:D2960') ;
 exy1 = xlsread('book1.xlsx','Sheet1','E1:E2960') ;
 s1 = xlsread('book1.xlsx','Sheet1','F1:F2960') ;
 t1 =  xlsread('book1.xlsx','Sheet1','AD1:AD2960') ;
 t2 = xlsread('book1.xlsx','Sheet1','AE1:AE2960') ;
 t3 =  xlsread('book1.xlsx','Sheet1','AF1:AF2960') ;
%residual strain
%
 ex2 = xlsread('book1.xlsx','Sheet1','K1:K2960') ;
 ey2 = xlsread('book1.xlsx','Sheet1','L1:L2960') ;
 exy2 = xlsread('book1.xlsx','Sheet1','M1:M2960') ;
  s2 = xlsread('book1.xlsx','Sheet1','N1:N2960') ;
 %residual strain
 %
 ex3 = xlsread('book1.xlsx','Sheet1','Q1:Q2960') ;
 ey3 = xlsread('book1.xlsx','Sheet1','R1:R2960') ;
 exy3 = xlsread('book1.xlsx','Sheet1','S1:S2960') ;
 s3= xlsread('book1.xlsx','Sheet1','T1:T2960') ;
 %residual strain
 %
 ex4 = xlsread('book1.xlsx','Sheet1','W1:W2960') ;
 ey4 = xlsread('book1.xlsx','Sheet1','X1:X2960') ;
 exy4 = xlsread('book1.xlsx','Sheet1','Y1:Y2960') ;
  S4 = xlsread('book1.xlsx','Sheet1','Z1:Z2960') ;

%ELASTIC LOADING STRAIN EVALUATION



     eax1 =ex1/2  ;% The amplitude of the overload strain x  ;
     sa1 =   s1       ;% The maxium stress amplitude  ;
    gamma1 = exy1    ;%The shear strain amplitude ;
    ta1 = t1;
%
      eax2 = (ex2+ex3)/2  ;% The amplitude of the overload strain x  ;
     sa2 =   s3-s2      ;% The maxium stress amplitude  ;
     gamma2 = (exy2+ exy3)/2  ;%The shear strain amplitude ;
     ta2 = t3-t2;

     b = -0.0835 ; c= -0.5142 ; ef = 0.476/sqrt(3) ; sf = 703/sqrt(3) ;
```

```
     if type ==3
     b = -0.0835 ; c= -0.5142 ; ef = 0.476 ; sf = 703 ;
end
%
 Nf1 = []   ; Nf2 = [ ] ;
 N1 = 1e4 ; N2= 1e5 ;
     for i = 1 : NoElem
% syms N1
% syms N2
g = 10 ; tol = 5e-3 ;

N1 = 0.5*exp((1/b)* ) ;
N2 = 0.5*exp((1/b)*log(abs(sa2(i)+ta2(i))/abs(ta2(i)))) ;


Nf1 = [Nf1  ; N1 ] ;
Nf2 = [Nf2  ;  N2] ;


    end
 figure
 fill(Ex',Ey',D')
```

8.5 Reading from Abaqus

This code isn't created by the writer of the thesis but it's available online ; It reads the Abaqus input file so the mesh can be created in Matlab and the results are comparable regardless whether they are created in Abaqus directly or from programming in Matlab . Also it's beneficial to create the important matrices required for MATLAB interactive toolbox CALFEM

```
    function [ Edof, Dof, Coord, Ex, Ey, NoDofs, NoNodes, NoElem, Enode ] = ...
           AbaqusToFEMGeneral( filename, elementType )
The interested readers are referred to florosd@chalmers.se where the full
integrated system of codes are provided for the sake of this mesh conversion
```

8.6 Elemental stiffness degradation code

The elemental stiffness degradation method described for fatigue damage and residual stress relaxation are implemented simultaneously with the use of Abaqus.

```
clear all
%
% limit endruence and limit elastic
sigma_endurence=0; % The endurance limit
sigma_elastic=355; % The yield strength value
elemumber=2960 ;   % The number of elements
alpha=1;           % Micro-crack closure effect
%
% Abaqus report files containing stress values must be added to the working path

% Initial stiffness value before any reduction
E_precedent=210000*ones(L,1);
file='abaqus1.rpt';% This is the file name
fid=fopen(file,'r');
a=[ ]
while(~feof(fid)),
   s=fgetl(fid);
% This can change slightly if Abaqus report gives diffeernt length of this line
   if strcmp(s,'------------------------'),
```

```
      biggmeshh3=fscanf(fid,'%f',[6,elemumber]);
     biggmesh3=biggmeshh3'
   end
end
fclose(fid)

%
L = elemumber ;

S113=biggmesh3(:,4);
% The Sines criteria equievlelent stress
sige= abs(S113) ;

for i=1:L
%This is the stiffness reduction rule
    E(i,1)=(E_precedent(i,1))*(1-(sige(i,1)/(sigma_elastic)));
end
%
% This is required for being an input in the keyword
toabaqus=[elenumb,E,0.3*ones(L,1)];

for i=1:L
    Mm(i,[1:8])='Part-1-1' ;
end
for i=1:L
    ca(i,1)=',';
end
for i=1:L
    do(i,1)='.';
end
abb=[Mm,do,num2str(toabaqus(:,1)),ca,
num2str(toabaqus(:,2)),ca,num2str(toabaqus(:,3))]


  dlmwrite('stiffness.txt',abb,'')
 type stiffness.txt
```

8.7 Rainflow counting algorithm

```
    % RFC-call
% Read input data in the form of max-min-stresses
clear all
close all
clf

% RAINFLOW COUNT
input history
[mid,range]=rfc_skeleton(history); % Call the function that does the RFC

% Check that the largest range is captured
max_range = range(end)
if max_range ~= max(range)
    disp('Missed largest range ')
end

amplitude = range*0.5;
figure(1)
errorbar(mid,amplitude)
figure(2)
h = normplot(amplitude)


% FATIGUE LIFE EVALUATION
fatlim = 'y' % Account for the fatigue limit? (y / n)
criterion = 'SWT' % Mid stress criterion
% Parameters: mid stress, stress range, criterion, account for fatigue limit
Nf=a(mid, range, criterion, fatlim);

disp('=====')
disp('Fatigue life evaluation using and SN-curve and the SWT mid stress criterion.')
if fatlim == 'y'
    disp('The fatigue limit is accounted for.')
else
    disp('The fatigue limit is not accounted for.')
end
disp('The component can sustain ')
disp(num2str(Nf))
disp('repetitions of the current load sequence, which contains')
disp(num2str(length(amplitude)))
disp('stress cycles. Consequently, the component can in total sustain')
disp(num2str(length(amplitude).*Nf))
disp('stress cycles.')
disp('')
disp('The equivalent damage of the load sequence is ')
D = 1/Nf;
disp(num2str(Nf))
disp('[-]')
```

9 APPENDIX B: Material proprieties change with temperature

Table 7: Temperature effect on the material properties

Conductivity	Density	Elasticity	Poisson's ratio	Expansion coefficient	Specific heat	Temperature
(W/(mK))	Ton/mm^3	MPa	-	-	(J/(kg K))	C
14.6	7.90E-09	198500	0.294	1.70E-05	462000000	0
15.1	7.88E-09	193000	0.295	1.74E-05	496000000	100
16.1	7.83E-09	185000	0.301	1.80E-05	512000000	200
17.9	7.79E-09	176000	0.31	1.86E-05	525000000	300
18	7.75E-09	167000	0.318	1.91E-05	540000000	400
20.8	7.66E-09	159000	0.326	1.96E-05	577000000	600
23.9	7.56E-09	151000	0.333	2.02E-05	604000000	800
32.2	7.37E-09	60000	0.339	2.07E-05	676000000	1200
33.7	7.32E-09	20000	0.342	2.11E-05	692000000	1300
120	7.32E-09	10000	0.388	2.16E-05	700000000	1500

Table 8: The plasticity degradation with the presence of thermal loads

Yield stress	Plastic strain	Temprature
MPa	-	C
265	0	20
387.5	0.05	20
186	0	200
320.65	0.05	200
155	0	400
299.8	0.05	400
138	0	600
286	0.05	600
112	0	700
216.8	0.05	700
91	0	800
113	0.05	800
50	0	900
50	0.05	900
25	0	1000
25	0.05	1000
21	0	1100
21	0.01	1100
10	0	1500
10	0.01	1500

10 REFERENCES

References

A. Pirondi, N. B. (2003). *Modeling ductile damage under fully reversed cycling.* Computational Materials Science 26 129–141.

Aeran, A., Siriwardane, S. C., Mikkelsen, O., and Langen, I. (2017). *A new nonlinear fatigue damage model based only on SN curve parameters*, volume 103. Elsevier.

Aid, A., Bendouba, M., Aminallah, L., Amrouche, A., Benseddiq, N., and Benguediab, M. (2012). *An equivalent stress process for fatigue life estimation under multiaxial loadings based on a new non linear damage model*, volume 538. Elsevier.

Aravas, N. (1987). *On the numerical integration of a class of pressure-dependent plasticity models*, volume 24. Wiley Online Library.

Asma Manai, Hedi Hassis, A. K. (2017). *A pragmatic anisotropic Damage Fatigue Model Based on a failure criterion and its gradient.* www.iosrjournals.org.

Banvillet, A. (2001). *Prévision de durée de vie en fatigue multiaxiale sous chargements réels: vers des essais accélérés.*

Björn åkesson, M. (2013). *Steel Structures.* Chalmers university of technology.

Bouchard, P.-O., Bourgeon, L., Fayolle, S., and Mocellin, K. (2011). *An enhanced Lemaitre model formulation for materials processing damage computation*, volume 4. Springer.

Carlson, R., Kardomateas, G., and Bates, P. (1991). *The effects of overloads in fatigue crack growth*, volume 13. Elsevier.

Chaboche, J. and Lesne, P. (1988). *A non-linear continuous fatigue damage model*, volume 11. Wiley Online Library.

Chandrakanth, S. and Pandey, P. (1995). *An isotropic damage model for ductile material*, volume 50. Elsevier.

Cheng, G. and Plumtree, A. (1998). *A fatigue damage accumulation model based on continuum damage mechanics and ductility exhaustion*, volume 20. Elsevier.

Chow, C. and Wei, Y. (1991). *A model of continuum damage mechanics for fatigue failure*, volume 50. Springer.

Corp, D. S. S. (2017). *fe-safe USER GUIDE.* Simulea.

Dattoma, V., Giancane, S., Nobile, R., and Panella, F. (2006). *Fatigue life prediction under variable loading based on a new non-linear continuum damage mechanics model*, volume 28. Elsevier.

D.Floros (2018). *abaqusMesh2Matlab: Program for extracting FE-mesh data.* https://se.mathworks.com/matlabcentral/fileexchange/67437-abaqusmesh2matlab.

Dowling, N. E. (2012). *Mechanical behavior of materials: engineering methods for deformation, fracture, and fatigue.* Pearson.

Gao, H., Huang, H.-Z., Zhu, S.-P., Li, Y.-F., and Yuan, R. (2014). *A modified nonlinear damage accumulation model for fatigue life prediction considering load interaction effects*, volume 2014. Hindawi.

Hibbitt, Karlsson, and Sorensen (2001). *ABAQUS/Standard user's manual*, volume 1. Hibbitt, Karlsson & Sorensen.

Kariyawasam, K. and Mallikarachchi, H. (2015). *Simulation of Low Cycle Fatigue with Abaqus/FEA.*

Leitner, M., Khurshid, M., and Barsoum, Z. (2017). *Stability of high frequency mechanical impact (HFMI) post-treatment induced residual stress states under cyclic loading of welded steel joints*, volume 143. Elsevier.

Lemaitre, J. and Chaboche, J.-L. (1994). *Mechanics of solid materials*. Cambridge university press.

Miner (1954). *MA. Cumulative damage in fatigue*. J Appl Mech 1945:A159–64.

Peerlings, R. H. J. (1999). *Enhanced damage modelling for fracture and fatigue*.

Pirondi, A., Bonora, N., Steglich, D., Brocks, W., and Hellmann, D. (2006). *Simulation of failure under cyclic plastic loading by damage models*, volume 22. Elsevier.

Runesson, K., Steinmann, P., Ekh, M., and Menzel, A. (2006). *Constitutive modeling of engineering materials—theory and computation*.

Schubnell, J., Farajian, M., Däuwel, T., and Shin, Y. (2018). *Numerical fatigue life analysis of a high frequency mechanical impact treated industrial component based on damage mechanics models*, volume 49. Wiley Online Library.

Shen, C. (2012). *Contribution à l'étude du cumul de dommage en fatigue multiaxiale*.

Silitonga, S., Maljaars, J., Soetens, F., and Snijder, H. (2013). *Survey on damage mechanics models for fatigue life prediction*, volume 58.

Simulia learning community (2017). *Abaqus weld interface*. Katherine corey.

Simulia learning community (2018). *Workshop 1 3D Welding Simulations Abaqus Welding Interface*. Dassault Systèmes.

Tai, W. H. and Yang, B. X. (1986). *A new microvoid-damage model for ductile fracture*, volume 25. Elsevier.

Tian, J., Liu, Z.-M., and He, R. (2012). *Nonlinear fatigue-cumulative damage model for welded aluminum alloy joint of EMU*, volume 34. China Railway Society, 10 Fuxing Rd. Beijing 100844 China.

Van Do, V. N., Lee, C.-H., and Chang, K.-H. (2015). *High cycle fatigue analysis in presence of residual stresses by using a continuum damage mechanics model*, volume 70. Elsevier.

Wang, M., Fei, Q., and Zhang, P. (2016). *A modified fatigue damage model for high-cycle fatigue life prediction*, volume 2016. Hindawi.

Wang, T. and Lou, Z. (1990). *A continuum damage model for weld heat affected zone under low cycle fatigue loading*, volume 37. Elsevier.

Xiao, Y. (2004). *A multi-mechanism damage coupling model*, volume 26. Elsevier.

Xiao, Y.-C., Li, S., and Gao, Z. (1998). *A continuum damage mechanics model for high cycle fatigue*, volume 20. Elsevier.

Xie, X.-f., Jiang, W., Luo, Y., Xu, S., Gong, J.-M., and Tu, S.-T. (2017). *A model to predict the relaxation of weld residual stress by cyclic load: Experimental and finite element modeling*. Elsevier.

Zhang, L., Liu, X.-s., Wang, L.-s., Wu, S.-h., and Fang, H.-y. (2012). *A model of continuum damage mechanics for high cycle fatigue of metallic materials*, volume 22. Elsevier.

Zhang, M., Meng, Q., Hu, W., Shi, S., Hu, M., and Zhang, X. (2010). *Damage mechanics method for fatigue life prediction of Pitch-Change-Link*, volume 32. Elsevier.